Charge States and Charge-Changing Cross Sections of Fast Heavy Ions Penetrating Through Gaseous and Solid Media*

HANS-DIETER BETZ

Physics Department, Laboratory for Nuclear Science, Massachusetts Institute of Technology, Cambridge, Massachusetts 02139

This review surveys the experimental and theoretical situation concerning charge states and charge-changing cross sections of heavy ions up to and including uranium, which penetrate through gaseous and solid targets with velocities primarily in the range $v_0 < v < Zv_0$ ($v_0 = e^2/\hbar = 2.188 \times 10^8$ cm/sec). Particular emphasis is given to ions with atomic numbers in the range $16 \leq Z \leq 92$. The published literature is covered through August 1971. General physical and mathematical relations are outlined which describe the composition of charge states in a heavy-ion beam which passes through matter. Recent experimental techniques and methods of data analysis are summarized. Extensive experimental results on heavy-ion equilibrium charge state distributions, average equilibrium charge states, and cross sections for capture and loss of one or more electrons in single encounters with target atoms are presented and critically examined. The data extend to ions as heavy as uranium and energies up to ~400 MeV. Systematic trends are emphasized and generalizations are discussed which allow interpolations and to some extent extrapolations of the data to be made to ranges which have not been investigated experimentally. Attention is given to the cross sections for multiple-electron loss which are relatively large but which are poorly understood. We deal with effects of residual ion excitation on charge-changing collisions in the light of recent experimental results. It is shown that the average equilibrium charge of heavy ions can be approximated by utilizing both theoretical concepts which originate from the work of Bohr and Lamb, and semiempirical relations which are based on observed regularities of the data. Recent interpretations of phenomena associated with density effects, i.e., with the increase of projectile ionization which is observed for increasing target densities, are scrutinized and refinements of the theory by Bohr and Lindhard are explored.

CONTENTS

* Supported by U.S. Atomic Energy Commission under Contract AT(11-1)3069.

I. INTRODUCTION

The charge of high-speed ions passing through matter fluctuates due to electron capture and loss processes which occur with high probabilities in ion–atom collisions. Interest in these charge-changing phenomena developed from early studies of alpha rays and fission fragments, and has grown considerably since energetic beams of heavy ions in high-charge states became available from particle accelerators. The most recent attention has been stimulated in connection with the design of new powerful heavy-ion accelerators in which charge exchange plays an essential role. Besides practical demands for the prediction of ionic charge states and charge changing-cross sections of fast heavy ions, it has been realized for a long time that the study of charge states, i.e., of electron capture and loss phenomena, is an important source of information about atomic collisions and processes in complex atomic systems.

The purpose of the present article is to review experimental results and theoretical approaches concerning the formation of charge states of heavy ions in collisions with target atoms in dilute gases, dense gases, and solids. Throughout this paper, particular emphasis is given to projectiles with atomic numbers in the range $16 \leq Z \leq 92$ and the notation "heavy ion" usually refers to ions in that range. However, since systematic trends of certain ion properties extend beyond that range, we will often refer to experimental and basic theoretical results obtained for ions with $Z < 16$, including hydrogen atoms and ions. Heavy-ion velocities of present interest lie primarily in the range $v_0 < v < Zv_0$ ($v_0 = e^2/\hbar = 2.188 \times 10^8$ cm/sec). This implies that we deal in most cases with those ions which are highly ionized, but which still carry many electrons in their atomic shells. The interactions between these partially stripped ions and matter are extremely complicated, and are difficult to predict. The lack of adequate comprehensive theories often requires that we pursue a phenomenological approach. Therefore, we emphasize the description and illustration of typical experimental results, and we reproduce important portions of the reviewed data on average equilibrium charge states in gaseous and solid targets and charge-changing cross sections in tabular and graphical form.

The first specific theoretical interest in charge states of heavy ions arose in connection with studies of velocity-range relations for fission fragments. In order to estimate the energy loss of the fragments it appeared necessary to calculate their ionic charge states at all velocities during the slowing down process. Such calculations have been performed by Lamb (1940), Bohr (1940, 1941), Knipp and Teller (1941), and Brunings, Knipp, and Teller (1941). In a well-known treatise, Bohr (1948) presented a first extensive theory of charge-changing processes, including some rough estimates for electron capture and loss cross sections for fission fragments. Those parts of that theory which deal with heavy ions have been refined by Bohr and Lindhard (1954): this includes an attempt to account for the density effects observed by Lassen (1951a, b). Some numerical calculations of charge-changing cross sections have been carried out for fission fragments by Bell (1953).

The first data on the charge exchange of heavy ions was obtained from the studies of uranium fission fragments. Lassen (1951a, b) investigated ionic charge state distributions for the light group ($Z \simeq 38$, $v \simeq 6v_0$) and for the heavy group ($Z \simeq 54$, $v \simeq 4v_0$) of fission fragments passing through various gaseous and solid targets. He was the first to observe the theoretically expected density effects which have become quite important in the field of heavy-ion stripping: higher degrees of ionization are obtained when ions emerge from solids rather than from gases (density effect in solids, see Sec. VI.2), and when the pressure of a target gas is increased (density effect in gases, see, Sec. VI.1). In the years following Lassen's work, experimental studies of charge exchange processes were limited almost entirely to ions with $Z \leq 18$. It is not surprising that hydrogen and helium projectiles have been investigated most extensively. These ions are readily available and are easily stripped to the bare nucleus at energies below 100 keV and 1 MeV, respectively. A review of experimental results on charge-changing collisions of hydrogen and helium atoms and ions at velocities above $0.045v_0$ ($E > 0.2$ keV) has been given by Allison (1958). A summary of additional data on hydrogen, helium, and some heavy ions including fission fragments has been prepared by Allison and Garcia-Munoz (1962). Nikolaev (1965) reviewed experimental and theoretical studies of electron capture and loss by ions which lie primarily in the range $3 \leq Z \leq 18$, and he systematized and generalized many of the results which were available at that time. His comprehensive article contains very useful background information.

Heavier ions with high velocities were not investigated in detail until cyclotrons and linear accelerators could be utilized to produce monoenergetic beams of a great variety of heavy ions. Since 1962, systematic data on heavy ions up to and including uranium, with energies ranging from ~ 1 MeV to almost 200 MeV has been accumulated mainly by using tandem van de Graaff accelerators by research groups at Heidelberg in Germany, and Oak Ridge, Tennessee, and Burlington and Cambridge, Massachussets, in the United States. The experimental results obtained by these groups represent a significant fraction of the recent data which is relevant to this review. Extensive information is now available about ionic charge state distributions and average equilibrium charge states of heavy ions passing through gases and solids. For a long time, data on electron capture and loss cross sections has been sparse and disconnected, but in recent years a number of detailed measurements of charge-changing probabilities have been carried out for a few selected

projectiles and targets such as, for example, bromine and iodine stripped in hydrogen, helium, nitrogen, and oxygen. However, especially at energies above ~ 60 MeV, more systematic work must be done before a sufficiently complete picture is attained.

In this review, we have attempted to give a comprehensive and critical survey of the published literature about charge states and charge-changing cross sections of fast heavy ions. The review covers the literature up to August, 1971. We have concentrated on the discussion of those charge-changing collisions which occur with relatively large probabilities, and affect essentially all beam particles penetrating through a target. This implies that we exclude the discussion of collisions with very small impact parameters in which the projectiles are scattered out of the main direction of the beam, and which give rise to heavy-ion induced inner-shell excitation phenomena. Furthermore, questions concerning the energy loss of heavy ions are, though related, not part of the present review and receive only passing attention.

Section II summarizes the most important purely mathematical relations between charge state populations, target thickness, and charge-changing cross sections. Section III surveys experimental methods and techniques of data analysis. Section IV presents the theoretical and experimental results on cross sections for loss and capture of one or more electrons; systematic trends are pointed out and the need for substantially improved theories is demonstrated. In Sec. V we focus on various aspects associated with equilibrium charge state distributions. It is shown that average equilibrium charge states can be approximated both theoretically on the basis of simple physically reasonable though relatively arbitrary assumptions, which originate from the pioneering work of Bohr (1940, 1941) and Lamb (1940), and empirically on the basis of general experimentally observed regularities. Section VI deals with the density effects. It includes the discussion of discrepancies between theory and recent experimental observations and a possible solution. A list of the most frequently used symbols is given in the Glossary.

II. MATHEMATICAL DESCRIPTION OF THE EQUATIONS FOR CHARGE-CHANGING PROCESSES

1. Differential Equations for Charge State Nonequilibrium

When an ion of charge q collides with atoms or molecules of a target gas, the ion may capture or lose one or more electrons on each encounter. The probabilities for these processes are described by cross sections $\sigma(q, q')$, where q and q' denote the charge which the ion carries before and after a single charge-changing collision. Very often, especially in theoretical investigations, σ is given in units of cm^2/atom; in the following, however, we prefer units of cm^2/molecule because charge exchange in complex target molecules is frequently discussed. Cross sections are sometimes written in the form $\sigma(q, q\pm n)$, where positive and negative signs characterize electron loss and capture by the ions, respectively; and in the form $\sigma(q, q+n)$, with positive and negative values of n for loss and capture, respectively. It is also customary to use subscripts in order to distinguish cross sections for capture (σ_c) and loss (σ_l). Values $|n|=1$ refer to single loss and capture cross sections, i.e., to collisions in which the ion captures or loses only a single electron, and $|n|>1$ refers to multiple capture and loss cross sections, i.e., to single collisions in which the ion captures or loses more than one electron. According to experimental evidence, capture of more than one electron is a relatively unlikely process, whereas simultaneous loss of several electrons in a single collision is a very probable process which cannot be neglected, especially for heavy ions penetrating through heavy gases. Apart from their dependence on q and n, cross sections may vary strongly with nuclear charge and velocity of the projectiles, and with the nuclear charge of the target atoms.

The variation of the charge composition of an ion beam penetrating through a gasesous target is described by a system of linear coupled differential equations

$$dY_q(x)/dx=\sum_{q'\neq q}[\sigma(q', q)\,Y_{q'}(x)-\sigma(q, q')\,Y_q(x)], \tag{2.1}$$

where Y_q denotes the fraction of the ions which carries the charge q ($\sum_q Y(q)=1$), and x, depending on the units chosen for σ, is the number of atoms/cm^2, or molecules/cm^2 in the path of the ions. In principle, q and q' may vary within the range $-1\leq q\leq Z$; however, actual charge distributions show a limited width, and most of the values Y_q are exceedingly small. For practical purposes, it is usually sufficient to retain a number of charge states which, depending on Z, lies between ~ 10 and ~ 15. In particular, since the ion velocities of present interest are not smaller than v_0, the terms Y_{-1} will always be neglected.

Though the purely mathematical derivation of Eq. (2.1) is straight forward and needs no lengthy explanation, it is important to point out some restrictions on its use. Equation (2.1) takes into account only those collisions in which the charge of the ions is really changed, and it does not include elastic collisions or encounters which lead only to excitation of the ions. Also excluded are processes in which, for example, one electron is captured and lost shortly thereafter, perhaps as the result of an Auger process, before the ion undergoes another collision or enters the charge analyzing system. It is further assumed that the gas target is sufficiently dilute so that the ions, possibly excited in collisions, always have enough time to return to their ground state before any subsequent charge changing collision occurs. Then, all cross sections $\sigma(q, q')$ in

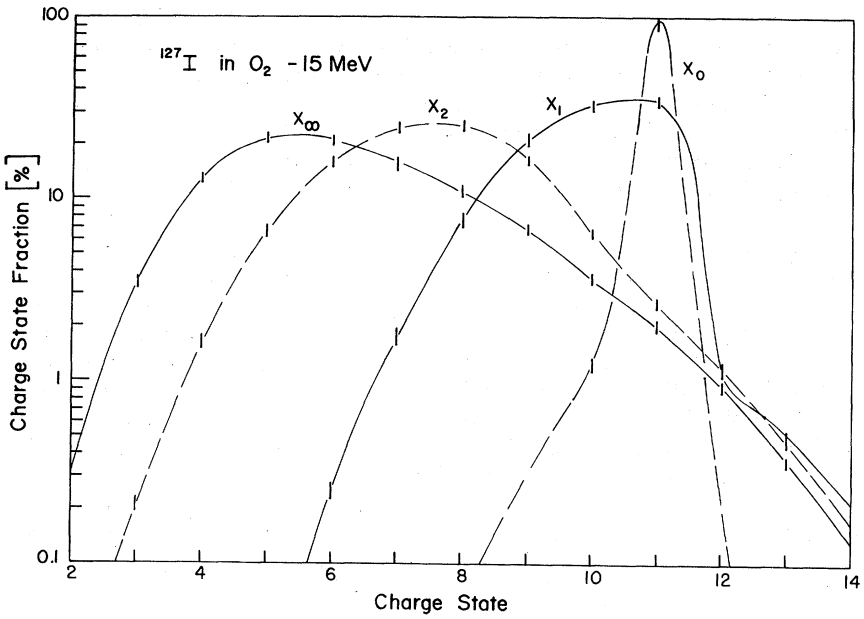

FIG. 2.1. Calculated nonequilibrium charge state distributions for 15-MeV iodine ions with initial charge +11, stripped in dilute oxygen; from Betz and Wittkower (1972a). The underlying set of multiple capture and loss cross sections $\sigma(q, q')$ consists of experimental values for $5 \leq q \leq 11$, and of extrapolated values for $q \leq 4$ and $q \geq 12$. Charge states are indicated near each curve. Experimental charge state fractions which have been measured at target thickness zero served as initial conditions for the integration of Eq. (2.1) and are indicated by arrows on the left-side ordinate. Charge equilibrium is reached at a target thickness of only $\sim 10^{16}$ molecules/cm^2, corresponding to 0.53 μg/cm^2.

Eq. (2.1) are strictly associated with the ground state of ions with charge q. In addition, it is necessary that the target be so thin that the average energy loss per ion in the target is negligible. Finally, it is assumed that the beam which emerges from the target is observed essentially in the forward direction. We do not deal with the angular dependence of the cross sections. In addition, it is assumed that the two methods of increasing x: (i) increasing the length of the target cell at constant gas pressure, and (ii) increasing the gas density within a cell of constant length, are equivalent. Provided that the above conditions are met, all probabilities $\sigma(q, q'; v, Z, Z_T)$ are constant for a given set of the indicated parameters and represent a consistent set which allows one to integrate Eq. (2.1) and, for given initial conditions, to predict the variation of the charge fractions along the path of the beam.

When only a few charge states are influential, simple analytical solutions of Eq. (2.1) can be found. Examples for a three-component system have been given by Allison (1958). For fast heavy ions, where many more charge states are important, a numerical integration is convenient. Since the accuracy $\delta Y/Y$ of the computed charge fractions need not necessarily be better than $\sim 0.1\%$, a simple Runge–Kutta integration is adequate. Figures 2.1 and 2.2 show examples of calculated non-

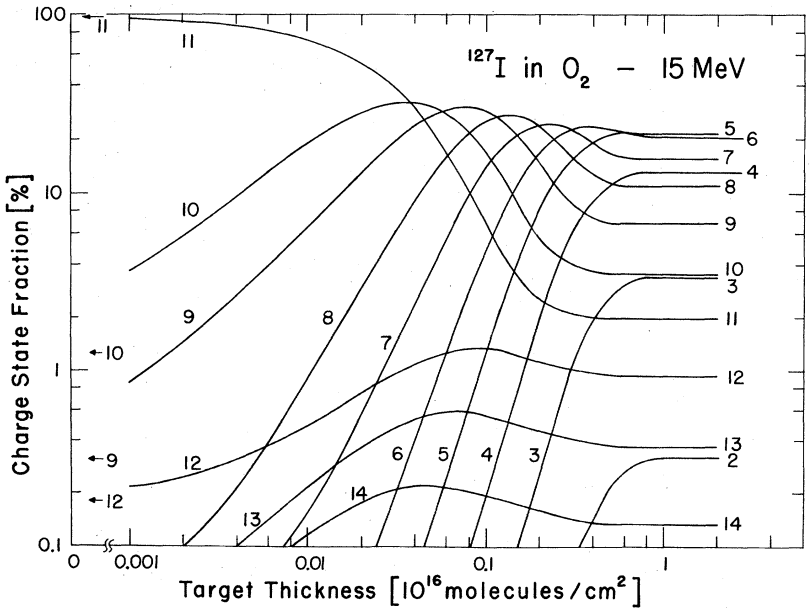

FIG. 2.2. Charge state distributions for 15-MeV iodine ions in oxygen, taken from Fig. 2.1 at four target thicknesses: $x_0 = 0$ (incident experimental distribution), $x_1 = 3.54 \times 10^{14}$, $x_2 = 1.86 \times 10^{15}$, and $x_\infty = 10^{16}$ molecules/cm^2 (equilibrium). The calculated fractions are indicated by vertical bars; the envelopes are drawn as smooth curves to guide the eye and to demonstrate the peculiar shapes of the distributions.

equilibrium charge state distributions for 15-MeV iodine ions passing through dilute oxygen gas. Figure 2.1 illustrates typical behavior of the growth curves $Y_q(x)$. For example, charge fractions which are small at low target thicknesses increase steadily until they reach at most one maximum, decrease by varying amounts, and approach an equilibrium value. Figure 2.2 demonstrates the different shapes of charge state distributions $Y_x(q)$ during approach towards equilibrium.

Without significant modifications, Eq. (2.1) can not be used for a description of charge exchange in dense gaseous targets or in solids. We will show in Sec. VI that especially in gaseous equilibrium targets the conditions for having a "dilute" target are extremely difficult to realize. At present, the many questions primarily concerning excitation and deexcitation processes preclude the suggestion of the required practical modifications of Eq. (2.1).

2. Charge State Equilibrium

Under the ideal circumstances which we have specified in Sec. II.1, each charge state fraction of an ion beam reaches a certain equilibrium value which does not change when the target thickness is further increased, and which is independent of the initial distribution of charge states in the beam incident on the target. To distinguish from nonequilibrium fractions Y_q we will denote equilibrium charge state fractions by F_q: Eq. (2.1) yields for each charge state q

$$\sum_{q'\neq q}[F_{q'}\sigma(q', q)-F_q\sigma_t(q)]=0, \qquad (2.2.a)$$

where $\sigma_t(q)$ denotes the total charge-changing cross section for ions with charge q,

$$\sigma_t(q)=\sum_{q'\neq q}\sigma(q, q').$$

Equation (2.2.a) implies that the number of particles which populate the fraction F_q is equal to the number which depopulate it. According to the definition of charge equilibrium, it is also evident that the number of particles populating a range of fractions with charges below q must be equal to the number of particles which depopulate that range; hence, we have for each q

$$\sum_{q'<q\leq q''}{}_{q',q''}[F_{q'}\sigma(q', q'')-F_{q''}\sigma(q'', q')]=0. \qquad (2.2.b)$$

When only cross sections for capture and loss of a single electron are considered, Eq. (2.2b) reduces to the simple relation

$$F(q)\sigma(q, q+1)=F(q+1)\sigma(q+1, q). \qquad (2.3)$$

Equation (2.3) is often useful for light ions, but it is much less significant for the description of equilibrium distributions of heavy ions, especially because the cross sections for multiple electron loss become highly influential.

When a complete set of cross sections $\sigma(q, q')$ is given, it is possible to calculate the corresponding equilibrium fractions $F(q)$ from the cross sections without integrating Eq. (2.1). In order to perform that calculation, it is convenient to reduce the redundant system Eq. (2.2.a) by means of the additional equation $\sum_q F(q)=1$. For simplicity, let us assume that the relevant charges are in the range $1<q<r$. When we substitute, for example,

$$F(r)=1-\sum_{q=1}^{r-1}F(q),$$

Eq. (2.2.a) becomes an inhomogeneous system of $r-1$ independent equations which we may describe as follows:

$$\mathbf{CF}=\mathbf{G}. \qquad (2.4.a)$$

Here $\mathbf{C}$ represents a square matrix of full rank $r-1$, and $\mathbf{F}$ and $\mathbf{G}$ are vectors with $r-1$ components:

$$C_{qq'}=\begin{cases}\sigma(q', q)-\sigma(r, q); & q\neq q'\\ -\sigma_t(q')-\sigma(r, q); & q=q'\end{cases}; \qquad G_q=-\sigma(r, q), \qquad (2.4.b)$$

and $\mathbf{F}$ contains the first $r-1$ equilibrium charge state fractions which may be written in the form

$$\mathbf{F}=\mathbf{C}^{-1}\mathbf{G}. \qquad (2.5)$$

The inverted matrix $\mathbf{C}^{-1}$ can be obtained by means of standard routines; in the present case, the inversion is particularly simple because all diagonal elements in $\mathbf{C}$ are different from zero.

An important quantity is the average or mean equilibrium charge which is defined by

$$\bar{q}=\sum_q qF(q). \qquad (2.6)$$

The values of $\bar{q}$ are generally not integers. In case of symmetrical distributions, $\bar{q}$ coincides with that charge $\hat{q}$ for which the smoothed curve $F(q)$ assumes its maximum. The charge associated with the most intense fraction has often been referred to as the most probable charge; we will not make use of that notation because it may lead to ambiguities, especially in the case of very broad distributions. Another characteristic parameter is the width of a charge distribution which is defined by

$$d=[\sum_{q'}(q'-\bar{q})^2F(q')]^{1/2}. \qquad (2.7)$$

In case of a precise Gaussian distribution, d is related to the full half-width h, and to the full e^{-1}-width, Γ, by

$$h=d(\ln 2)^{1/2}; \qquad \Gamma=2d\sqrt{2}. \qquad (2.8)$$

Charge distributions are not always symmetrical. As a measure of the degree of asymmetry, it is convenient to define a skewness parameter of the distribution

$$s=\sum_{q'}(q'-\bar{q})^3F(q')/d^3, \qquad (2.9)$$

where $\bar{q}$ and d denote the average charge and distribution width defined in Eqs. (2.6) and (2.7), respectively.

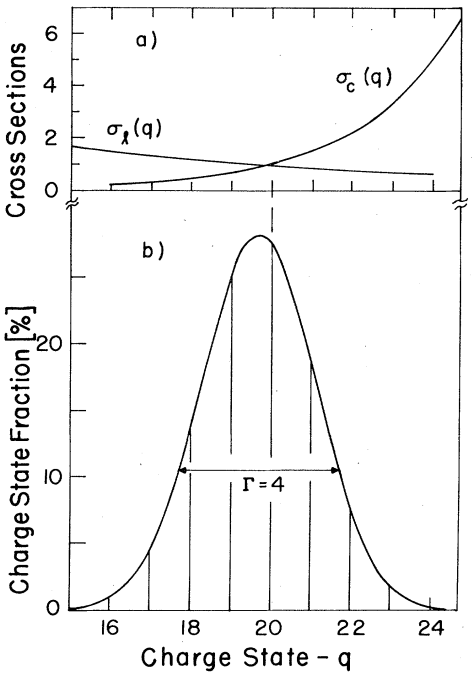

FIG. 2.3. (a) Hypothetical cross sections for capture and loss of a single electron, taken from Eq. (2.10) with $b_c=0.4$, $b_l=0.1$, and $q_x=20$; (b) corresponding Gaussian equilibrium charge state distribution which is centered symmetrically around $q_0=19.7$ and has a width $d_0=1.43$.

3. Relations between Charge-Changing Cross Sections and Equilibrium Charge State Distributions

It has been demonstrated in Sec. II.3 that simple procedures allow equilibrium charge state distributions to be calculated from a given set of cross sections. The reverse procedure cannot be carried out. Still, an equilibrium distribution reflects certain trends of the underlying cross sections. In the following, we will discuss the problem of drawing conclusions on cross sections from a given equilibrium distribution. This is of practical significance because it is much easier to measure equilibrium distributions than complete sets of charge-changing cross sections.

A known distribution $F(q)$ reflects only certain combinations of ratios of cross sections, not their absolute values. For example, when only single capture and loss is considered, $F(q)$ allows one to deduce directly ratios of capture and loss cross sections from Eq. (2.3). No such simple relation holds when multiple-electron capture and loss cross sections are present. However, since heavy-ion cross sections $\sigma(q, q\pm n)$ are found to show remarkable regularities, especially in their dependence on q and n, one expects to find some general relations at least for $\bar{q}$, d, and s which represent good approximations in many practical cases. We will present such relations derived from the study of those mathematically simple systems of cross sections which, for the present limited purpose, are acceptably near to real systems of cross sections.

Let us assume that cross sections for capture and loss of a single electron can be represented by curves of exponential form

$$\sigma(q, q-1)=A_c \exp[b_c(q-q_0)],$$
$$\sigma(q, q+1)=A_l \exp[-b_l(q-q_0)]. \quad (2.10)$$

Provided that we choose $A_c=A_l \exp[(b_l-b_c)/2]$, it can be shown (Bell, 1953) that Eq. (2.10) yields a Gaussian equilibrium distribution around q_0,

$$F(q)=(2\pi d^2)^{-1/2} \exp[-(q-q_0)^2/(2d^2)], \quad (2.11)$$

where the width depends only on the sum of the two parameters b_c and b_l,

$$d=(b_c+b_l)^{-1/2}. \quad (2.12)$$

Due to the symmetry of $F(q)$, the mean charge is equal to q_0 and, since $F(q)$ is Gaussian, $\bar{q}$ is related to the root-mean-square charge by $\overline{q^2}-(\bar{q})^2=d^2$. When $b_c\neq b_l$, the symmetry of $F(q)$ remains unaffected, but the charge q_x, for which σ_c and σ_l are of equal magnitude, differs by a relatively small amount from q_0, given by

$$q_0-q_x=(b_c-b_l)/[2(b_c+b_l)]. \quad (2.13)$$

Figure 2.3 shows a schematic example of cross sections and resulting equilibrium charge state distributions for $b_c=0.4$, $b_l=0.1$, and $q_x=20$. As a next step, we take into account multiple cross sections. Let us assume that the cross sections for transfer of n electrons amount to a fraction of the corresponding cross sections for single-electron transfer which is independent of the initial charge. Thus, we may write ($k_n^c<1$, $k_n^l<1$)

$$\sigma_c(q, q-n)=k_n^c\sigma_c(q, q-1),$$
$$\sigma_l(q, q+n)=k_n^l\sigma_l(q, q+1), \quad (2.14)$$

where the constants k^c and k^l depend only on n. The effects of multiple cross sections on the equilibrium distribution are threefold. First, the average charge will be shifted by a certain amount $\Delta\bar{q}_0$; second, the distribution width may be increased by a factor $\bar{k}$; and third, $F(q)$ may become asymmetrical. From Eqs. (2.10) and (2.14) we find, in a good approximation,

$$\Delta\bar{q}_0=d_0^2[\ln(\textstyle\sum nk_n^l/\sum nk_n^c)], \quad (2.15)$$

and

$$d=d_0\bar{k}$$
$$=d_0[\textstyle\sum n^2k_n^l/(2\sum nk_n^l)+\sum n^2k_n^c/(2\sum nk_n^c)]^{1/2}, \quad (2.16)$$

where d_0 refers to the distribution width which is obtained in the absence of multiple cross sections. In Eq. (2.15), the sum over k_n^l and k_n^c covers all multiple-electron transfer processes which are defined in Eq. (2.14). Equation (2.15) implies that multiple capture

cross sections shift $F(q)$ towards lower-charge states, and multiple loss cross sections towards higher-charge states. No net shift results in the particular hypothetical case of capture and loss cross sections for which the two sums in Eq. (2.15) become equal.

The effects of multiple cross sections on the asymmetry of equilibrium distributions depend in a complicated way on all values $k_n{}^c$ and $k_n{}^l$, and are not easily described in detail. However, some general trends are obvious: (i) multiple capture enhances the intensity of charge fractions on the left side, and multiple loss enhances the fractions on the right side of a distribution; the asymmetry increases (ii) when the values of k_n increase, and (iii) when higher values of n are taken into account. Figure 2.4 illustrates this situation for the particular case in which multiple-electron loss has been considered in the form $k_n{}^l=k_0{}^{n-1}$. Figure 2.4a shows some cross sections for $k_0=0.6$, and Fig. 2.4b presents

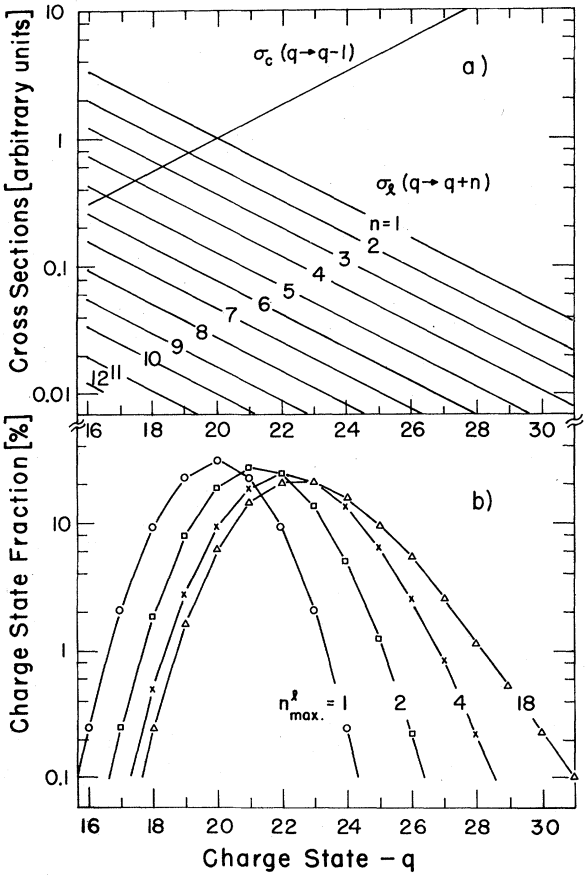

FIG. 2.4. (a) Hypothetical set of charge-changing cross sections for capture and loss of a single electron, taken from Eq. (2.10), with $b_c=b_l=0.3$ and $q_0=20$, and for loss of n electrons, taken from Eq. (2.14), with $k_n=k_0{}^{n-1}$ and $k_0=0.6$. The number n is indicated near each curve. (b) Equilibrium charge state distributions which result from the set of cross sections (a) by taking into account multiple loss for $n\leq n_{\max}{}^l$. Values $n_{\max}{}^l=$ 1, 2, 4, and 18 have been chosen and are indicated near each distribution. The skewness s of the resulting distributions amounts to 0, 0.11, 0.28, and 0.58, respectively.

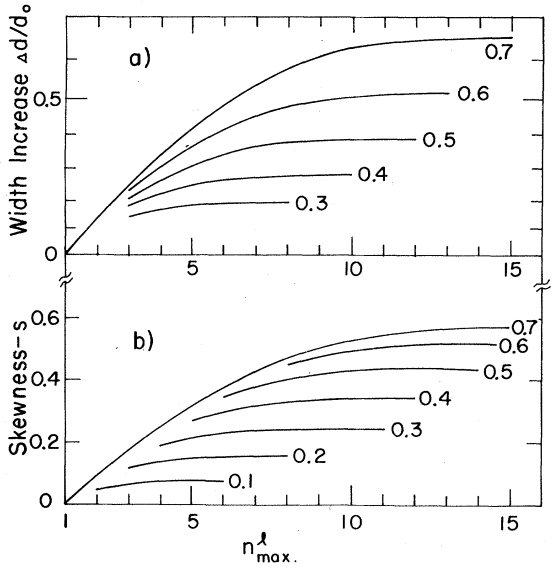

FIG. 2.5. (a) Relative increase of the charge state distribution width, $(d-d_0)/d_0$, and (b) skewness s of equilibrium distributions, as a function of $n_{\max}{}^l$. The associated equilibrium distributions have been calculated from charge-changing cross sections for capture and loss of a single electron, taken from Eq. (2.10) with $b_c=b_l=0.25$, and for loss of n electrons, taken from Eq. (2.14) with $k_n=k_0{}^{n-1}$ and $n\leq n_{\max}{}^l$. Several values of k_0 have been chosen and are indicated near each curve.

the distributions resulting from several maximum values of n, $n_{\max}{}^l$. The width increases approximately as given by Eq. (2.16), and the corresponding asymmetry increases with $n_{\max}{}^l$ until it reaches a saturation value which, for $k_0<0.8$, is roughly given by $s\simeq 1.2k_0/d_0$. Figure 2.5 shows these two effects in greater detail. Figure 2.5a shows the relative increase of the width, $(d-d_0)/d_0$ and Fig. 2.5b gives the skewness of the equilibrium charge state distributions as a function of $n_{\max}{}^l$. The significant parameter is the value of k_0, i.e., the relative magnitude of the multiple loss cross sections. It can be seen that very pronounced asymmetries require both k_0 and $n_{\max}{}^l$ to be relatively large, and vice versa. It will become evident from Secs. IV and V that the cases shown here for large values of $n_{\max}{}^l$, though grossly simplified, are quite typical for heavy ions, with the smaller and larger values of k_0 corresponding to light and heavy target atoms, respectively.

Both theoretical and experimental charge-changing cross sections are often approximated by power functions,

$$\sigma_c(q, q-1) \propto (q/q_0)^{a_c},$$
$$\sigma_l(q, q+1) \propto (q_0/q)^{a_l}. \qquad (2.17)$$

Within a suitable range of charge states around q_0, this system of cross sections may be regarded as an approximation of the exponential system, Eq. (2.10), provided that we choose the parameters a_c and a_l in such a way that the derivatives $\partial\sigma/\partial q$ for the two systems become equal at $q=q_0$, i.e.,

$$b_c=a_c/q_0, \qquad b_l=a_l/q_0. \qquad (2.18)$$

Compared with the exponential system, we now obtain ratios $\sigma_c(q)/\sigma_l(q)$ which are smaller for $q<q_0$, and larger for $q>q_0$. It follows from Eq. (2.3) that, compared with a Gaussian distribution, the equilibrium fractions decrease less rapidly on the right side than on the left side. Thus, even in the absence of multiple cross sections, $F(q)$ will show a certain asymmetry which, though very small for higher values of q_0, may be quite pronounced at low values of q_0. The addition of multiple cross sections according to Eq. (2.14) results in essentially the same effects as discussed above for the exponential system Eq. (2.10) with the exception that asymmetries are now somewhat stronger, especially for low q_0. Nevertheless, Eq. (2.12)–Eq. (2.16) will not significantly change and, together with Eq. (2.18), remain useful approximations. Incidentally, it is interesting to note that Eqs. (2.12) and (2.18) imply that, for constant $\bar{k}$, a constant width of an equilibrium distribution can be observed for increasing q_0 only when the sum of the exponents (a_c+a_l) increases linearly with q_0, i.e., when the dependence of the cross sections on the initial charge becomes stronger.

Another useful relation concerns the alteration of given cross sections and the resulting change of the mean charge. When all capture and loss cross sections defined by Eqs. (2.10) or (2.17), as well as all multiple-electron capture and loss cross sections, are changed by a charge-independent factor f_c and f_l, respectively, the average equilibrium charge will shift approximately by

$$\Delta\bar{q}=d_0^2 \ln (f_l/f_c). \tag{2.19}$$

III. EXPERIMENTAL METHODS AND DATA ANALYSIS

1. Apparatus and Experimental Methods

Allison (1958) has summarized a variety of experimental methods which have been used in connection with studies of hydrogen and helium projectiles; and Nikolaev (1965) reviewed the techniques which have been employed by the groups at Moscow and Kharkov in their studies of light ions ($Z\leq 7$) at energies below approximately 10 MeV, and of heavier ions ($Z\leq 36$) below approximately 5 MeV. Most of the recent data on heavy ions up to and including uranium, in the energy range from $\sim$1 MeV to $\sim$180 MeV has been obtained by means of experimental setups based on similar principles, except that tandem Van De Graaff accelerators served as a fast-particle source, and solid state counters as detection devices. For example, Fig. 3.1 illustrates schematically the experimental arrangement for charge state measurements with gaseous and solid targets which has been used, with modifications, by the groups at Heidelberg and at Oak Ridge, and Fig. 3.2, together with Table III.1, shows the apparatus which has been employed by the groups at Burlington and Cambridge. The three fundamental elements of these arrangements are (1) the beam preparation system, consisting of an accelerator producing ions of different charge states, and a charge monochromator to select ions of a unique charge state; (2) the target, consisting of either a pumped cell containing the target gas, or of provisions to insert foil targets into the beam; and (3) a detection system, consisting of an anlyzer to separate the beam emerging from the target into the various charge state components, and a detector system to determine the relative intensities of the charge state components. Some details of these elements which are relevant to the measurement of charge state distributions will be discussed in the following three sections.

a. Beam Preparation

Preparation of a suitable heavy-ion beam requires considerable effort with regard to ion sources, acceleration, and beam handling system. Fundamental implications arise from the fact that heavy ions readily change their ionic charge during and after acceleration even in glancing collisions with atoms. This feature of heavy ions causes many experimental difficulties, but it can also be exploited in various ways. Mainly under that aspect, we will describe procedures which have been used most frequently in order to obtain beams of specific masses and energies from tandem Van de Graaff accelerators.

In the conventional operation of tandem accelerators (Almqvist *et al.*, 1962; Rose *et al.*, 1965), negative ions, i.e., negative single atoms or more complex negatively charged molecules are accelerated through the first half of the machine. At the high-voltage terminal at the center of the accelerator, the ions pass through a stripper target which consists of either a windowless gas target or a foil, and emerge in various positive charge states q_A. In the second half of the accelerator, ions with different q_A gain different energy, and a discrete spectrum results containing energies $E(q_A)=U(1+\delta+q_A)$, where U denotes the terminal voltage, and δ is a small correction which depends on preacceleration and composition of the injected negative ions. However, the discrete energy spectrum is generally superimposed by a continuous one. Some ions may undergo additional charge-changing collisions in the residual gas anywhere along their path during the second half of acceleration which, on the average, increases their charge and, thus, increases their energy by variable amounts. On the one hand, this continuous spectrum is not desired in the normal mode of operation. On the other hand, since its relative intensity increases when heavier ions are accelerated, one may choose to enhance it even more by admitting small amounts of gas throughout the second half of the acceleration system. This procedure is called continuous stripping (Moak *et. al.*, 1963) and has the advantage of producing small beams of significantly increased energy. An example of an energy spectrum of that kind is shown in Fig. 3.3. The groups at Oak Ridge and Heidelberg have frequently applied

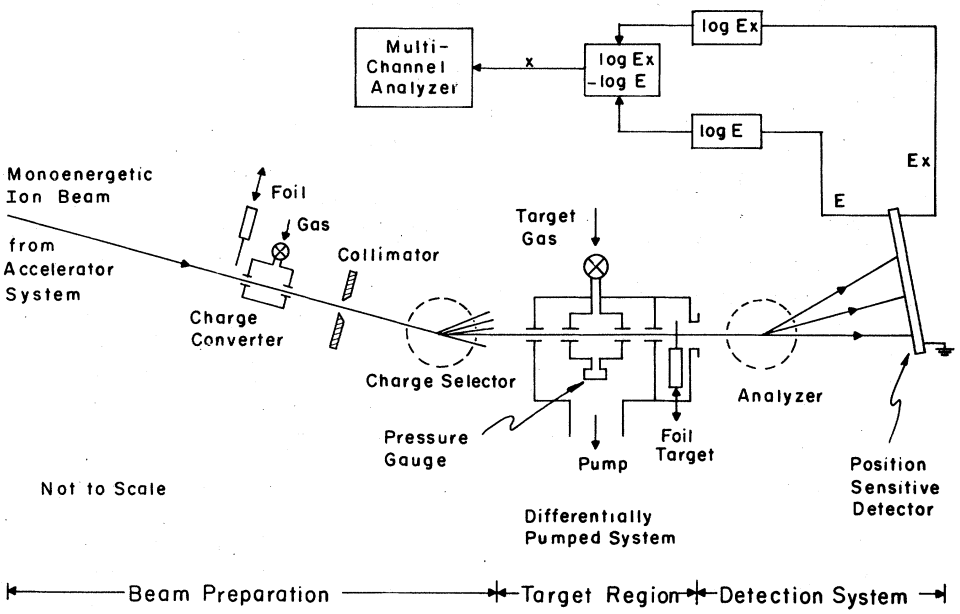

FIG. 3.1. Principal elements of the experimental arrangements used by the groups at Oak Ridge (Moak *et al.*, 1968) and Heidelberg (Beltz *et al.*, 1966; Angert *et al.*, 1968; and Möller *et al.*, 1968) for charge state measurements with gaseous or solid targets.

that technique in order to accelerate heavy ions up to energies of ~100 MeV though the maximum terminal voltage of their machines was less than 7 MV. An alternative which has sometimes been used to obtain higher charge states and, thus, higher energies is to insert one or more additional foil strippers into the path of the beam in the second half of the acceleration (Grodzins *et al.*, 1967).

The entire accelerated beam is directed into a magnet which filters out particles of constant rigidity, $mE/q^2=$ constant. In most cases, this eliminates all mass impurities in the beam which were not removed from the injected beam, or which result from the breakup of injected complex negative molecules in the terminal stripper. For the desired mass, the deflected beam then contains a spectrum of discrete energies, $E(q) \propto q^2$. In the presence of continuous stripping, the beam contains a large number of these energies, but in its absence a monoenergetic beam can be obtained. It is obvious, however, that magnetic selection alone does not guarantee a unique mass. Final discrimination, if required, can be achieved either by means of additional electrostatic deflection which is proportional to E/q, or electronically in the detector system.

TABLE III.1. Dimensions and pumping characteristics of the differentially pumped gas cell which is shown in Fig. 3.1; from Ryding *et al.* (1969b).

Apertures (circular)	Diameter	Length
A_2 outer cell entrance	1 mm	Knife edge
A_3 inner cell entrance	0.5 mm	Knife edge
A_4 inner cell exit	1.2 mm	2.2 mm
A_5 outer cell exit	2.5 mm	5.0 mm
A_6 movable outer cell exit	0.2 mm	Knife edge
Inner cell length (inside dimension)	2.83 cm, 3.65 cm	
Outer cell length (inside dimension)	13.5 cm	
Maximum beam divergence from inner cell entrance	±20 mrad	
Pumping speed of P_1	300 liter/sec	
Pumping speed of P_2	800 liter/sec	
Base pressure above P_2	$\sim 2\times10^{-7}$ Torr	
Pressure rise above P_2 at 1 Torr inner cell pressure	3×10^{-6} Torr	

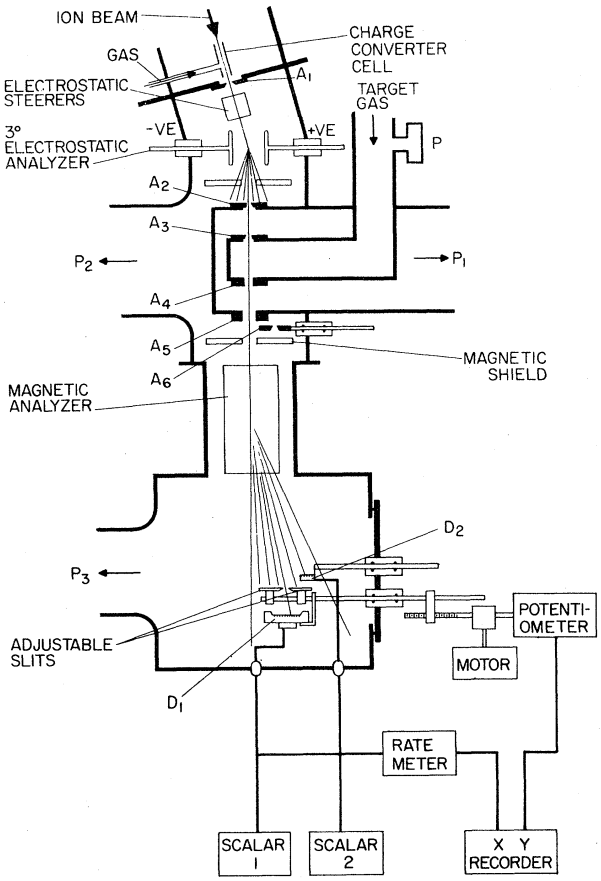

FIG. 3.2. Experimental apparatus used by the Burlington group (Ryding *et al.*, 1969b) for charge state measurements with gaseous or solid targets. Detailed characteristics of the differentially pumped gas cell are listed in Table III.1.

Of critical importance is the stability of the beam. Effects of continuous stripping, charge exchange in the beam line between accelerator and target, and scattering on apertures in the beam line may contribute to production of secondary beams with a broad range of rigidities. Difficulties in stabilizing a beam of small intensity may arise when this beam is a spatially close neighbor of a secondary beam of different energy but of relatively high intensity. Continuous and careful observation of the actual beam is then imperative. Preferably, the beam line should be kept under a vacuum which is sufficiently high to reduce most of the undesired charge exchange in the residual gas.

It is often desirable to vary the charge of the incident beam particles within a considerable range without affecting the energy. The availability of many different initial charge states is essential for accurate and comprehensive cross section measurements (see Sec. III.2), and provides a practical test of charge equilibrium by establishing the independence of a charge distribution of the incident charge state (see Sec. II). There are limited possibilities for selection of these charge states by choosing different parameters for the acceleration process. In certain experiments, this procedure has the advantage that the distance between the location where the charge states are produced and the target cell can be made very long. Thus, ions which are formed in an excited state at the high-voltage terminal have a good chance to de-excite to the ground state before they enter the target cell. However, instead of changing the many acceleration parameters, it is usually more convenient to produce the desired initial charge states in a charge converter cell which is located in front of the actual target cell (Fig. 3.1.). The charge converter consists of a windowless gas cell into which small amounts of gas are admitted. A significant extension of the resulting charge spectrum to higher-charge states is obtained when the gas target is replaced by a foil; this technique has been employed by the Heidelberg group. The desired charge state is then filtered out by a charge selector and passed on to the target cell. At Oak Ridge, the ions were selected by a beam-switching magnet; the groups at Heidelberg and at Burlington utilized a 15° and 3° electrostatic deflector, respectively.

When only equilibrium charge state fractions are to be measured, a variation of the incident charge is not imperative though it may be of practical value for testing charge equilibrium. In the case that charge converter and selector are not part of the setup, it becomes possible to investigate charge distributions for different energies simultaneously. The accelerated beam is filtered only by a magnet so that it contains ions with a number of energies $E(q) \propto q^2$ which are all passing through the target. Energy discrimination is easily achieved with solid state detectors (see Sec. III.1.c). This technique, combined with continuous stripping in the accelerator, has been employed by the Heidelberg group in an early series of equilibrium charge state measurements (Betz *et al.*, 1966).

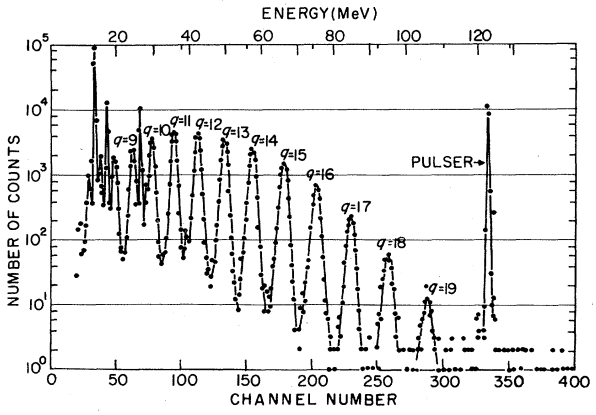

FIG. 3.3. Pulse height spectrum of iodine ions stripped continuously in the Oak Ridge 7-MV tandem van de Graaff accelerator. The ions are deflected through a 90° magnet onto a silicon surface barrier detector; from Moak *et al.* (1963).

b. Targets

Solid targets. A variety of solid targets ranging from beryllium to uranium compounds have been used for the measurement of heavy-ion charge state distributions. In the majority of the cases, the foils were self-supporting but thin enough not to produce excessive energy loss or scattering of the beam particles. Experience has shown that even the thinnest available foils were usually thick enough to establish at least approximate charge state equilibrium of heavy ions. This implies that measurements of charge state nonequilibrium is severely hindered if not impossible. However, it has been consistently observed that the equilibrium thickness, x_∞, increases with the energy of the projectiles. For example, in a carbon foil, x_∞ increases for bromine ions from ~ 5 $\mu g/cm^2$ at 40 MeV to ~ 25 $\mu g/cm^2$ at 140 MeV (Moak *et al.*, 1967, 1968). Equilibrium conditions are verified when either different incident charge states or foils of different thickness produce identical charge distributions. Obviously, the latter technique is unsatisfactory when foils are so thick that the energy loss is significant and leads to a noticeable reduction of the mean charge. Incidentally, when only relatively thick foils are used, the measured charge distribution should be associated with the energy of the emergent beam. Effects of multiple Coulomb scattering are usually ignored, but they become significant for thick and heavy target materials, and may render the resolution of adjacent charge states difficult. For the design of such experiments it is often useful to estimate the mean scattering angles; this can be performed, for example, by means of either the statistical theory of Williams (1939, 1940), as discussed by Bethe and Ashkin (1953), and Cline *et al.* (1969), or the classical theory by Meyer (1971). The latter work contains useful comments concerning the applicability of various theories for multiple and plural scattering of heavy ions.

Effects on equilibrium charge state distributions due to surface contaminations or to aging of foils have not been reported; this is in marked contrast to the results of investigations of light projectiles at low energies (Allison, 1958). With regard to the lifetime of foils, it is important to note that heavy-ion beams have far more damaging effects than light-ion beams. Heavy-ion currents of $\gtrsim 1$ μA usually destroy thin foils within minutes. However, intensities of accelerated heavy ion beams are mostly of the order of nA or less and, especially when solid state detectors are employed, intensities on the target must not be excessive; a typical rate might be $\lesssim 10^5$ particles/sec. Such low-beam currents do not affect the performance of foils during many successive experiments.

Gaseous targets. The large probabilities for charge exchange of heavy ions in even the thinnest self-supporting foils make it impossible to separate a gaseous target by foil windows from the high vacuum in the beam line. Thus, windowless differentially pumped systems are being used, as is shown in Figs. 3.1 and 3.2. Pressure gradients can be attained which are sufficiently high to allow pressures in the central target cell to rise to ~ 1 Torr without having serious effects on the vacuum in the beam line. Figure 3.2 and Table III.1 describe in detail the system which has been used by the Burlington group (Ryding *et al.*, 1969b). The thickness of a gas target is given by

$$x = NLP/(RT) \qquad [\text{molecules/cm}^2], \qquad (3.1)$$

where N is Avogadro's number, L the cell length, P the target gas pressure, R the gas constant, and T the temperature of the target gas. For $T = 15°$, Eq. (3.1) becomes

$$x = 3.35 \times 10^{16} LP \qquad [\text{molecules/cm}^2], \qquad (3.2)$$

where L is in centimeters, and P in Torr. Due to the gas flow out of the apertures of the cell system, a certain correction ΔL must be contained in L. For the setup used by the Burlington group, where L ranged from 2.83 cm to 3.65 cm, ΔL was determined carefully, and was found to amount to only 0.1 cm (Ryding *et al.*, 1969a).

Thicknesses of a few $\mu g/cm^2$ are usually sufficient to produce charge state equilibrium in low-energy heavy-ion beams ($E < 100$ MeV). For 15-MeV iodine ions in oxygen, x_∞ is less than 0.5 $\mu g/cm^2$ (see Fig. 2.1). Consequently, scattering of the beam is seldom excessive and charge states are easily separated (see Fig. 3.4). The Oak Ridge group worked with cells of effective lengths between 12 cm and 168 cm, and the Heidelberg group used $L = 20$ cm and 110 cm. The use of long cells was partly motivated by the attempt to exclude effects of residual ion excitation. It happened, however, that atomic lifetimes of ions excited in charge-changing collisions are often long enough to influence charge state measurements even in long cells (see Sec. VI.1.d).

When suitable needle valves are utilized to admit the target gas, it is no problem to adjust the pressure in the cell quickly to a desired value and to keep it constant at that value within, say, 1%. The more critical part is the exact measurement of P; uncer-

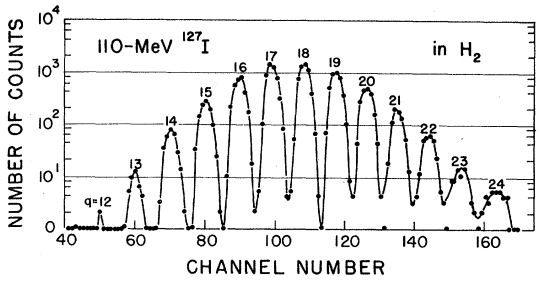

FIG. 3.4. Charge state spectrum of 110-MeV iodine ions stripped in hydrogen at 0.6 Torr in a gas cell of length 50 cm, recorded with a position-sensitive detector, 2 cm in length. The abscissa gives the deflection of each charge component in the analyzing electric field; from Moak *et al.* (1968).

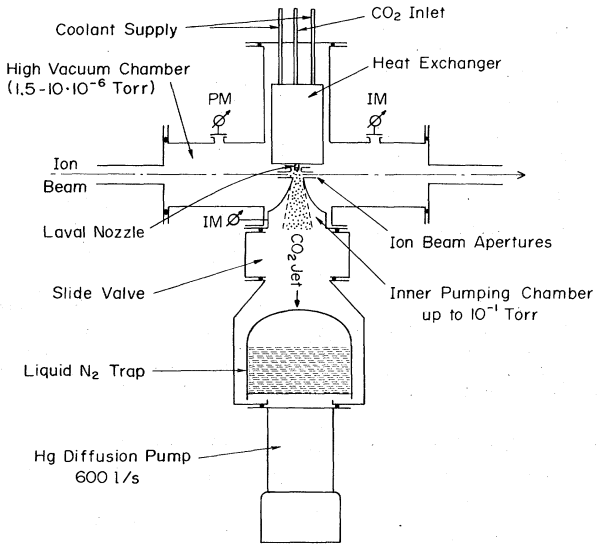

FIG. 3.5. Apparatus for a transverse supersonic jet target of carbon dioxide; from Franzke *et al.* (1972).

tainties in P are directly reflected in experimental cross section values. In the range above $\sim 2\times 10^{-4}$ Torr capacitance diaphragm-type differential pressure gauges can be used to determine P with an accuracy of better than $\sim 3\%$ (Utterback and Griffith, 1966). Systems of that kind have been employed by the groups at Oak Ridge and Burlington.[1] Pressures below $\sim 2\times 10^{-4}$ Torr are somewhat more difficult to determine, and with the use of conventional manometers, such as ionization gauges, one must expect errors $\gtrsim 10\%$. The Heidelberg group used Varian nude gauges which are accurate within 5%–10%. Measurements at these low pressures are required mainly when cross sections are to be determined from experiments utilizing long target cells.

In a few cases, investigators have used the gap in a deflection magnet as target gas cell. On the one hand, this technique results in a very complicated charge spectrum which extends continuously across the detector plane. On the other hand, it is an ideal method for the measurement of total charge-changing cross sections. The intensity $Y_q(x)$ of a particular charge fraction is measured at a fixed position in the detector plane, and, for a constant deflecting field, as a function of increasing thickness of the target gas (attenuation method). The resulting exponential decay $Y_q(x) \propto \exp(-\sigma_t(q)x)$ allows one to determine $\sigma_t(q)$ independent of all other charge-changing cross sections $\sigma(q', q'')$ with $q' \neq q$.

Jet targets. Transverse supersonic jet stripper targets are an alternative to differentially pumped gas cells. Their principal advantage is, for most purposes, that a lower vacuum can be maintained in the beam line while the stripper is operated at its highest thickness. Beringer and Roll (1957) constructed a mercury jet and observed an increase in the pressure in the beam line of less than 3×10^{-7} Torr for jet thicknesses up to 20 $\mu g/cm^2$. Assemblies of mercury jets have also been reported by Fogel *et al.* (1956), Dawton (1961), and Bethge and Günther (1964), though these investigations were aimed primarily at the production of negative ions. A water vapor jet has been built by Roos *et al.* (1965), and jets of carbon dioxide, nitrogen, and argon have been tested by Borovik *et al.* (1963) and Busol *et al.* (1964). Charge exchange work on heavy ions has been carried out by the Heidelberg group with jets of mercury and carbon dioxide (Franzke *et al.*, 1967, 1971, 1972). Figure 3.5 shows the apparatus used by Franzke *et al.* (1972). Thicknesses of these jets which have been achieved range up to $\sim 1.5\times 10^{17}$ molecules/cm^2 and are sufficiently high to establish charge state equilibrium for heavy ions at least at energies below ~ 100 MeV. Target thicknesses below $\simeq 4\times 10^{14}$ molecules/cm^2 could not be reached; consequently, charge-changing cross sections have been difficult to measure with these jet strippers.

[1] MKS Baratron (MKS Instruments Inc., Burlington, Massachusetts).

c. Detection System

The charge states in the beam emergent from the target are spatially separated by an analyzer as shown in Figs. 3.1 and 3.2. Both electrostatic and magnetic deflection systems have been used. The detection of the relative number of ions in each charge state group is performed most conveniently by means of solid state surface barrier detectors. These detectors can be employed when the ions have sufficient energy to penetrate through the dead layer on the entrance surface of the detector. Typically, 25 $\mu g/cm^2$ gold layers are used in which fission fragments, for example, lose an energy of ~ 0.5 MeV. Thus, heavy ions with energies higher than a few MeV can be counted with an efficiency of practically 100%—regardless of their incident charge state, including $q=0$. Moreover, the detector signal is proportional in height to the energy of the ions which are deposited in the depleted region. Since one has to consider comparatively short ranges, the detector serves as a useful heavy-ion energy spectrometer even when the depleted zone is of modest depth. In all cases reported, the energy resolution of these detectors was high enough to discriminate the incident beams with preselected distinct energies (see Sec. III.1.a). An important limitation in the use of solid state detectors in heavy-ion work is their susceptibility to radiation damage under heavy ion bombardment. Usually, the tolerable maximum exposure amounts to $\sim 10^8$ events/cm^2. This makes it imperative to monitor the detector signals constantly during the runs in order to detect the development of dead spots on the detector surface, which reduce the counting and energy discrimination efficiency and should be avoided.

Figure 3.2 shows how two silicon detectors D1 and D2 were used by the Burlington group in order to measure the relative intensity of the charge components in a

beam. One charge fraction at a time is detected with D1, but in order to perform the correct normalization independent of beam intensity fluctuations, another fraction is recorded simultaneously with D2 (Ryding *et al.*, 1969b). One advantage of that technique is that very small fractions can be measured with high precision and without accumulating the excessive number of counts from very intensive charge components. This is of particular importance for the measurement of extremely small charge changing cross sections.

A very significant version of solid state detectors are the position sensitive detectors which give both a signal proportional to the ion energy, $S_1 \propto E$, and simultaneously a signal proportional to the position of ion impact relative to one end of the sensitive detector area, $S_2 \propto Ex$.[2] The main advantage of these detectors is that entire charge state spectra can be recorded simultaneously, i.e., normalization problems are eliminated and the measuring time is minimized. Figure 3.1 indicates one possible mode of operation. The detector signals are processed in a quotient circuit and the resulting signal $S_3 \propto x$ is fed directly into a multichannel analyzing system. The groups at Oak Ridge and Heidelberg have utilized this technique. Figure 3.4 shows a charge spectrum obtained in the way described for 110-MeV iodine ions; charge states range from 12+ to 24+ and are clearly resolved, though each of the line is broadened because of the relatively poor energy resolution which solid state detectors exhibit for very heavy ions. Except for this, the lines would be almost ten times as sharp. Sufficient position resolution requires the minimum particle energy, $E_{\min}$, to be somewhat higher than in the case in which the detectors are used only as counters. For iodine ions, a realistic value of $E_{\min}$ is approximately 10 MeV. At present, commercially available detectors have a sensitive area as long as 5 cm. A quotient circuit which has frequently been used has been described by Strauss and Brenner (1965), and consists essentially of logarithmic and exponential amplifiers. It is also feasible to record charge state spectra simultaneously for different ion energies by exploiting the energy resolution characteristics of the detector and by utilizing a two-dimensional multichannel analyzer. Such a technique has been used by the Heidelberg group in a series of measurements which were aimed at equilibrium charge state distributions. It is also worth noting that a charge spectrum for a particular energy can be recorded without the use of a sophisticated quotient circuit. For example, the signal S_2 can be taken in coincidence with a selected energy signal S_1 or, when only a single energy is present in the beam, S_2 may be used directly as the x signal.

Hvelplund *et al.* (1972) have shown that reasonable position resolution for ions with energies as low as ~100 KeV can be obtained by using an open electron multiplier. They replaced the original collector of an ordinary electron multiplier by a resistive plate, and were able to record as many as four charge states simultaneously.

The accuracy of measured charge fractions is determined mainly by the statistical errors. When as many as 10^4–10^5 counts are accumulated in a particular charge state, the statistical error can practically be neglected; however, fractions with relative intensities below ~1% often have errors as large as 10%. Fluctuations in the thickness of thin targets, or energy loss and effects of scattering from thick targets may give rise to additional uncertainties.

2. Data Treatment and Analysis

We may consider normalized charge state distributions $Y_q(x)$ as the direct experimental information which is provided by the measurement of charge changing processes. No further analysis is required when only equilibrium charge state fractions $F(q)$ are desired, but considerable effort must be spent in order to determine individual charge-changing cross sections $\sigma(q, q')$ of heavy ions from measured nonequilibrium distributions. We will briefly describe some of the aspects which are important for such an analysis.

a. Cross Section Analysis with Least-Squares Techniques

Most investigators have employed approximate solutions of Eq. (2.1) in the particular range of small target thicknesses in which mainly single collision events occur. The principle of such approximations is the following: When a beam is incident in a single charge state q_i, increasing target thickness results in a linear increase in the fractions of the neighboring charge states:

$$Y(q, x) \simeq \sigma(q_i, q)x;$$

where

$$Y(q')|_{x=0} = 1; \quad q' = q_i$$
$$= 0; \quad q' \neq q_i. \tag{3.3}$$

The validity of Eq. (3.3) is restricted to the range $\sigma(q_i, q)x \ll 1$, though some extension may be achieved by taking into account the decrease of $Y(q_i)$ and terms of higher order. Details of this so-called slope method have been critically discussed in a paper by Datz *et al.* (1970). It turned out that this method or a variation of it is often unsatisfactory.

A complete analysis comprises application of the well-known least-squares technique as discussed by Datz *et al.* (1970) and Betz *et al.* (1971a). The values of $\sigma(q, q')$ are determined from that technique in such a way that an exact integration of Eq. (2.1) yields charge fractions which reproduce best the experimentally measured fractions in a least-squares sense. When an arbitrary set of cross sections $\sigma^{(i)}$ is assumed, the corresponding least-squares sum is defined by

$$S = \sum_{m=1}^{m_0} W_m (Y_m - Z_m)^2, \tag{3.4}$$

[2] Available from Nuclear Diodes, Prairie View, Illinois.

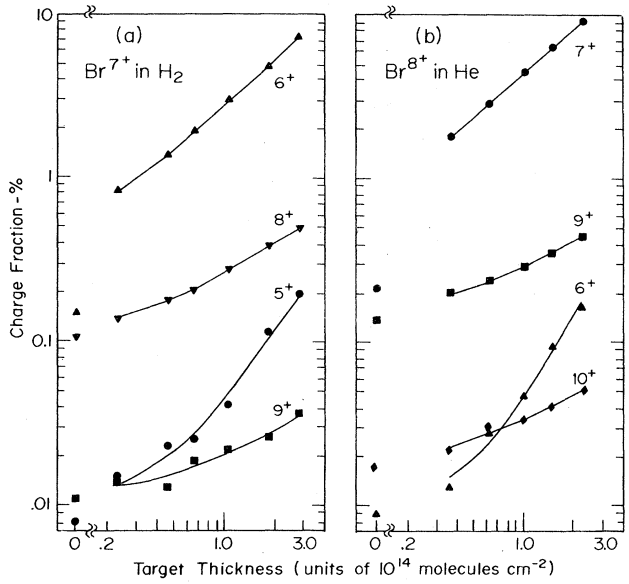

FIG. 3.6. Nonequilibrium charge state distributions for 14-MeV bromine ions passing through hydrogen (a) and helium (b). The incident fractions with charge 7+ and 8+, respectively, are not displayed. The solid lines are calculated from the final set of cross sections and originate, in the analysis, from the data points at target thickness zero; from Betz *et al.* (1971a).

where Y_m and Z_m are the experimental and calculated charge fractions, respectively, and W_m are the weighting factors chosen with respect to the experimental uncertainties of Y_m and x_m. The index m covers all nonzero charge fractions which have been measured for all charge states, target thicknesses x_m, and different nonequilibrium distributions belonging to the same cross section set. When we arrange the relevent n_0 cross sections as a vector $\boldsymbol{\sigma}$, the weights W_m in a diagonal $m_0 \times m_0$ matrix $\mathbf{W}$, and the differences $Y_m - Z_m$ in a vector $\Delta\mathbf{Y}$, minimization of S yields an improved set of cross sections

$$\boldsymbol{\sigma}^{(i+1)} = \boldsymbol{\sigma}^{(i)} + (\mathbf{A}^T\mathbf{W}\mathbf{A})^{-1}\mathbf{A}^T\mathbf{W}\Delta\mathbf{Y}, \qquad (3.5)$$

where the derivatives $A_{mn} = \partial Z_m / \partial \sigma_n$ form a rectangular $m_0 \times n_0$ matrix $\mathbf{A}$. In general, nonlinearities in the system make it necessary to repeat the minimization steps several times. However, more than two or three iterations may be needed only when the initially assumed cross sections differ too much from the best values, or when nonequilibrium distributions cover ranges of higher target thicknesses. Applicability of the least-squares technique is restricted neither by the particular initial conditions $Y_q|_{x=0}$ which are given from the experiment, nor by deviations from a linear increase $Y_q(x) \propto x$ for small values of x. This is important because it is a quite typical observation that charge fractions in general do not increase linearly with x even when x is small. Figures 2.1 and 3.6 illustrates that very clearly.

A decisive advantage of the least-squares technique is that the uncertainties in the determined cross sections are obtained simultaneously with the minimization procedure by

$$\delta\sigma_n^{(i+1)} = [(\mathbf{A}^T\mathbf{W}\mathbf{A})_{nn}^{-1}]^{1/2}. \qquad (3.6)$$

Especially the values of those cross sections which have a minor influence on the nonequilibrium charge distribution can hardly be regarded as a reliable result, without having considered the associated uncertainties according to Eq. (3.6). In such cases, the fact that calculated distributions reproduce the experimental distributions well does not guarantee the correctness of these cross section values. Another useful result of the described least-squares technique concerns the correlation between any two of the cross sections involved, which is described by the coefficients

$$B_{nn'} = [\mathbf{A}^T\mathbf{W}\mathbf{A}]_{nn'}^{-1}[\delta\sigma_n^{(i+1)}\delta\sigma_{n'}^{(i+1)}]^{-1/2} \qquad (B_{nn'} \leq 1), \qquad (3.7)$$

where $\delta\sigma_n^{(i+1)}$ and $\delta\sigma_{n'}^{(i+1)}$ are given by Eq. (3.6). For example, in the case shown in Fig. 3.6.a of bromine ions with initial charge 7+ passing through hydrogen at 14 MeV, the cross sections $\sigma(7, 5)$ and $\sigma(6, 5)$ are strongly correlated with each other, $B = -0.848$, and cannot be determined independent of each other.

b. Cross Section Analysis in the Presence of Residual Ion Excitation

A severe complication in the analysis of heavy-ion cross sections from typical experimentally obtained nonequilibrium charge state distributions arises from the fact that the conditions for having a dilute target gas are not fulfilled. It happened that lifetimes of excited heavy ions are often almost two orders of magnitude longer than was anticipated on simple theoretical grounds (see Sec. VI.1). Thus, cross sections associated with excited states of the ions must be taken into account and their influence must be expected to increase with increasing density of the target gas. This implies that the cross sections in Eq. (2.1) are no longer constant and, instead, depend on x. Though Eq. (2.1) is then invalid, we indicate two cases in which it remains useful without formal changes.

A first possibility consists in evaluating a single nonequilibrium distribution measured at low target densities. The least-squares fit yields well-defined cross sections $\sigma(q_i, q)$ which refer to the particular state of excitation of the incident ions, not necessarily identical with the ground state. However, some of these cross sections are correctly obtained only when other cross sections $\sigma(q', q'')$, which are associated with an average excitation of ions with charge q' formed inside the target cell, are determined from the same fit. We illustrate that situation by discussing the example which is shown in Fig. 3.6a. The incident bromine ions with charge 7+ have been formed in the terminal of the accelerator and traveled a sufficiently long path

($\sim 10^3$ cm) to allow radiative de-excitation before entering the target cell. Thus, the resulting cross sections $\sigma(7, q')$ refer to the ground state of Br^{7+}. In contrast, the value obtained for $\sigma^*(6, 5)$ from the same data set reflects added contributions from excited states. Nearly all ions with charge 6+ have been formed inside the target cell by electron capture, often into excited states. The related lifetimes are indeed long enough so that those ions of charge 6+ which pick up another electron in the target cell may still be substantially excited when that second collision $6+\rightarrow 5+$ occurs. Consequently, $\sigma^*(6, 5)$ refers to a certain average excitation of the Br^{6+} ions. Since $\sigma^*(6, 5)$, in the example considered, is strongly correlated with $\sigma(7, 5)$, it is essential to include $\sigma^*(6, 5)$ as a free variable in the least-squares fit, in order to obtain a reliable result for $\sigma(7, 5)$. On the one side, it is not justified to perform the fit by neglecting second-order processes, i.e., $\sigma^*(6, 5) = 0$; this would lead to a value of $\sigma(7, 5)$ which is too high. On the other side, one can not assume that $\sigma^*(6, 5)$ is equal to the value $\sigma(6, 5)$ which has been determined from a separate fit of a nonequilibrium distribution, where ions with $q_i = 6$ were incident in states with an average excitation close to zero; this would lead to a value of $\sigma(7, 5)$ which is too small. Incidentally, in the case discussed, $\sigma^*(6, 5)$ and $\sigma(6, 5)$ were found to be 1.40 and 2.66×10^{-16} cm^2/molecule, respectively. This example is quite typical for heavy ions and demonstrates the difficulty of determining relatively small cross sections for double capture.

A second possibility of using Eq. (2.1) in the presence of residual ion excitation has been discussed by Ryding *et al.* (1970c). They performed a least-squares fit of nonequilibrium distributions in a small range of densities and interpreted the constant cross sections in Eq. (2.1) as average effective cross sections, σ_{eff}. Then, by applying the same procedure consecutively to other density ranges, it was possible to determine σ_{eff} as a function of the residual ion excitation (see Sec. VI.1).

IV. CROSS SECTIONS FOR ELECTRON CAPTURE AND LOSS

Charge-changing cross sections for electron capture and loss by fast heavy ions in collisions with target atoms or molecules provide the fundamental basis for all accurate and compact descriptions of ionic charge states which are produced in ion–atom encounters. Numerous investigators have devoted considerable effort to the calculation and measurement of these cross sections. While reasonable agreement could be obtained between theory and experiment in the simplest cases, such as for protons moving through atomic hydrogen, the processes involved in the capture and loss of electrons by heavy ions are in general so intricate as to defy precise and comprehensive description. The major part of the theoretical treatments has been based on simplified models and relatively arbitrary assumptions. It is not surprising, therefore, that these models can claim only approximate validity in restricted regions of the basic parameters Z, v, q, and Z_T. However, most theories were developed prior to 1956, i.e., at a time when practically no experimental information on heavy-ion cross sections was available. It may be expected that future theoretical studies will benefit from the many experimental results which have accumulated since then. In Sec. IV.1, we outline briefly some of the important existing approaches which give useful insight into the processes associated with charge-changing collisions and which make important contributions to our understanding of these complex phenomena.

Experimental work on charge-changing cross sections of heavy ions has intensified in recent years. To date, most of the measurements have been carried out with bromine and iodine projectiles with extensive variations of the parameters q, v, and Z_T. These and other available data are presented in Sec. IV.2, along with a discussion of the trends, and relations to theory.

1. Theoretical Studies

The first extensive theory about cross sections for electronic charge exchange was presented by Bohr (1948). He derived analytical expressions for capture and loss of an electron by light and heavy ions passing through both light and heavy target gases. Bell (1953) computed numerically, on a classical basis, cross sections for electron capture and loss by typical fission fragments stripped in light and heavy gases at low densities. In a refinement of Bohr's work, Bohr and Lindhard (1954) attempted on the basis of simple classical and statistical arguments to give a comprehensive interpretation of capture and loss by highly charged heavy ions. Gluckstern (1955) modified Bell's model in order to calculate cross sections for ions of intermediate atomic number, $8 \leq Z \leq 18$, passing through various dilute gases.

All of these authors realized the complexity of the charge-changing phenomena, and their theoretical treatments are usually based on physically reasonable but relatively arbitary assumptions. It must be expected, therefore, that the application of these theories is limited and, as later experiments have shown, that many of the suggested models need substantial modifications. For example, all of the theoretical calculations mentioned above have been limited to capture and loss of a single electron. The possibility of multiple-electron transfer in single collisions has been realized, but it has generally been assumed that the probability for these events is very small. However, experiments have shown that multiple-electron loss occurs with relatively high probability; typically, the cross section for removing more than one electron in a single encounter is often larger than the single-electron loss cross section. This must be taken into account when experimental cross sections are compared with theoretical ones. In all theoretical approaches, orbital electron velocities play an essential role. However, the considerable ambigu-

ities which arise from the difficulties in defining these velocities in multi-electron ions have generally not been taken into account.[3] In the following discussion, we concentrate on charge exchange by ions which are initially in the ground state; the effects of residual ion excitation on charge-changing collisions of heavy ions will be treated separately in Sec. VI.

a. Theory of Bohr

In a first and relatively simple case, Bohr (1948) considered loss by fast light ions which move through light media. He argued that, especially when the orbital dimensions of the target electrons are larger than or comparable to those of the electron to be lost from the ion, the ionizing effects of the electrons and nucleus of the target on the ion are approximately independent of each other. Thus, Bohr applies the so-called free collision approximation in which the binding forces may be disregarded, and which is valid when the ion velocity is large compared to v_0 or, more precisely, when $\kappa = b/\lambda\!\!\!^{-} \ll 1$, where $\lambda\!\!\!^{-}$ denotes the de Broglie wavelength divided by 2π of the ion's electron in question, and b is the collision diameter. In the case of particles which repel each other, b represents the minimum distance of approach in a head-on collision, and, in the absence of screening effects, is given by $2e_1e_2/(\bar{m}v^2)$, where e_1 and e_2 are the charges, and $\bar{m}$ is the reduced mass of the colliding particles. Of course, for $\lambda\!\!\!^{-} \gg b$, classical mechanical ideas, such as orbits of the particles during the encounter, completely fail to account for the individual collision effects. Nevertheless, Bohr gives quite an illustrative description, and arrives at a cross section for electron loss,

$$\sigma_l = 4\pi a_0^2 Z^{-2}(Z_T^2 + Z_T)(v_0/v)^2. \tag{4.1}$$

Application of that formula is of course not restricted to light ions as long as the condition $\kappa \ll 1$ is fulfilled. The accuracy of Eq. (4.1) has been studied by Dmitriev and Nikolaev (1963). In the particular case of hydrogen and helium targets, they use the Born approximation which, for the case considered, gives results which are identical to those obtained in the free collision approximation. They assumed in accord with Bohr that their approximation is valid when v is considerably greater than the orbital velocity u of the lost electron, so that the loss cross section can be assumed to be equal to the effective cross section for scattering of a free electron of velocity v by an atom of the medium, accompanied by an energy transfer to the electron which exceeds its binding $m_e u^2/2$. A decisive difference between their theory and the one by Bohr is that they allow for screening of the Coulomb field of the target nuclei by the electrons of the medium. This causes a noticeable reduction of Bohr's loss cross sections, Eq. (4.1), especially when $u \lesssim Z^* v_0$, where Z^* is the effective charge of the target nuclei.

[3] See the discussion in Sec. V.2.c.

When light ions are stripped in targets with intermediate values of Z_T, Bohr points out that the firmly bound electrons and nuclei in the target will, even in close collisions, no longer act independently on the electrons of the ion. Then, by taking into account the resulting screening effects, he finds

$$\sigma_l \simeq \pi a_0^2 Z_T^{2/3} Z^{-1} v_0/v. \tag{4.2}$$

In the case of light ions penetrating through heavy targets, no specific loss cross sections are derived apart from the rough estimate that σ_l is of the order of πa_0^2, and largely independent of Z_T and v.

As regards electron capture, Bohr emphasizes that these processes are more difficult to estimate because at least three particles take part in the exchange of energy and momentum, whereas electron loss is essentially a two-body problem. For the cross section for capture, of an electron bound to a nucleus Z_2, by a nucleus Z_1, the Born approximation gives useful results for $\kappa_1 \ll 1$ and $\kappa_2 \ll 1$ (Brinkmann and Kramers, 1930). However, electron capture by light ions in heavier targets is not readily described by the Born approximation or by means of classical pictures. The principal reason for that, Bohr argues, is mainly that those electrons will be captured which have an orbital velocity comparable with v corresponding to $\kappa \approx 1$. Thus, Bohr applied statistical considerations and represents the capture cross section of, say, alpha particles in heavy targets in the form

$$\sigma_c \sim \sigma' f n_e. \tag{4.3}$$

Here, σ' denotes the cross section for a collision in which the ion transfers an energy of the order of $m_e v^2/2$ to an atomic electron with an orbital velocity u, and is approximated by $\sigma' = 4\pi a_0^2 Z^2 v_0^4/(u^2 v^2)$, provided that the ion can be assumed to be a point charge. The probability that capture results from such a collision is represented by the factor f and amounts, for the case considered, to $f \sim (Zv_0/v)^3$. Furthermore, n_e stands for the number of electrons in a target atom with orbital velocities close to u, and is given, on the basis of a statistical model, by $n_e = Z_T^{1/3} u/v_0$. Consequently, for $u \simeq v$, Eq. (4.3) becomes

$$\sigma_c \sim 4\pi a_0^2 Z^5 Z_T^{1/3} (v_0/v)^6. \tag{4.4}$$

Nikolaev (1957, 1965) applied the statistical concept Eq. (4.3) to nitrogen ions stripped in hydrogen, nitrogen, and argon, and arrived at expressions which differ somewhat from Eq. (4.4).

Compared to light ions, capture and loss of heavy projectiles present a more complicated situation. This difference is largely due to the fact that heavy ions, though highly charged, carry a large number of bound electrons. In addition, contrary to previously discussed cases, highly charged ions may bind electrons in states with orbital velocities $u > v$. An important part of Bohr's theory is the following argument: on the one hand, collisions with the target atoms will most likely result in the removal of electrons with $u \lesssim v$, but loss of

electrons with $u \gg v$ is impossible, as he claims, or at least very improbable. On the other hand, electrons are readily captured into states of orbital velocities $u \gtrsim v$, but capture into states with $u \ll v$ is very improbable. This implies that a heavy ion on the average carries a number of bound electrons approximately corresponding to the number of electrons in the neutral projectile for which $u > v$ (see also Sec. V.1).

In his estimate of the loss cross section of heavy ions in light targets, Bohr uses the above arguments and finds, in analogy to Eq. (4.1)

$$\sigma_l \sim 4\pi a_0^2 Z^{1/3} Z_T^2 (v_0/v)^3. \tag{4.5}$$

In estimating σ_c, Bohr relies on analogies to the reverse case, i.e., to capture of light ions in heavy targets. Utilizing the symmetry of Brinkmann and Kramers' expression with regard to Z and Z_T, Bohr interchanges Z and Z_T in Eq. (4.4), and approximates

$$\sigma_c \sim 4\pi a_0^2 Z^{1/3} Z_T^5 (v_0/v)^6. \tag{4.6}$$

Finally, in heavy targets, Bohr assumes that capture or loss are likely to take place whenever ion and target atom interpenetrate in a collision. Considerations of radial extensions lead to a symmetrical expression

$$\sigma_l \sim \sigma_c \sim \pi a_0^2 (Z^{1/3} + Z_T^{1/3}) (v_0/v)^2. \tag{4.7}$$

b. Theory of Bell

Bell (1953) computed numerically, on a classical basis, cross sections for capture and loss of a single electron by fission fragments passing through dilute gases of hydrogen, helium, oxygen, and argon. Since he was most interested in ratios of cross sections in order to obtain average equilibrium charge states, he treats capture and loss by similar methods, thereby expecting certain cancellation of errors inherent in his methods. He emphasizes, however, that an approach different from the classical one might be better justified.

As regards electron capture, Bell argues that a perturbation or Born approximation method is not valid, since the charge states of the heavy ions are of the order of the atomic number of the heavy target atoms. On the basis that electrons will be captured in fairly high quantum states, he chooses a classical approach. In considering the possible capture of any electron, he ignores the polarization effect of the ion on the gas atom until the force exerted by the ion on the electron to be captured becomes equal to the force binding the electron in the atom. Thereafter, when the electron is liberated, he ignores the interaction of the electron with the atom and considers the newly liberated electron to be captured only if its total energy in the rest frame of the ion is negative. Space and velocity distributions of the target electrons are calculated from the statistical model by Fermi and Thomas, and the total capture cross section is obtained by summing over all individual capture cross sections for each target electron.

Some consequences of Bell's procedure are quite illustrative. First, electrons are preferentially captured when their initial orbital velocities are close to the ion velocity. This implies, as in Bohr's theory, that lightly bound electrons are seldom captured by fast heavy ions. Second, the electronic structure of a gas atom disintegrates as the ion passes by. For example, when a typical uranium fission fragment collides with an oxygen atom, the fragment liberates the first electron in the atom at a distance of $\sim 10 a_0$; for an impact parameter of $\sim 0.65 a_0$, the atom retains only its K electrons when the most violent part of the collision occurs. Very few of the liberated electrons can be captured by the fragment; most of them will simply escape. Third, total capture cross sections are nearly twice as large in argon as in oxygen (a result due to the number of electrons in the atoms which are available for capture and have $u \approx v$), and tend in general to increase slightly with Z_T, though the increase becomes slower with larger Z_T.

Bell argues that electron loss should preferably be treated by quantum-mechanical perturbation theory. However, since this is too cumbersome to be readily carried out, he discusses a simplified approach and describes the collision between gas atoms and fragment electrons by classical mechanics. He justifies that procedure on the basis of the large quantum numbers of the electrons involved, and because of the coincidence of classical and perturbation methods when the field of the target atom is approximated by means of a Coulomb potential. Thus, he uses the Fermi–Thomas model and calculates the loss cross sections essentially from a detailed consideration of the momentum which is transferred in a collision to an electron of the ion. Apart from the fundamental question of the validity of that classical approach, the resulting loss cross sections depend critically on the assumptions about the effective charge q_T of the target atom during the collision. In a simple interpretation of his results, Bell concludes that an electron is lost from an ion only when it passes the target atom closely enough so that the fragment electron penetrates the remaining electronic structure of the ionized target atom.

In an attempt to calculate cross sections in hydrogen and helium, Bell modifies his theory mainly by taking into account the detailed velocity distribution instead of the Fermi–Thomas distribution of the target electrons. It turns out that weakly bound electrons in light targets are easily liberated at large distances from an approaching ion, but are captured only with difficulty. However, Bell's quantitative treatment of that case is doubtful. Especially in hydrogen, the largely reduced capture cross sections lead to an increase in the average equilibrium charge which is in marked disagreement with experiments.

c. Theory of Bohr and Lindhard

Based on the theoretical treatise on the effects associated with the passage of atomic particles though

matter (Bohr 1948, Sec. IV.1.a), Bohr and Lindhard (1954) presented a comprehensive interpretation of those particular aspects which concern highly charged ions. They argue in accord with Bell, that a rigorous treatment of electron capture and loss processes presents great complications, and apply instead simple mechanical considerations partially based on the circumstance that the binding states in the ion involved in capture and loss are specified by high quantum numbers.

Electron loss is considered as an ionization process, i.e., as being a question of energy transfer to electrons in the ion sufficient for electron escape. According to the free collision approximation discussed in Sec. IV.1.a, the loss cross section for a particular electron is given by the cross section for energy transfer greater than $m_e u^2/2$ in a collision between a free electron at rest and a heavy particle with charge q_T and velocity v,

$$\sigma_l{}^i = 4\pi a_0{}^2 q_T{}^2 [v_0{}^2/(uv)]^2 \{1-[u/(2v)]^2\}, \qquad (u \leq 2v) \tag{4.8}$$

where the upper limit of energy transfer is given by $2m_e v^2$. The total loss cross section per ion is then obtained by summing $\sigma_l{}^i$ over all electrons in the ion with orbital velocities $u \leq 2v$. Bohr and Lindhard estimate the velocity distribution from the simplest Fermi–Thomas model, $dn/dv = A^{1/3}/v_0$, and the integration of Eq. (4.8) yields a more specific loss cross section than the ones given by Bohr in his earlier work [Eqs. (4.5)–(4.7)],

$$\sigma_l = \pi a_0{}^2 q_T{}^2 Z^{1/3} (v_0/v^*)^3, \tag{4.9}$$

where v^* is the orbital velocity of the most loosely bound electron in the ground state of the ion, close to v, and q_T stands for the atomic number Z_T of light gases, or for the effective charge of heavy gas atoms. In the latter case, they interpret q_T as the average equilibrium charge which would result for the projectile when ion and target are interchanged, $q_T = Z_T{}^{1/3} v/v_0$. In order to estimate the dependence $\sigma_l(q)$, v^* is approximated by $v_0 q Z^{-1/3}$, and Eq. (4.8) becomes

$$\sigma_l = \pi a_0{}^2 Z_T{}^{2/3} Z^{4/3} q^{-3} (v/v_0)^2. \tag{4.10}$$

Electron capture is treated in a manner similar to the method of Bell except that they (Bohr and Lindhard) consider only the energy and not also the momentum of the electron, and that the velocity distribution of the target electrons is estimated only roughly from the Fermi–Thomas model. Taking into account the number of electrons with velocities $u \sim v/2$ which can be captured by a heavy ion from a heavy target atom, they develop an expression which is more sophisticated than Bohr's early result Eq. (4.7),

$$\sigma_c = \pi a_0{}^2 Z_T{}^{1/3} q^2 (v_0/v)^3. \tag{4.11}$$

Essentially the same functional dependence may be obtained from Eq. (4.3) where, with $u \sim v/2$, $\sigma' = \pi a_0{}^2 q^2 (v_0/v)^4$, $f=1$, and $n_e = Z_T{}^{1/3} v/(2v_0)$. Nikolaev (1965) emphasizes that the deviation of Eq. (4.11) is based on the assumption that the electron to be captured can be treated as a classical particle having a reasonably well-defined velocity $u \approx v/2$. In view of the uncertainty principle and the relevant orbital dimensions, that assumption is justified only when q is sufficiently high, $q \gtrsim q_c = Z^{1/3} v/v_0$. As a consequence, when this specific estimate for q_c is correct, Eq. (4.11) is invalid just in the range of charge states around $\bar{q}$. However, the criterion for determining q_c is not a sharp one—a fact which precludes the literal interpretation of Nikolaev's estimate for q_c and, like in many other cases, leaves considerable uncertainty as to what range of validity should be practically associated with the theoretical approximation. It is interesting to note that Nikolaev's argument to restrict Eq. (4.11) to $q \gtrsim q_c$, which is approximately equivalent to the condition of having an ion charge which is sufficiently high so that the ion can be treated as a point charge during the collision, implies that σ_c is independent of Z—in accord with Eq. (4.11). However, we will discuss experimental evidence in Sec. IV.2.a which supports the estimate $q_c > \bar{q}$, i.e., Eq. (4.11) is probably inapplicable for $q \simeq \bar{q}$ and, thus, cannot be used in these cases together with Eq. (4.10) in order to describe the balance between electron capture and loss.

As regards electron capture by heavy ions in light target gases, Bohr and Lindhard note in accord with Bell that a concept should be applied which differs from the one used for heavy target gases—otherwise, capture cross sections would become essentially zero. They explain the possibility of capture of very weakly bound target electrons on the basis that electron release is a gradual process, and that it takes a certain time before it can be completed. Thus, there is a *small* chance that a loosely bound electron will remain with the atom until the highly charged ion approaches closely enough so that capture can take place. They give a cursory estimate

$$\sigma_c = \pi a_0{}^2 q^3 (v_0/v)^7 \nu^{*2}/\nu^3 \tag{4.12}$$

where ν^* and ν characterize screening effects in the target atom and an effective quantum number, respectively.

d. Other Theories

Gluckstern (1955) modifies Bell's theory in order to account for capture and loss by ions of intermediate atomic numbers, $8 \leq Z \leq 18$, passing through dilute gases of hydrogen, nitrogen, argon, and mercury. He argues that Bell's capture cross sections are too large because they contain contributions of all electrons in a target atom. One should *not* sum the individual capture cross sections especially in collisions with small impact parameters, but should instead consider, at any impact parameter r_0, the probability of capturing *any* electron. In a rough estimate, Gluckstern accounts for that by

simply reducing the capture cross sections calculated from Bell's original model to 40 percent of their original values. With regard to electron loss from K and L shells, Gluckstern assumes that the electrons in an ion are located in concentric shells with radii chosen to match the known ionization potentials. Then, he obtains the loss cross section from considerations similar to ones employed by Bohr (1948) and Bell, except that he determines q_T on the basis of a classical concept involving the impact parameter. From the resulting cross sections, Gluckstern calculates equilibrium charge state distributions and average charges. He compares his calculations with some experimental results on nitrogen, oxygen, and neon ions by Hubbard and Lauer (1955), Reynolds *et al.* (1954), and Stephens and Walker (1954), and obtains reasonable agreement for $\bar{q}$, but the predicted widths of the distributions are significantly larger than the measured ones. It is interesting to note the observation by Gluckstern that Bell's capture cross sections are independent of Z—a fact which was not explicitly mentioned by Bell—and vary approximately as $\sigma_c \propto q^2/v^{3.5}$.

Nikolaev (1957) pointed out that Gluckstern's method of determining σ_c is inapplicable because it is based on classical concepts which are valid only when $\kappa = 2qv/v_0 \gg 1$. However, in the cases considered, q is low, and v is between $3v_0$ and $6v_0$, so that $\kappa \approx 1$. Nikolaev instead uses Bohr's statistical approach Eq. (4.3) and, by taking into account the effective charge of the ions which is seen by the electron to be captured, derives for nitrogen ions, with charge states between 2 and 4 and velocities between $2v_0$ znd $5v_0$, the somewhat different expression

$$\sigma_c \approx 4\pi a_0^2 q^3 (v_0/v)^6 n_e, \tag{4.13}$$

where $n_e = 1$ in hydrogen and $n_e = Z_T^{1/3} v/v_0$ in nitrogen, argon, or other heavy gases.

In a refined treatment of Massey's adiabatic criterion, Drukarev (1959, 1967) derives an expression for the ion velocity v_m where a maximum of σ_c occurs. He predicts that v_m depends on the energy defect of the collision, $\Delta E = E_i - E_f$, where E_i and E_f approximate the binding energy of the electron before and after its capture. In particular, Drukarev concludes that v_m is proportional to $|\Delta E|$ and $|\Delta E|^{1/2}$ for $|\Delta E| \ll E_i$ and $|\Delta E| \simeq E_i$, respectively. The usefulness of this concept has been experimentally demonstrated by Pivovar *et al.* (1969). However, as has been pointed out by Wittkower and Gilbody (1967), precise application of the simple adiabatic maximum rule is complicated by the fact that the effective value of $|\Delta E|$ for many collisions may be modified considerably by the formation of excited products or by a possible pseudocrossing of the potential energy curves of the initial and final systems.

Nikolaev (1965) notes that Bohr's general conceptions and Massey's adiabatic criterion as discussed by Drukarev (1959, can also be used to explain a maximum in the loss cross section as a function of v. When v is smaller than the velocity u of the electron being removed, σ_l must increase with increasing v because of the adiabatic nature of the collision. For $v > u$, σ_l must diminish with increasing v because the interaction time becomes shorter. Maxima in $\sigma_l(v)$ should therefore lie close to $v = u$. However, it will be shown in Sec. IV.2 that the experimentally observed maxima are substantially shifted to higher values of v, and especially for heavy ions are so broad that it becomes difficult to determine their location. Unfortunately, none of the above theoretical formulas derived for σ_l allows for such a maximum.

Refinements of Bohr's formula Eq. (4.1) have been discussed for the particular case of loss of K electrons by hydrogenlike ions (Dmitriev *et al.*, 1965) and by heliumlike ions (Senashenko *et al.*, 1968). As regards electron capture by bare nuclei with $Z > 1$, Nikolaev (1965) approximates $\sigma_c(Z, Z-1)$ on the basis of theoretical results by Brinkmann and Kramers (1930) and Schiff (1954), and he obtains the useful scaling equation

$$\sigma_c(Z, Z-1) \approx Z^2 [v/(2v_0)]^3 \sigma_p(1, 0) \qquad [Z > v/(2v_0)], \tag{4.14.a}$$

$$\approx Z^5 \sigma_p(1, 0) \qquad [Z < v/(2v_0)], \tag{4.14.b}$$

where $\sigma_p(1, 0)$ is the capture cross section for protons of the same velocity in the same medium. He also notes that Eq. (4.14.a), when Z is replaced by q, should hold for any ion of sufficiently high charge q. Values $\sigma_p(1, 0)$ are available from experimental and theoretical work. Among the extensive literature on charge exchange by protons and atomic hydrogen in gases we give a few of the more comprehensive references: experimental results are contained in reviews by Allison (1958), Allison and Garcia-Munoz (1962), Welsh *et al.* (1967), and in a paper by Toburen *et al.* (1968); theoretical formulations have been presented by Bates and Carroll (1962), Bates (1962), Dalgarno (1964), Nikolaev (1966), and Bates and Mapleton (1967).

Electron capture into excited states. A question of particular interest concerns the states into which electrons are captured by fast heavy ions. Quantum-mechanical calculations of electron capture cross sections have been reported only for simple cases such as protons, helium ions, or hydrogenlike ions passing through hydrogen, helium, and hydrogenlike atoms. For heavy ions, only speculative arguments are available.

It is quite illustrative to discuss briefly the results which have been obtained in the simple cases. Oppenheimer (1928) showed that alpha particles capture electrons from hydrogen atoms mainly into s states with cross sections which, for sufficiently high velocity,

are simply given by

$$\sigma_n = \sigma_1/\nu^3, \qquad (v \gg v_0), \tag{4.15}$$

where ν denotes the principal quantum number. Since capture into other than s states is neglected, Eq. (4.15) implies that capture into the ground state, σ_1, accounts for about 83% of the total capture cross section per ion. In a qualitative picture, capture is much more likely to occur into the $1s$ state than into νs states because the $1s$ electron is more tightly bound and has the larger spread in momentum space. Brinkmann and Kramers (1930) improved Oppenheimer's work but arrived also at Eq. (4.15). Jackson and Schiff (1953) and Schiff (1954) refined the calculations of Brinkmann and Kramers by taking into account the full interaction potential in the Born approximation, and find that for protons passing through atomic hydrogen in the energy range between 25 and 100 keV, i.e., in the range where $\bar{q}$ is close to $\frac{1}{2}$, σ_1 amounts to about two-thirds of the total capture cross section, whereas it approaches Oppenheimer's value at high velocities. In addition, they show that at velocities $v \approx v_0$ capture into the $2p$ state is larger than into the $2s$ state. Bates and Dalgarno (1953) confirm Jackson and Schiff's results and extend the calculations to various other final states of the electrons captured by protons in hydrogen. It has been pointed out by Bates and Carroll (1962) and Dalgarno (1964) that all the calculations mentioned above are still not exact, but are probably good enough to render Eq. (4.15) a useful approximation. Thomas and Bent (1967) measured absolute single-collision cross sections for the formation of various excited states of neutral helium atoms by the impact of 0.15- to 1.0-MeV protons and deuterons, and Thomas (1967) compared the results of that work with theoretical calculations which are based on existing models. Vinogradov and Shevel'ko (1970) performed calculations on the formation of states of hydrogen projectiles excited by electron pick-up in single collisions with complex target atoms and find reasonable agreement with experimental data when electron capture from inner shells is taken into account.

Unfortunately, conclusions have not been extended to collisions which involve partially stripped heavy ions and heavier targets. Bell (1953) states that in those cases electrons will necessarily be captured into fairly high quantum states. Bohr and Lindhard (1954) estimate on general grounds that fast heavy ions capture electrons from light and heavy targets into states of very high and modestly high excitation, respectively. A crude experimental test of the latter assumptions will be discussed in Sec. VI.1.

Radiative electron capture. In the preceding sections we discussed the capture of bound electrons, and we argued that the relevant models do not allow those electrons to be captured which are essentially free. Clearly, these models become unsatisfactory when one takes into account the possibility of radiative electron capture. In such cases, the emission of a photon allows conservation of energy and momentum. Bethe and Salpeter (1957) derived the following total cross section for the capture of a free electron into the $1s$ orbit of a bare nucleus

$$\sigma_R = 9.1\times10^{-21}\left(\frac{E_B E'}{E_\gamma}\right)^2 \frac{\exp\,(-4E'\ \text{arctg}\ E'^{-1})}{1-\exp\,(-2\pi E')}\ (\text{cm}^2),$$

where E_B is the binding energy of the electron after capture, E_γ is the energy of the emitted photon, and $E' = [E_B/(E_\gamma - E_B)]^{1/2}$. In this derivation, it has been assumed that the relative velocity between electron and nucleus is not too large so that retardation effects can be neglected. A rough approximation for the total cross section for capturing a free electron into *any* of the bound states with principal quantum number ν, valid up to energies E_γ of approximately $10E_B$, is ($E_\nu = E_B/\nu^2$)

$$\sigma_{R,\nu} \simeq 1.96\pi^2(e^2\hbar/m_e{}^2c^3)[E_B{}^2/E_\gamma(E_\gamma - E_\nu)]\nu^{-3} \qquad (E_\gamma < 10E_B).$$

It is evident that free electrons are most likely to be captured into the innermost empty, or partially unfilled shell. For radiative capture of an electron by a positive ion, screening corrections must be applied.

Although radiative capture occurs with relatively small probabilities, it is nevertheless important in many cases. For example, in most recent investigations, Betz and Schnopper (1972), Betz *et al.* (1972), and Schnopper *et al.* (1972) measured the x-ray spectra produced by highly stripped chlorine and bromine ions in collisions with various targets. Due to the high ion velocities investigated in these experiments ($v \leq 2.56\times10^9$ cm/sec) radiative capture by the ions resulted in the emission of unusually energetic x-rays. For example, 120-MeV chlorine ions ($\bar{q} \simeq 14^+$) produced significant amounts of x-rays with energies up to $E_\gamma \simeq 5.5$ keV, though the energy of the characteristic K x-ray band does not exceed $\sim$2.82 keV. The measured cross sections σ_R are as large as $\sim 2\times10^{-22}$ cm^2, in close agreement with theory. Clearly, further explorations of radiative electron capture processes are desirable.

2. Experimental Results and Comparison with Theory

This section presents a tabulation and some characteristic graphical illustrations of charge-changing cross sections which have been reported for heavy ions in the velocity range of present interest, as well as a critical discussion of these experimental results. Table IV.1 lists the values of $\sigma(q, q+n)$ as a function of the basic parameters arranged in the order Z, E, Z_T, n, and q. The units are 10^{-16} cm^2/molecule. All listed cross sections have been measured individually mainly by means of the techniques discussed in Sec. III. Excluded are those cross sections which have been determined indirectly by using, for example, combinations of other cross sections with equilibrium charge state fractions.

In general, relatively large cross sections, and especially the ones for single-electron capture and loss, have small errors ($\sim$10%) which are essentially due to

TABLE IV.1. Experimental charge-changing cross sections $\sigma(q, q')$ of chlorine, argon, bromine, krypton, and iodine ions in gases, as a function of the projectile energy. All cross sections are given in units of 10^{-16} cm²/molecule and are arranged in the order of increasing initial charge q, and increasing number of transferred electrons, $n=q'-q$. Target gases are H_2 (H2), He (HE), N_2 (N2), O_2 (O2), air (AIR), CO_2 (CO2), N_2O (N2O), CH_4 (CH4), C_3H_6O (C1), Ar (AR), and Kr (KR). The reference numbers listed for each cross section identify the source of the data and are explained at the bottom of the Table. The values of the capture cross sections ($q'<q$) may be influenced by residual ion excitation. Further explanations are given in the text, Sec. IV.1.

q	q'	σ	Ref.
	$Z=17$ $M=35$		
	4.00 MeV, H2		
1	0	0.320	d
2	1	0.819	d
3	2	1.890	d
4	3	3.200	d
5	4	5.050	d
2	0	0.002	d
3	1	0.017	d
4	2	0.068	d
5	3	0.121	d
1	2	3.090	d
2	3	1.720	d
3	4	0.966	d
4	5	0.445	d
5	6	0.210	d
1	3	0.461	d
2	4	0.152	d
3	5	0.058	d
4	6	0.020	d
1	4	0.035	d
2	5	0.021	d
3	6	0.007	d
1	5	0.004	d
2	6	0.004	d
1	6	0.001	d
	$Z=18$ $M=40$		
	1.41 MeV, HE		
1	0	0.560	k
2	1	2.730	k
3	2	3.750	k
4	3	6.600	k
2	0	0.034	l
3	1	0.140	l
4	2	0.410	l
0	1	6.600	g
1	2	1.100	g
2	3	1.060	g
3	4	0.880	g
4	5	0.560	g
1	3	1.000	h
2	4	0.325	h
3	5	0.045	h
1	4	0.157	h
2	5	0.015	h
1	5	0.009	h
	1.41 MeV, N2		
1	0	1.140	k
2	1	6.100	k
3	2	11.700	k
4	3	19.200	k
2	0	0.160	l
3	1	1.040	l
4	2	2.000	l
4	1	0.168	l
0	1	25.000	g
1	2	4.860	g
2	3	3.720	g
3	4	2.020	g
4	5	0.780	g
1	3	2.600	h
2	4	1.400	h
3	5	0.530	h
4	6	0.132	h
1	4	1.140	h
2	5	0.370	h
3	6	0.116	h
1	5	0.272	h
2	6	0.106	h
1	6	0.084	h
	1.41 MeV, AR		
1	0	0.850	k
2	1	5.250	k
3	2	10.500	k
4	3	21.000	k
2	0	0.880	l
3	1	1.000	l
4	2	2.400	l
0	1	27.800	g
1	2	5.350	g
2	3	3.180	g
3	4	1.500	g
1	3	1.860	h
2	4	1.010	h
3	5	0.315	h
1	4	0.820	h
2	5	0.230	h
3	6	0.116	h
1	5	0.184	h
2	6	0.100	h
	1.41 MeV, KR		
1	0	1.830	k
2	1	10.000	k
3	2	17.500	k
4	3	29.500	k
2	0	0.194	l
3	1	1.580	l
4	2	4.200	l
3	0	0.080	l
4	1	0.680	l
0	1	17.500	g
1	2	4.300	g
2	3	2.700	g
3	4	1.230	g
4	5	0.880	g
1	3	1.850	h
2	4	0.700	h
3	5	0.230	h
1	4	0.615	h
2	5	0.123	h
	3.51 MeV, H2		
3	2	5.000	k
4	3	8.500	k
5	4	12.400	k
6	5	16.400	k
	3.51 MeV, HE		
3	4	1.010	g
4	5	0.510	g
5	6	0.185	g
3	5	0.130	h
4	6	0.084	h
	3.51 MeV, N2		
3	2	4.540	k
4	3	8.800	k
5	4	13.700	k
6	5	19.600	k
3	4	2.680	g
4	5	1.600	g
5	6	0.570	g
3	5	1.020	h
4	6	0.470	h
5	7	0.110	h
3	6	0.200	h
	3.51 MeV, AR		
2	1	3.500	k
3	2	4.700	k
4	3	8.400	k
5	4	14.000	k
6	5	19.000	k
7	6	25.500	k
3	4	2.600	g
4	5	1.300	g
5	6	0.660	g
3	5	0.780	h
4	6	0.330	h
5	7	0.130	h
3	6	0.140	h
4	7	0.088	h
	3.51 MeV, KR		
3	2	5.400	k
4	3	14.500	k

TABLE IV.1 (*Continued*)

q	q'	σ	Ref.
5	4	19.500	k
6	5	27.700	k
3	4	2.300	g
4	5	0.800	g
4	6	0.320	h
5	7	0.155	h
	40.00 MeV, N2		
6	5	0.070	i
13	12	1.360	i
13	11	0.320	i
13	10	0.130	i
6	7	1.160	i
13	14	0.040	i
6	8	0.680	i
6	9	0.260	i
6	10	0.090	i
6	11	0.026	i
	40.00 MeV, AR		
6	5	0.017	i
13	12	0.830	i
13	11	0.190	i
13	10	0.065	i
6	7	0.860	i
13	14	0.015	i
6	8	0.400	i
6	9	0.130	i
6	10	0.066	i
6	11	0.027	i
	400.00 MeV, N2		
16	15	0.006	i
17	16	0.010	i
18	17	0.014	i
13	14	0.114	i
13	15	0.014	i
13	16	0.002	i
	400.00 MeV, AR		
13	12	0.001	i
17	16	0.013	i
17	15	0.001	i
	$Z=35$ $M=79$		
	6.00 MeV, HE		
2	1	1.080	b
3	2	2.580	b
4	3	5.140	b
5	4	7.120	b
6	5	9.970	b
7	6	9.300	b
8	7	13.000	b
9	8	16.600	b
3	1	0.033	b
4	2	0.159	b
5	3	0.392	b
6	4	0.684	b
7	5	0.740	b
8	6	0.310	b
9	7	0.250	b
2	3	1.980	b
3	4	1.250	b
4	5	0.832	b
5	6	0.442	b
6	7	0.230	b
7	8	0.124	b
8	9	0.040	b
9	10	0.025	b
2	4	0.445	b
3	5	0.313	b
6	8	0.022	b
2	5	0.160	b
	10.00 MeV, HE		
3	2	0.898	b
4	3	1.970	b
5	4	3.380	b
6	5	5.530	b
7	6	5.160	b
8	7	7.680	b
9	8	10.400	b
10	9	13.400	b
5	3	0.056	b
6	4	0.104	b
7	5	0.154	b
8	6	0.086	b
3	4	1.250	b
4	5	0.854	b
5	6	0.560	b
6	7	0.320	b
7	8	0.173	b
8	9	0.106	b
9	10	0.060	b
10	11	0.038	b
3	5	0.331	b
4	6	0.195	b
5	7	0.131	b
6	8	0.048	b
	13.90 MeV, H2		
6	5	3.170	e
7	6	3.110	e
8	7	5.290	e
10	9	11.100	e
6	4	0.002	e
6	7	0.326	e
7	8	0.188	e
8	9	0.122	e
10	11	0.096	e
6	8	0.031	e
7	9	0.028	e
8	10	0.029	e
	13.90 MeV, HE		
6	5	3.540	e
8	7	5.220	e
10	9	11.300	e
6	4	0.690	e
8	6	0.410	e
10	8	0.292	e
6	7	0.563	e
8	9	0.220	e
10	11	0.101	e
6	8	0.093	e
8	10	0.049	e
6	9	0.041	e
	13.90 MeV, AR		
6	5	7.490	e
8	7	12.200	e
10	9	20.800	e
6	4	0.239	e
8	6	0.127	e
10	8	0.857	e
6	7	1.150	e
8	9	0.416	e
10	11	0.363	e
6	8	0.432	e
8	10	0.401	e
6	9	0.238	e
	14.00 MeV, H2		
4	3	0.640	b
5	4	1.220	b
6	5	2.660	b
7	6	2.740	b
8	7	4.190	b
6	4	0.007	b
7	5	0.016	b
8	6	0.006	b
4	5	0.740	b
5	6	0.450	b
6	7	0.286	b
7	8	0.162	b
8	9	0.118	b
4	6	0.130	b
5	7	0.075	b
6	8	0.021	b
7	9	0.010	b
8	10	0.009	b
4	7	0.027	b
4	8	0.004	b
	14.00 MeV, HE		
4	3	0.738	b
5	4	1.390	b
6	5	2.740	b
7	6	3.140	b
8	7	4.450	b
9	8	6.110	b
10	9	8.180	b
7	5	0.038	b
9	7	0.037	b
10	8	0.022	b
4	5	0.819	b
5	6	0.555	b
6	7	0.429	b
7	8	0.228	b
8	9	0.166	b
9	10	0.111	b
4	6	0.195	b

TABLE IV.1 (*Continued*)

q	q'	σ	Ref.
5	7	0.155	b
6	8	0.037	b
7	9	0.019	b
	25.00 MeV, H2		
7	6	0.298	e
8	7	0.559	e
9	8	0.923	e
10	9	1.370	e
11	10	2.130	e
7	8	0.278	e
8	9	0.197	e
9	10	0.128	e
10	11	0.106	e
11	12	0.082	e
7	9	0.021	e
8	10	0.010	e
9	11	0.018	e
10	12	0.015	e
11	13	0.020	e
7	10	0.001	e
9	12	0.016	e
	25.00 MeV, HE		
7	6	0.586	e
8	1	7.120	e
9	8	1.850	e
11	10	3.610	e
7	8	0.365	e
8	9	0.303	e
9	10	0.206	e
11	12	0.164	e
7	9	0.087	e
8	10	0.081	e
9	11	0.042	e
11	13	0.074	e
7	10	0.024	e
9	12	0.024	e
	25.00 MeV, AR		
7	6	1.250	e
9	8	4.150	e
7	8	0.921	e
9	10	0.564	e
7	9	0.364	e
9	11	0.373	e
7	10	0.220	e
7	11	0.136	e
	41.67 MeV, H2		
7	6	0.021	f
8	7	0.054	f
7	8	0.287	f
8	9	0.247	f
7	9	0.021	f
8	10	0.025	f
7	10	0.002	f
8	11	0.011	f
	41.67 MeV, AR		
7	6	0.099	f
8	7	0.203	f
7	8	0.929	f
8	9	0.056	f
7	9	0.302	f
8	10	0.289	f
7	10	0.197	f
8	11	0.180	f
7	11	0.126	f
8	12	0.152	f
7	12	0.106	f
8	13	0.098	f
7	13	0.073	f
8	14	0.072	f
7	14	0.052	f
8	15	0.370	f
7	15	0.031	f
	$Z=36$ $M=84$		
	2.97 MeV, HE		
3	2	4.000	k
4	3	6.800	k
3	4	1.130	g
4	5	0.580	g
	2.97 MeV, KR		
3	2	21.500	k
4	3	30.300	k
3	1	2.400	l
4	2	4.200	l
	2.97 MeV, N2		
3	2	12.600	k
4	3	18.600	k
3	1	1.300	l
4	2	2.940	l
3	4	2.080	g
4	5	1.320	g
	$Z=53$ $M=127$		
	4.50 MeV, H2		
1	0	1.220	m
2	1	5.060	m
3	2	11.800	m
4	3	17.100	m
3	1	0.312	m
4	2	1.060	m
1	2	5.170	m
2	3	3.330	m
3	4	1.690	m
4	5	1.110	m
1	3	1.600	m
2	4	1.060	m
3	5	0.484	m
1	4	0.484	m
	5.00 MeV, H2		
2	1	3.540	c
3	2	9.390	c
4	3	14.600	c
5	4	18.000	c
6	5	20.800	c
7	6	18.500	c
8	7	22.000	c
9	8	31.000	c
10	9	36.000	c
11	10	41.000	c
12	11	47.000	c
13	12	53.000	c
14	13	67.000	c
15	14	85.000	c
2	0	0.025	c
3	1	0.256	c
4	3	0.801	c
5	3	1.990	c
6	4	1.650	c
7	5	1.190	c
2	3	2.740	c
3	4	1.650	c
4	5	0.965	c
5	6	0.345	c
6	7	0.197	c
7	8	0.044	c
2	4	0.700	c
3	5	0.266	c
4	6	0.104	c
5	7	0.023	c
6	8	0.019	c
2	5	0.136	c
4	7	0.019	c
	5.00 MeV, O2		
2	1	2.860	c
3	2	8.330	c
4	3	14.100	c
5	4	17.100	c
6	5	20.300	c
7	6	16.700	c
8	7	30.000	c
9	8	34.000	c
10	9	40.000	c
11	10	44.000	c
12	11	51.000	c
13	12	62.000	c
14	13	81.000	c
3	1	0.219	c
4	2	1.150	c
5	3	2.800	c
6	4	3.950	c
7	5	6.140	c
2	3	3.620	c
3	4	2.730	c
4	5	1.860	c
5	6	1.010	c
6	7	0.764	c
7	8	0.511	c
2	4	1.620	c
3	5	1.460	c
4	6	1.060	c
5	7	0.545	c
6	8	0.321	c
7	9	0.189	c

TABLE IV.1 (*Continued*)

q	q'	σ	Ref.
2	5	1.02	c
3	6	1.010	c
4	7	0.776	c
5	8	0.184	c
6	9	0.124	c
3	7	0.247	c
	6.00 MeV, HE		
2	1	1.120	b
3	2	3.460	b
4	3	6.760	b
5	4	9.330	b
6	5	10.500	b
7	6	10.400	b
8	7	13.400	b
9	8	17.700	b
4	2	0.057	b
5	3	0.273	b
6	4	0.418	b
7	5	0.811	b
8	6	0.640	b
9	7	0.910	b
2	3	2.600	b
3	4	1.500	b
4	5	1.270	b
5	6	0.761	b
6	7	0.587	b
7	8	0.294	b
8	9	0.168	b
9	10	0.034	b
2	4	0.983	b
3	5	0.732	b
4	6	0.321	b
5	7	0.211	b
6	8	0.078	b
2	5	0.492	b
3	6	0.239	b
4	7	0.110	b
2	6	0.153	b
	9.50 MeV CO2		
3	2	4.500	p
4	3	10.200	p
5	4	14.000	p
6	5	18.500	p
7	6	21.500	p
8	7	25.000	p
2	3	6.600	p
3	4	5.400	p
4	5	4.500	p
5	6	2.800	p
6	7	2.600	p
7	8	1.600	p
8	9	1.250	p
2	4	3.400	p
3	5	2.900	p
4	6	2.400	p
5	7	1.600	p
6	8	1.400	p
7	9	0.700	p
2	5	1.900	p
3	6	1.400	p
4	7	2.200	p
5	8	1.100	p
6	9	0.900	p
	10.00 MeV, H2		
3	2	3.210	c
4	3	5.990	c
5	4	9.080	c
6	5	13.700	c
7	6	18.100	c
8	7	18.300	c
10	9	27.000	c
11	10	31.000	c
12	11	36.000	c
13	12	41.000	c
14	13	53.000	c
15	14	62.000	c
16	15	72.000	c
17	16	88.000	c
18	17	99.000	c
9	8	24.000	c
3	1	0.144	c
4	2	0.300	c
5	3	0.499	c
6	4	0.735	c
7	5	1.06	c
8	6	0.272	c
3	4	1.890	c
4	5	1.320	c
5	6	0.807	c
6	7	0.724	c
7	8	0.669	c
8	9	0.372	c
3	5	0.686	c
4	6	0.405	c
5	7	0.332	c
6	8	0.183	c
7	9	0.319	c
3	6	0.369	c
4	7	0.230	c
5	8	0.152	c
6	9	0.348	c
	10.00 MeV HE		
3	2	1.980	b
4	3	4.460	b
5	4	6.280	b
6	5	7.350	b
7	6	7.710	b
8	7	10.600	b
9	8	13.000	b
4	2	0.027	b
5	3	0.117	b
6	4	0.185	b
7	5	0.511	b
8	6	0.272	b
9	7	0.500	b
3	4	1.630	b
4	5	1.340	b
5	6	0.847	b
6	7	0.744	b
7	8	0.471	b
8	9	0.336	b
9	10	0.199	b
3	5	0.717	b
4	6	0.463	b
5	7	0.349	b
6	8	0.194	b
7	9	0.124	b
3	6	0.328	b
4	7	0.180	b
5	8	0.092	b
	10.00 MeV, O2		
3	2	3.240	c
4	3	6.980	c
5	4	9.950	c
6	5	14.600	c
7	6	15.100	c
8	7	20.500	c
9	8	24.100	c
10	9	30.200	c
11	10	34.000	c
12	11	40.000	c
13	12	45.000	c
14	13	59.000	c
15	14	70.000	c
16	15	77.000	c
3	1	0.062	c
4	2	0.312	c
5	3	0.738	c
6	4	1.320	c
7	5	3.160	c
8	6	3.450	c
9	7	4.050	c
10	8	6.090	c
3	4	2.690	c
4	5	2.110	c
5	6	1.400	c
6	7	1.070	c
7	8	0.700	c
8	9	0.600	c
9	10	0.414	c
3	5	1.370	c
4	6	0.992	c
5	7	0.705	c
6	8	0.366	c
7	9	0.390	c
8	10	0.220	c
9	11	0.247	c
3	6	1.010	c
4	7	0.690	c
5	8	0.397	c
6	9	0.250	c
	10.00 MeV, AR		
4	3	6.740	c
4	5	2.230	c
4	6	0.879	c
4	7	0.497	c

TABLE IV.1 (*Continued*)

q	q'	σ	Ref.
4	8	0.233	c
4	9	0.157	c
	12.00 MeV, H2		
5	4	6.390	n
5	3	9.017	n
5	6	0.716	n
5	7	0.214	n
	12.00 MeV N2		
5	4	8.630	n
5	3	0.402	n
5	6	1.500	n
5	7	0.791	n
5	8	0.574	n
	12.00 MeV, O2		
5	4	8.400	n
5	3	0.386	n
5	6	1.510	n
5	7	0.903	n
5	8	0.602	n
	12.00 MeV, CO2		
5	4	10.300	n
5	3	0.619	n
5	6	1.870	n
5	7	1.170	n
5	8	0.888	n
	12.00 MeV, N2O		
5	4	10.800	n
5	3	0.539	n
5	6	1.790	n
5	7	1.030	n
5	8	0.871	n
	12.00 MeV, AIR		
9	8	26.300	o
13	12	45.500	o
15	14	62.200	o
16	15	85.200	o
17	16	73.000	o
18	17	77.000	o
	12.00 MeV, CH4		
5	4	11.200	n
5	3	0.612	n
5	6	1.480	n
5	7	0.641	n
5	8	0.417	n
	12.00 MeV, C1		
5	4	8.540	n
5	3	0.441	n
5	6	1.460	n
5	7	0.812	n
5	8	0.499	n
	13.69 MeV, N2		
5	4	7.200	a
6	5	16.820	a
6	7	2.420	a
6	8	0.912	a
6	9	0.646	a
	15.00 MeV, H2		
5	4	2.810	c
6	5	3.080	c
7	6	5.250	c
8	7	7.720	c
9	8	11.500	c
10	9	16.600	c
11	10	20.900	c
12	11	26.000	c
13	12	29.000	c
14	13	39.000	c
15	14	44.000	c
16	15	51.000	c
17	16	60.000	c
6	4	0.134	c
7	5	0.040	c
8	6	0.287	c
9	7	0.095	c
10	8	0.298	c
5	6	0.778	c
6	7	0.703	c
7	8	0.391	c
8	9	0.221	c
9	10	0.140	c
10	11	0.106	c
5	7	0.201	c
6	8	0.172	c
7	9	0.099	c
8	10	0.064	c
5	8	0.041	c
	15.00 MeV, HE		
4	3	2.260	b
5	4	3.210	b
6	5	4.020	b
7	6	5.590	b
8	7	7.410	b
9	8	9.390	b
10	9	12.200	b
6	4	0.044	b
7	5	0.240	b
8	6	0.063	b
9	7	0.163	b
10	8	0.282	b
4	5	1.240	b
5	6	0.906	b
6	7	0.837	b
7	8	0.545	b
8	9	0.452	b
9	10	0.386	b
10	11	0.258	b
4	6	0.483	b
5	7	0.437	b
6	8	0.278	b
4	7	0.275	b
5	8	0.152	b
	15.00 MeV, O2		
5	4	5.800	c
6	5	7.710	c
7	6	10.700	c
8	7	13.400	c
9	8	16.100	c
10	9	21.500	c
11	10	24.400	c
12	11	28.000	c
13	12	32.000	c
14	13	40.000	c
15	14	45.000	c
16	15	55.000	c
17	16	63.000	c
18	17	72.000	c
5	3	0.222	c
6	4	0.332	c
7	5	1.230	c
8	6	0.685	c
9	7	1.600	c
10	8	3.310	c
11	9	5.220	c
5	6	1.730	c
6	7	1.430	c
7	8	0.889	c
8	9	0.774	c
9	10	0.583	c
10	11	0.444	c
11	12	0.415	c
5	7	1.020	c
6	8	0.662	c
7	9	0.487	c
8	10	0.442	c
9	11	0.316	c
10	12	0.268	c
11	13	0.245	c
5	8	0.579	c
6	9	0.413	c
7	10	0.361	c
8	11	0.349	c
9	12	0.270	c
10	13	0.199	c
5	9	0.399	c
6	10	0.356	c
7	11	0.328	c
8	12	0.236	c
9	13	0.151	c
5	10	0.362	c
6	11	0.216	c
7	12	0.227	c
8	13	0.120	c
5	11	0.303	c
6	12	0.173	c
7	13	0.147	c
5	12	0.182	c
6	13	0.074	c
5	13	0.094	c

TABLE IV.1 (*Continued*)

q	q'	σ	Ref.
	16.00 MeV, N2		
11	10	23.400	c
11	9	2.220	c
11	12	0.517	c
	16.00 MeV, AIR		
10	9	19.500	o
11	10	23.400	o
12	11	28.000	o
13	12	36.400	o
14	13	41.500	o
15	14	44.500	o
16	15	46.500	o
17	16	47.500	o
18	17	59.600	o
19	18	57.500	o
20	19	70.800	o
21	20	61.600	o
22	21	76.000	o
	18.64 MeV, N2		
6	5	8.820	a
7	6	11.840	a
8	7	19.180	a
6	7	2.580	a
7	8	1.728	a
	20.00 MeV, H2		
6	5	1.490	c
7	6	1.270	c
8	7	2.790	c
9	8	6.330	c
10	9	9.000	c
12	11	14.400	c
13	12	18.000	c
14	13	25.000	c
15	14	29.000	c
16	15	35.000	c
9	7	0.150	c
6	7	0.780	c
7	8	0.560	c
8	9	0.464	c
9	10	0.267	c
10	11	0.217	c
7	9	0.052	c
9	11	0.045	c
	20.00 MeV, O2		
6	5	4.580	c
7	6	5.510	c
8	7	7.520	c
9	8	13.500	c
10	9	16.000	c
12	11	20.000	c
13	12	23.500	c
14	13	33.000	c
15	14	38.000	c
16	15	43.500	c
7	5	0.100	c
8	6	0.602	c
9	7	0.803	c
6	7	2.200	c
7	8	1.050	c
8	9	0.860	c
9	10	0.659	c
10	11	0.538	c
6	8	1.120	c
7	9	0.525	c
8	10	0.316	c
9	11	0.295	c
10	12	0.260	c
7	10	0.345	c
8	11	0.255	c
9	12	0.244	c
	24.36 MeV, N2		
6	5	4.860	a
7	6	5.140	a
8	7	13.740	a
9	8	14.980	a
10	9	21.200	a
6	7	2.700	a
7	8	2.140	a
8	9	1.802	a
9	10	1.542	a
10	11	1.370	a
7	9	1.016	a
8	10	0.968	a
9	11	0.920	a
7	10	0.576	a
8	11	0.306	a
9	12	0.518	a
7	11	0.348	a
8	12	0.260	a
9	13	0.478	a
	24.40 MeV, CO2		
5	4	2.150	p
6	5	3.600	p
7	6	4.800	p
8	7	8.400	p
9	8	11.000	p
10	9	13.200	p
11	10	15.000	p
4	5	4.800	p
5	6	3.700	p
6	7	3.300	p
7	8	2.600	p
8	9	2.000	p
9	10	1.500	p
4	6	2.500	p
5	7	1.800	p
6	8	1.330	p
7	9	1.200	p
8	10	1.100	p
9	11	0.910	p
4	7	1.200	p
5	8	0.620	p
6	9	0.860	p
7	10	0.650	p
8	11	0.480	p
9	12	0.680	p
	25.00 MeV, H2		
10	9	3.510	c
14	13	13.000	c
15	14	16.000	c
10	8	0.010	c
10	11	0.205	c
	25.00 MeV, O2		
10	9	7.690	c
14	13	21.000	c
15	14	25.000	c
10	8	1.080	c
10	11	0.533	c
	30.81 MeV, N2		
6	5	2.320	a
7	6	2.200	a
8	7	5.120	a
9	8	9.980	a
10	9	12.780	a
14	13	31.800	a
15	14	31.400	a
16	15	35.600	a
17	16	35.200	a
6	7	3.080	a
7	8	2.380	a
8	9	1.946	a
9	10	1.540	a
10	11	1.440	a
7	9	0.904	a
10	12	0.944	a
7	10	0.404	a
10	13	0.580	a
7	11	0.628	a
10	14	0.428	a
7	12	0.410	a
	38.04 MeV, N2		
8	7	2.200	a
9	8	5.200	a
10	9	9.660	a
11	10	9.880	a
10	8	0.130	a
8	9	2.360	a
9	10	2.260	a
10	11	1.562	a
10	12	0.906	a
10	13	0.750	a
10	14	0.442	a
10	15	0.248	a
	38.10 MeV, CO2		
6	5	0.830	p
7	6	1.050	p
8	7	2.230	p
9	8	4.050	p

TABLE IV.1 (*Continued*)

q	q'	σ	Ref.
10	9	6.600	p
11	10	9.600	p
12	11	11.200	p
13	12	12.500	p
5	6	4.750	p
6	7	4.000	p
7	8	3.150	p
8	9	2.500	p
9	10	2.100	p
10	11	1.500	p
11	12	1.150	p
5	7	2.390	p
6	8	1.900	p
7	9	1.350	p
8	10	1.000	p
9	11	1.050	p
10	12	0.930	p
11	13	0.540	p
5	8	1.160	p
6	9	0.960	p
7	10	0.830	p
8	11	0.740	p
10	13	0.310	p
11	14	0.450	p
	46.03 MeV, N2		
9	8	3.140	a
10	9	5.300	a
11	10	7.480	a
12	11	10.640	a
9	7	0.084	a
10	8	0.048	a
12	10	0.186	a
9	10	1.804	a
10	11	1.328	a
11	12	1.830	a
12	13	1.404	a
9	11	1.184	a
10	12	0.890	a
11	13	0.420	a
12	14	0.448	a
9	12	0.694	a
10	13	0.628	a
11	14	0.708	a
12	15	0.326	a
9	13	0.312	a
10	14	0.262	a
11	15	0.422	a
12	16	0.214	a
9	14	0.080	a
10	15	0.118	a
11	16	0.206	a
9	15	0.044	a
10	16	0.048	a
	54.78 MeV, N2		
10	9	2.220	a
11	10	3.560	a
12	11	5.480	a
13	12	8.940	a
17	16	13.540	a
18	17	15.580	a
11	12	2.080	a
12	13	1.624	a
12	14	0.978	a
12	15	0.582	a
12	16	0.330	a
12	17	0.148	a
12	18	0.050	a
	54.80 MeV, CO2		
8	7	0.660	p
9	8	1.420	p
10	9	2.450	p
11	10	3.350	p
12	11	5.000	p
13	12	7.000	p
14	13	8.800	p
15	14	10.100	p
16	15	11.000	p
7	8	3.800	p
8	9	3.300	p
9	10	2.850	p
10	11	2.400	p
11	12	1.930	p
12	13	1.600	p
13	14	1.380	p
14	15	1.100	p
15	16	0.940	p
7	9	1.950	p
8	10	1.600	p
9	11	1.490	p
10	12	1.100	p
11	13	0.850	p
12	14	0.720	p
13	15	0.480	p
7	10	0.980	p
8	11	0.830	p
9	12	0.700	p
10	13	0.850	p
11	14	0.780	p
12	15	0.480	p
	64.28 MeV, N2		
12	11	3.680	a
13	12	4.440	a
13	14	1.484	a
	110.00 MeV, H2		
12	11	0.016	j
12	13	0.100	j
12	14	0.380	j
12	15	0.010	j
12	16	0.003	j
	110.00 MeV, HE		
12	11	0.065	j
12	13	0.160	j
12	14	0.060	j
12	15	0.020	j
12	16	0.007	j
12	17	0.004	j
	110.00 MeV, AR		
12	11	0.090	j
12	13	0.700	j
12	14	0.400	j
12	15	0.180	j
12	16	0.120	j
12	17	0.070	j
12	18	0.050	j
12	19	0.037	j
12	20	0.030	j
12	21	0.024	j
12	22	0.020	j
12	23	0.014	j
12	24	0.011	j
	162.00 MeV, O2		
17	18	0.600	j
17	19	0.200	j
17	20	0.120	j
17	21	0.080	j
17	22	0.060	j
17	23	0.040	j
17	24	0.022	j
17	25	0.010	j
17	26	0.002	j

[a] Angert *et al.* (1968), and Möller *et al.* (1968).
[b] Betz *et al.* (1971a).
[c] Betz and Wittkower (1972a).
[d] Betz and Wittkower (1972b).
[e] Datz *et al.* (1970).
[f] Moak (1967).
[g] Dmitriev *et al.* (1962a).
[h] Dmitriev *et al.* (1962b).
[i] Main (1967).
[j] Moak *et al.* (1968).
[k] Nikolaev *et al.* (1961a).
[l] Nikolaev *et al.* (1962b).
[m] Ryding *et al.* (1969a).
[n] Wittkower and Betz (1971b).
[o] Ryding *et al.* (1971b).
[p] Franzke *et al.* (1972).

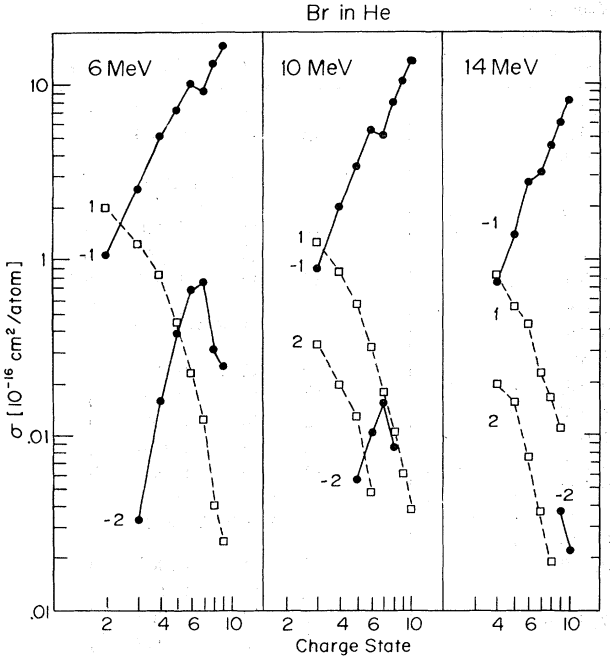

FIG. 4.1. Cross sections $\sigma(q, q+n)$ in units of 10^{-16} cm^2/molecule for electron capture (solid lines) and electron loss (dashed lines) by bromine ions passing through helium at energies of 6, 10, and 14 MeV, as a function of the initial ionic charge state q. The values of n are indicated near each curve. All data points are taken from Table IV.1 and from Betz *et al.* (1971a).

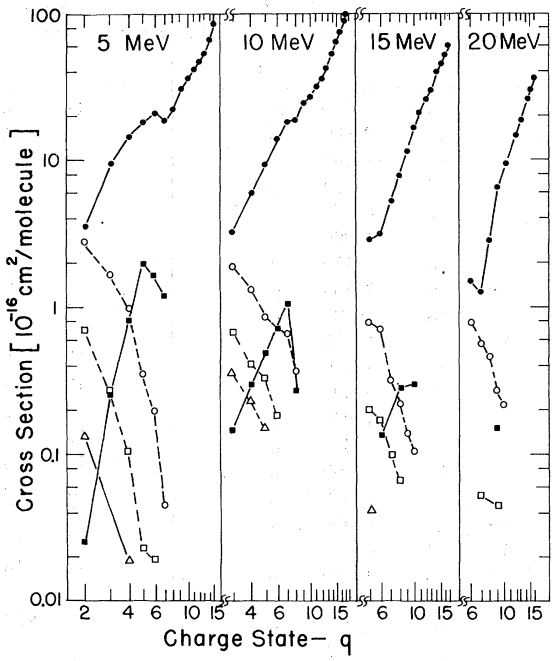

FIG. 4.3. Charge-changing cross sections $\sigma(q, q+n)$ in units of 10^{-16} cm^2/molecule for iodine ions passing through hydrogen at energies of 5, 10, 15, and 20 MeV, as a function of the initial ionic charge state q. The full symbols refer to electron capture, $n=-1$ (●), and $n=-2$ (■), and the open symbols refer to electron loss, $n=1$ (○), $n=2$ (□), and $n=3$ (△). All data points are taken from Table IV.1 and from Betz and Wittkower (1972a).

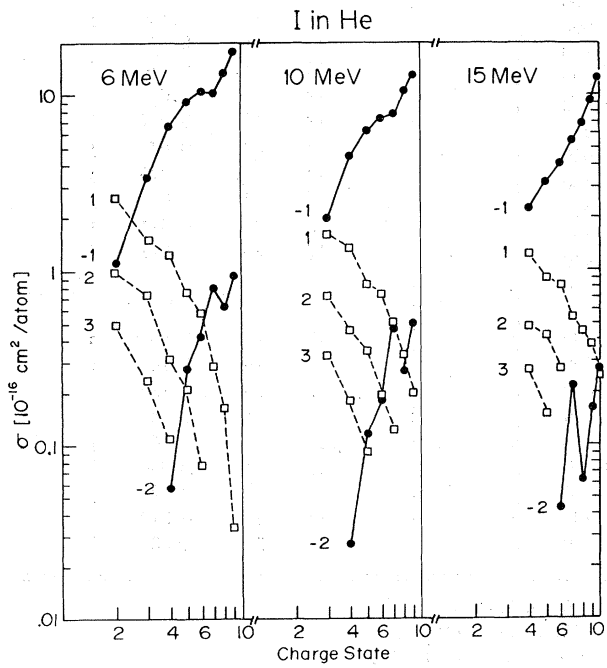

FIG. 4.2. Cross sections $\sigma(q, q+n)$ in units of 10^{-16} cm^2/molecule for electron capture (solid lines) and electron loss (dashed lines) by iodine ions passing through helium at energies of 6, 10, and 15 MeV, as a function of the initial ionic charge state q. The values of n are indicated near each curve. All data points are taken from Table IV.1 and from Betz *et al.* (1971a).

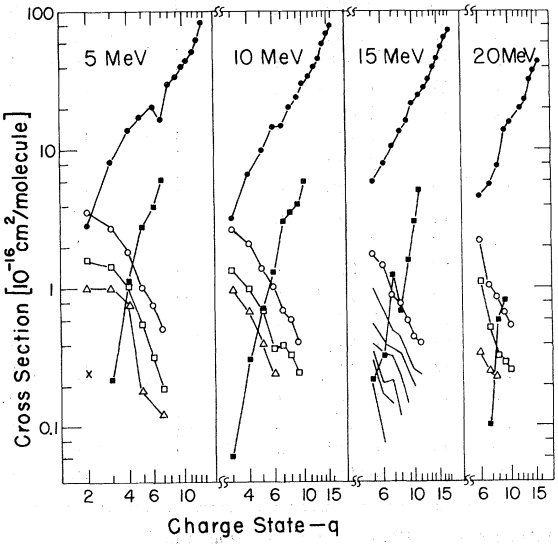

FIG. 4.4. Charge-changing cross sections $\sigma(q, q+n)$ in units of 10^{-16} cm^2/molecule for iodine ions passing through oxygen at energies of 5, 10, 15, and 20 MeV, as a function of the initial ionic charge state q. The full symbols refer to electron capture, $n=-1$ (●), and $n=-2$ (■); and the open symbols refer to electron loss, $n=1$(○), $n=2$ (□), $n=3$ (△), and $n=4$ (×). The location of the values of the multiple loss cross sections for $n\leq 7$ at 15 MeV is indicated by solid lines. All data points are taken from Table IV.1 and from Betz and Wittkower (1972a).

the difficulties of measuring the thickness of the target gas. In the case of cross sections for multiple-electron capture and loss, additional uncertainties arise due to the less accurate measurement of small charge fractions and also from the use of unsatisfactory techniques of analysis; absolute errors may then rise to as much as a factor of 2. The interpretation of the capture cross sections is often difficult because it is generally not known whether the measured values refer to the ground state or to the excited states of the ions; Sec. VI.1 will describe in detail how σ_c may decrease significantly when the excitation of the capturing ions is increased. Of those capture cross sections which have been measured for different residual ion excitation, only the largest values are listed in Table IV.1, corresponding to the ground state or to the states of lowest investigated excitation. A few of the listed values may be afflicted with further uncertainties because they were read off from small graphs, or because it was not known whether the cross sections have been given in units of cm²/atom or cm²/molecule. In some instances, the complete experimental data have been made available by the investigators and the cross sections have been re-evaluated using the least-squares technique described in Sec. III.2. In these cases, it was found that single capture and loss cross sections, as is to be expected, changed on the average by no more than 5%–10%, whereas multiple-electron transfer cross section, especially those for double electron capture, changed by as much as a factor of 2.

Characteristic trends in the data have been found by many investigators and are illustrated in Figs. 4.1–4.10 and are discussed in Sec. IV.2.a–e. Comparison with theory is necessarily hindered because most theoretical results are valid only in restricted ranges of the basic parameters, and these limitations are in general not clearly spelled out, or because no theory exists which appears to be applicable to the experimentally investigated case. For example, explicit theoretical formulas give simple power functions for the dependence of single capture and loss cross sections as a function of v, but most of the measurements have been performed in velocity ranges where the cross sections are near a maximum. Furthermore, the important processes of multiple-electron loss and multiple-electron capture have not yet received sufficient attention from theorists.

Several of the experimental results on cross sections which have been omitted from Table IV.1 deserve to be mentioned. Lo and Fite (1970) assembled cross sections for capture and loss in graphical form; the nuclear charge of the ions ranges from $Z=7$ to $Z=92$, but the energies do not exceed 2 MeV except in one case, and the initial charge states are limited essentially to $q=0$ and $q=1+$.[4]

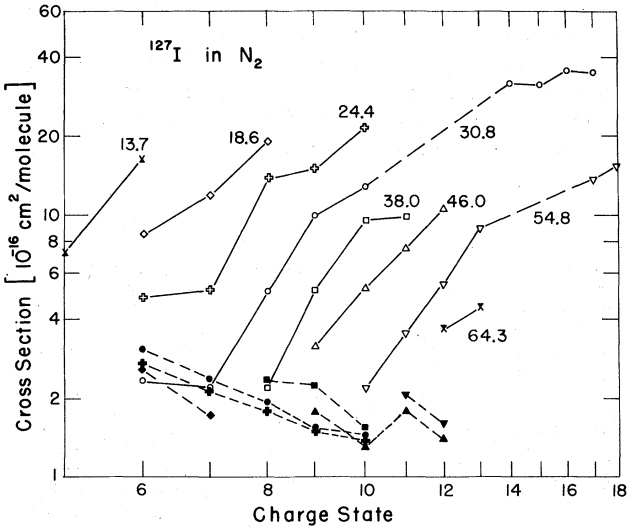

FIG. 4.5. Cross sections $\sigma(q, q\pm1)$ in units of 10^{-16} cm²/molecule for capture (open symbols) and loss (full symbols) of a single electron by iodine ions of various energies in collisions with nitrogen molecules, as a function of the initial ionic charge state q of the ions. Open and full symbols of the same kind refer to the same energy which is indicated in units of MeV near the curves for electron capture. All data points are taken from Table IV.1 and from Angert *et al.* (1968) and Möller *et al.* (1968).

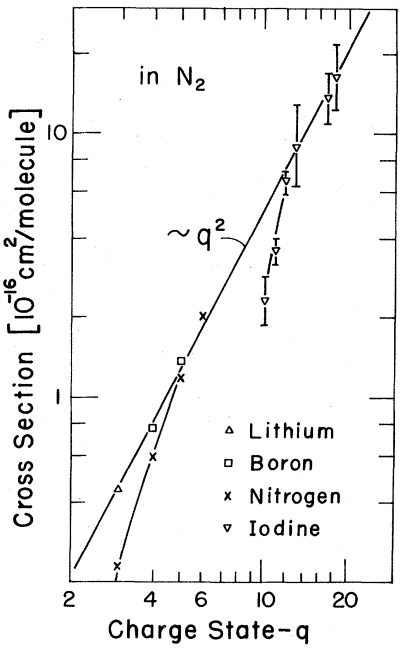

FIG. 4.6. Cross sections $\sigma(q, q-1)$ in units of 10^{-16} cm²/molecule for capture of a single electron by various ions of the same velocity $v=9.1\times10^8$ cm/sec in collisions with nitrogen molecules; from Angert *et al.* (1968).

[4] Lo and Fite do not specify whether they used units of cm²/atom or cm²/molecule. On the one hand, they reproduce results from many authors in units of cm²/molecule; on the other hand, they show almost identical cross sections for those cases in which both monoatomic and diatomic oxygen targets have been used, thereby favoring the interpretation of σ in units of cm²/atom (however, see Sec. IV.2.e).

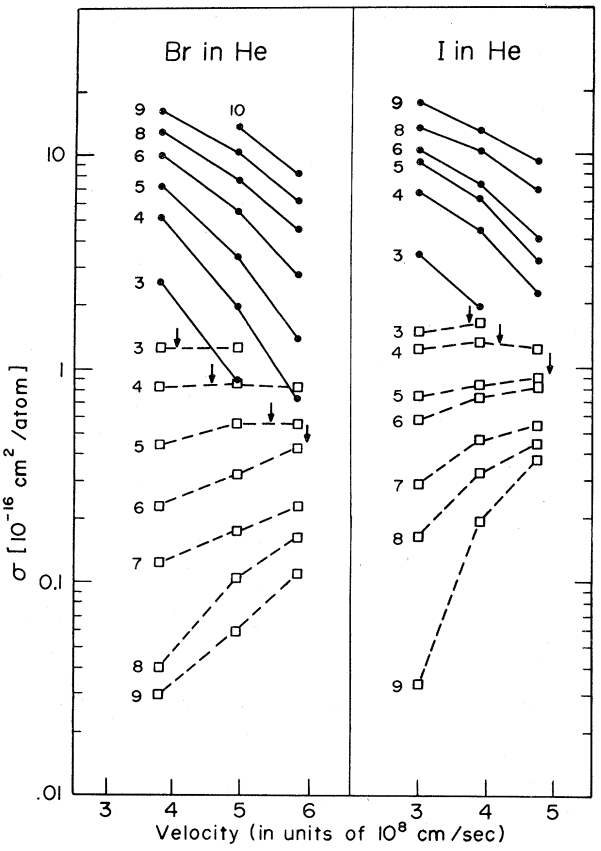

FIG. 4.7. Velocity dependence of cross sections for capture (solid lines) and loss (dashed lines) of a single electron by bromine and iodine ions passing through helium. The initial ionic charge state of the projectiles is indicated near each curve. All data points are taken from Table IV.1 and from Betz *et al.* (1971a).

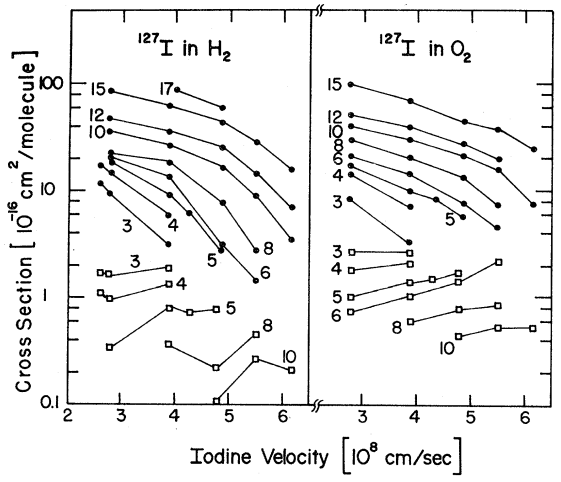

FIG. 4.8. Velocity dependence of cross sections for capture (full symbols) and loss (open symbols) of a single electron by iodine ions passing through hydrogen and oxygen. The initial ionic charge state of the projectiles is indicated near each curve. All data points are taken from Table IV.1 and from Ryding *et al.* (1969a), Wittkower and Betz (1971b), and Betz and Wittkower (1972a).

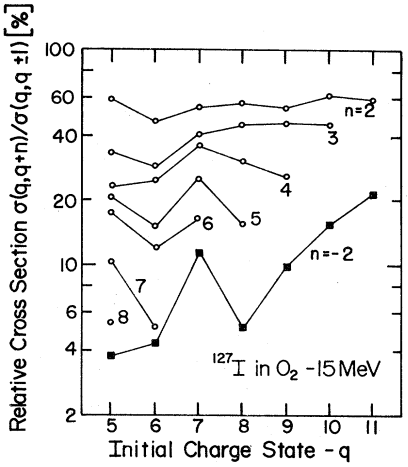

FIG. 4.9. Ratios of cross sections, $\sigma(q, q+n)/\sigma(q, q\pm1)$, in percent, between multiple- and single-electron transfer for 15-MeV iodine ions passing through oxygen, as a function of the initial ionic charge state q: ■, ratio for double capture ($n=-2$); O, ratio for multiple loss ($n\leq 8$). The values of n are indicated near each curve. The underlying cross section values are taken from Table IV.1 and from Betz and Wittkower (1972a).

a. Single-Electron Capture

Experimental results on cross sections $\sigma(q, q-1)$ for capture of a single electron by bromine and iodine ions passing through gases of hydrogen, helium, nitrogen, and oxygen are shown in Figs. 4.1–4.8. As is to be expected from theoretical considerations, $\sigma_c(q)$ generally increases with q as is illustrated in Figs. 4.1–4.6, though shell- and excitation effects may disturb that trend, and $\sigma_c(v)$ decreases with increasing v, though there is undoubtedly a maximum at low-ion velocities (see Figs. 4.7 and 4.8). Indications for a dependence of σ_c on Z near $q\simeq\bar{q}$ have been found which are not explicitly predicted theoretically. These and other trends will be discussed in the following sections.

Shell effects in σ_c. It is evident from Figs. 4.1–4.5 that

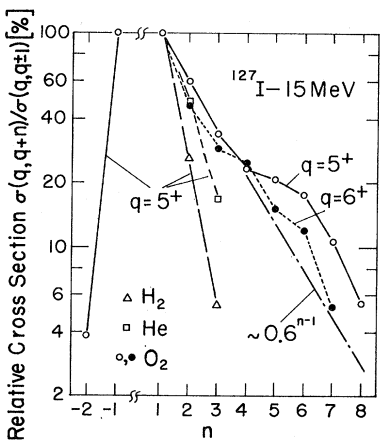

FIG. 4.10. Relative cross sections, $k_n=\sigma(q, q+n)/\sigma(q, q\pm1)$, in percent, for multiple-electron capture and loss of 15-MeV iodine ions with initial charge $q=5+$ passing through hydrogen (△), helium (□), and oxygen (○), and with initial charge $q=6+$ passing through oxygen (●). Also shown is the dependence $k_n=k_0^{n-1}$ with $k_0=0.6$. The underlying cross section values are taken from Table IV.1 and from Betz *et al.* (1971a), and Betz and Wittkower (1972a).

the continuous increase of $\sigma_c(q)$ is sometimes interrupted at the particular charge $q=7$, and $\sigma_c(7, 6)$ may lie considerably below $\sigma_c(6, 5)$. Clear evidence for that effect has been found by Datz *et al.* (1970) for bromine ions, and by Betz *et al.* (1971a) for iodine ions. Since charge state 7+ corresponds in both ion species to an electron configuration of a closed principal shell, the *M* or *N* shell, respectively, the anomalous behavior of $\sigma_c(7)$ has been interpreted as a shell effect. It appears quite plausible to assume that it is relatively difficult to capture an electron into a new shell though a clearcut theoretical explanation has not been given. The effect is found independent of the investigated target species, but seems to depend on the ion velocity. For iodine ions, $\sigma_c(7)$ shows a noticeable decrease relative to a smooth trend of $\sigma_c(q)$ for $E<15$ MeV (Figs. 4.2–4.4) and for $E\gtrsim 20$ MeV, whereas no effect of comparable magnitude is seen in the intermediate energy interval. Interestingly the velocity of 20-MeV iodine ions corresponds closely to the orbital velocity of the captured electron in the ground state of the 6+ ion. A more quantitative discussion of the shell effects is hindered by the uncertainties of the reported capture cross sections. Betz *et al.* (1971a) pointed out that residual ion excitation causes capture cross sections to decrease often by as much as a factor of ~ 2, so that an evaluation of the dependence of σ_c on q is fair only when corresponding states of residual excitation of the ions are compared, preferably ground states. Unfortunately, in most of the experiments it has not been determined to which excitation states the reported cross section values refer. Nevertheless, the existence of shell effects in the absence of residual ion excitation has been proven in several cases (Betz and Wittkower, 1972b). Further evidence for an anomalously decreased cross section $\sigma_c(7)$ of bromine and iodine ions may be seen in the fact that equilibrium charge state distributions of these ions often show slightly smaller values of the particular charge fraction $F(6)$ than one would expect from a smooth distribution (see Sec. V.4).

Dependence of σ_c on the ionic charge. It appears that apart from shell and excitation effects the over-all dependence of experimental single capture cross sections on the ionic charge q of heavy ions can be roughly approximated in the form

$$\sigma_c(q) \propto q^{a_c}. \tag{4.16}$$

The experimentally determined values of a_c may vary considerably depending on the different cases. There are strong indications for a systematic increase of a_c with the ion velocity, at least for charge states in the range around $\bar{q}$. Datz *et al.* (1970) find for bromine ions quite independent of the target gas (H_2, He, and Ar) a value of $a_c\approx 3.8$ at 13.9 MeV, and $a_c\approx 5.1$ at 25 MeV. Figure 4.1 shows for bromine ions $a_c\approx 2.0$, 2.7, and 3.2 at 6, 10, and 14 MeV, respectively, but no clear-cut dependence is revealed for iodine ions in helium, where a_c is between 2.5 and 3.0 (Fig. 4.2) at all investigated energies. Likewise, the results shown in Fig. 4.3 give $a_c\simeq 1.7$, 2.0, 3.1, and 3.7 for iodine ions in hydrogen at 5-, 10-, 15-, and 20 MeV, but no systematic trend is found for iodine at the same energies in oxygen where a_c lies between 2.0 and 2.5. For charge states which are close to $\bar{q}$ and smaller than a certain charge q_c, which will be discussed further below, Angert *et al.* (1968) deduced values between 2.3 and 5.4 for iodine ions passing through nitrogen (Fig. 4.5), and approximate their data by a purely empirical formula

$$\sigma_c = q^{3.81}(v_0/v)^{5.38}\times 10^{-16}\ [\text{cm}^2/\text{molecule}]$$
$$(q\lesssim q_c;\ 2\lesssim v/v_0\lesssim 4.5). \tag{4.17}$$

In addition, from their own work on iodine and from the investigations by Nikolaev *et al.* (1961a) on ions with atomic numbers in the range $2\leq Z\leq 7$ stripped in nitrogen, they approximate capture cross sections for $q\gtrsim q_c$, and find the semiempirical relation

$$\sigma_c(q, v) = 18.1q^{1.91}(v_0/v)^4\times 10^{-16}\ (\text{cm}^2/\text{molecule})$$
$$(q\gtrsim q_c). \tag{4.18}$$

Nikolaev *et al.* (1957) determined σ_c for nitrogen ions in nitrogen and argon, and approximate their results in the form

$$\sigma_c = 2\pi a_0^2 Z_T^{2/3} q^{5/2}(v_0/v)^5\ (\text{cm}^2/\text{atom}). \tag{4.19}$$

In a later study of nitrogen ions stripped in various gases, Nikolaev *et al.* (1961a) found that a_c increases from ~ 1.5 to ~ 3 in the velocity range $(2.6\text{–}8)\times 10^8$ cm/sec.

According to Eq. (4.11), Bohr and Lindhard assume that a_c does not depend on v and has a constant value which amounts to 3 in hydrogen and helium targets, and to 2 in heavier target gases. Likewise, Bell's calculations are consistent with $a_c=2$ (see Sec. IV.1.d), and do not account for the experimentally observed and sometimes systematic changes of a_c with the ion velocity. It is worth noting that an increase of a_c with v, at least in the range of charge states close to $\bar{q}$, is qualitatively consistent with the observation that the width d of equilibrium charge state distributions does not increase noticeably within wide ranges of ion velocitites. It has been shown in Sec. II that according to Eqs. (2.12) and (2.18), constant exponents a_c and a_l would lead to a broadening of the distributions when $\bar{q}$ increases. Thus, with a constant value of a_c, Bohr and Lindhard obtain the proportionality $d\propto(\bar{q})^{1/2}$ which could not be verified for ions with atomic numbers and velocities corresponding to typical fission fragments (see Sec. V.4.b).

Dependence of σ_c on Z. All explicit results from the theories outlined in Sec. IV.1 result in a strong dependence of σ_c on q, but do not predict an influence of Z. However, Angert *et al.* (1968) have demonstrated that there is a Z dependence which is quite pronounced in the cases they investigated. They plotted their capture cross sections according to Eq. (4.17) along

with values from other investigators interpolated for the same ion velocity. A typical result is shown in Fig. 4.6; for a given charge q, σ_c decreases when Z increases, provided that q is smaller than q_c. They conclude that q_c is a certain critical charge such that theoretical approaches which are based on the assumption that the capturing ion can be treated as a classical point charge during the collision are justified for $q \gtrsim q_c$, but break down for $q < q_c$ (see Sec. IV.1.d). Due to the limited data, an experimental determination of q_c is somewhat uncertain, but it seems that q_c depends at least on Z and v and, in the case of iodine ions, is substantially larger than $\bar{q}$. The data obtained by Datz *et al.* (1970), Betz *et al.* (1971a), and Betz and Wittkower (1972a) does not show an approach of a_c to values close to 2 or 3 when q increases, but their data does not extend to the energies which were used by Angert *et al.* Clearly, more experimental results are needed in order to clarify the situation.

If the observations and interpretation of q_c by Angert *et al.* are correct, formulas of the type of Eq. (4.11) or the more empirical approximations like Eq. (4.18) would not be valid in the range of charge states around $\bar{q}$, a range which is often of greatest interest, but could be used for $q \gtrsim q_c$, and perhaps even for extrapolations to very high charge states $q \gg \bar{q}$. On the basis of the present results it is still difficult to predict σ_c quantitatively for $q \gtrsim q_c$ because existing formulas for σ_c can be regarded as approximations only. For example, Eqs. (4.11) and (4.18) are different especially with regard to their velocity dependence though they give surprisingly close results for the particular case of ions passing through nitrogen with velocity $4.15 v_0$ (see Fig. 4.6).

Dependence of σ_c on the ion velocity. In qualitative agreement with theoretical estimates $\sigma_c(v)$ decreases with increasing ion velocity. This is also shown in Figs. 4.7 and 4.8. Quite independent of q, $\sigma_c(v)$ seems to have a maximum near $v \simeq v_0$ (see also Sec. IV.1.d and the discussion by Drukarev 1960, 1967). Since most of the data was obtained for ion velocities close to this maximum ($v/v_0 \leq 4.5$), a simple power function $\sigma_c(v) \propto v^{-p}$ can not be employed very successfully in order to describe the experimental results. When the power law is used, one finds that p increases monotonically from $\sim$0–2 at $v/v_0 \simeq 1$, to $\sim$4–6 at $v/v_0 \simeq 4.5$. In this range, no striking influence of Z_T is observable although it appears that p increases more strongly in light than in heavy targets. These results for bromine and iodine ions are similar to the ones obtained mainly for nitrogen and other light ions (Nikolaev *et al.*, 1961a). Furthermore, the general trend of $\sigma_c(v)$ for the investigated ions agrees with that of $\sigma_c(1, 0)$ for protons with the exception that p then assumes values which are larger by a factor of $\sim$2.

Based on theoretical assumptions, elaborated in Sec. IV.1, that those target electrons whose orbital velocities are close to the ion velocity are preferentially captured, one should expect p to increase much more in light targets than in heavy ones. When Z_T is large, ions of increasing velocity will still find target electrons with matching velocities, $u \simeq v$, i.e., electrons will then be captured from deeper shells. In the analogous case of protons, for example, Nikolaev (1966) shows that $\sigma_c(1, 0)$ decreases less rapidly whenever v comes close to the velocity u of target electrons.

Bohr and Lindhard's formula $\sigma_c(v) \propto v^{-3}$, Eq. (4.11), is intended to apply to typical fission fragments, i.e., also to $\sim$50-MeV iodine ions. However, on the basis of approximations of experimental results for iodine ions, Eq. (4.17) and Eq. (4.18), p was found to amount at least to 4 and possibly to larger values especially when q is close to $\bar{q}$.

Dependence of σ_c on Z_T. In general, $\sigma_c(Z_T)$ increases with Z_T, though this dependence becomes weaker for larger values of Z_T. At relatively low velocities of the order of v_0, σ_c does not depend dramatically on Z_T. Figure 4.8 shows, for example, that σ_c is only slightly smaller in hydrogen than in oxygen gas. The differences increase at higher ion velocities. Betz *et al.* (1971a) find almost identical capture cross sections for 14-MeV bromine ions ($v/v_0 = 2.66$) in hydrogen and helium (provided that the cross sections are given in units of cm^2/molecule); Datz *et al.* (1970) report cross sections ratios of 1:1.3:2.5 and 1:3:5 for bromine ions in hydrogen, helium, and argon at 13.9 MeV ($v/v_0 = 2.65$) and 25 MeV ($v/v_0 = 3.55$), respectively; Moak *et al.* (1968) found for 110-MeV iodine ions ($v/v_0 = 5.9$) ratios of $\sigma_c(12, 11)$ in hydrogen, helium, and argon which amount to 1:4:5.6, respectively. On the theoretical basis of Eqs. (4.11) and (4.12) one would expect much larger ratios in the above cases. Nevertheless, it may be concluded that the relatively small values of σ_c in hydrogen are responsible for the increase of the average equilibrium charge $\bar{q}$ relative to heavier target gases which is observed for very fast ions (see Sec. V.3.b).

An interesting anomaly of $\sigma_c(v)$ is observed especially in helium but also in other inert gases. In these cases, the maximum values of σ_c are unusually small and lie at considerably higher velocities. This effect can be seen in the data by Wittkower and Gilbody (1967) who measured capture cross sections $\sigma(1, 0)$ for neon, argon, and krypton ions passing through hydrogen and rare gases in the energy range 60–450 keV. Similar results have been obtained by Pivover *et al.* (1969) who studied $\sigma(1, 0)$ for lithium, sodium, and potassium ions in rare gases, and in sodium and potassium vapors at energies between 20 and 155 keV. They interpret the differences in the behavior of rare gases vs other gases on the basis of Drukarev's (1967) modified adiabatic criterion. The above experimental results are readily understood in view of the relatively large binding of the most weakly bound electrons in rare gases compared to other gases. For example, the first ionization potential of helium amounts to $\sim$25 eV, whereas it is $\sim$5 eV in sodium or potassium. Therefore,

it is reasonable to assume that it becomes difficult for slow ions with low charges to liberate electrons from, say, helium atoms. This corresponds to a decrease of the cross section σ' in Eq. (4.3) which leads to smaller capture cross sections. A further consequence of the steep decrease of $\sigma_c(v)$ for decreasing, low velocities in helium targets is an anomalous behavior of charge fractions (see Sec. V.3.b).

b. Multiple-Electron Capture

Table IV.1 contains a large number of multiple capture cross sections $\sigma(q, q-n)$ of heavy ions; some of the systematic trends are illustrated in Figs. 4.1–4.4, and in Fig. 4.9. As a rule, these cross sections are relatively small. For example, the ratio $k_{-2}=\sigma(q, q-2)/\sigma(q, q-1)$ amounts in all reported cases to less than $\sim 9\%$ in light targets. Most investigators encountered considerable difficulties in measuring double capture cross sections of heavy ions (see Sec. III.2), and experimental errors $\delta\sigma(q, q-2)$ are seldom below $\sim 50\%$. The problems are magnified in the case of cross sections for capture of more than two electrons, and results for $n>2$ have not been reported for ions with $Z>9$. We will, therefore, concentrate mainly on the discussion of double electron capture.

Figures 4.1–4.4 demonstrate that $\sigma(q, q-2)$ generally increases with the initial charge of the capturing ions. In most cases, bromine and iodine ions show a characteristic discontinuity in $\sigma(q, q-2)$ for $q=8$ which is just outside the error limits. Independent of the investigated target gases, $\sigma(8, 6)$ is smaller than $\sigma(7, 5)$. Betz *et al.* (1971a) attribute this effect to the influence of the $M\rightarrow N$ and $N\rightarrow 0$ shell transitions, respectively. As has been found in the case of single-electron capture, a final state appears to be somewhat less favored when electrons are to be captured into a new principal shell. Apart from these and other possible distortions, it is apparent that cross sections for double capture increase more strongly with q than the ones for single-electron capture. In all the data shown, $k_{-2}(q)$ increases with q, but it is not evident whether it reaches a constant value or decreases for $q\gg\bar{q}$. Figure 4.9 displays k_{-2} for 15-MeV iodine ions in oxygen, and k_{-2} increases from ~ 4 to 21% in the range of charge states between 5+ and 11+. The largest values have been found for 5-MeV iodine ions in oxygen where k_{-2} reaches 36% for $q=7+$ (Fig. 4.3).

It is a quite general observation that k_{-2} decreases when the ion velocity becomes higher, and increases—sometimes nonmonotonically—when targets with larger atomic numbers are used. The former observation implies that $\sigma(q, q-2)$ decreases more steeply with v than the single capture cross sections. As an example, it may be mentioned that the largest values of k_{-2} measured for iodine ions decrease in hydrogen from 9% at 4.5 MeV to 2.3% at 20 MeV, and in oxygen from 36% at 5 MeV to 8% at 20 MeV. The values in helium are mostly comparable though somewhat larger than the ones in hydrogen. Furthermore, k_{-2} increases with the nuclear charge of the projectile ions though shell effects may sometimes lead to nonmonotonic changes. These results agree qualitatively with the findings by Nikolaev *et al.* (1961b) for ions with $Z<18$ and $Z=36$ with initial charge states $q<7$ passing through gases of helium, nitrogen, argon, and krypton. Extending measurements of similar kind to higher velocities, Macdonald *et al.* (1971, 1972) investigated cross sections of oxygen and fluorine ions in helium, nitrogen, and argon and found characteristic maxima in the dependence of k_{-2} on the ion velocity.

Nikolaev *et al.* (1961b) point out that despite their smallness multiple capture cross sections have a decisive influence on equilibrium charge state distributions; most of the ions with $q\ll\bar{q}$ will in fact be formed by simultaneous capture of several electrons. This is easily understood by comparing the transition rates $\sigma(q', q)\times F(q')$ for a given charge state q under equilibrium conditions.

A theoretical treatment of double capture by helium nuclei in helium has been given by Gerasimenko and Rozentsveig (1956). The calculated values differ by a factor of only ~ 2 from comparable experimental results. Nikolaev (1965) relates measured values of $k_{-2}(q)$ to the ionization potential I_{q-2} of light ions and finds $k_{-2}\propto I_{q-2}^{3/2}$, provided that $k_{-2}<10\%$. Obviously, the probability for capturing several electrons in a single encounter depends critically on the degree of ion excitation. The total excitation I_t^* of an ion of initial charge q after effective capture of n electrons must be smaller than I_{q-n} and, thus, capture must proceed largely into ground states, especially when $n>2$. Otherwise, $I_t^*>I_{q-n}$ will lead to the ejection of one or more electrons due to rearrangement processes. Since electron capture by fast heavy ions is likely to occur preferentially into excited states at least for charge states $q\simeq\bar{q}$ (see S3c. VI.1), one may argue that I_t^* exceeds I_{q-n} after most collisions with $n\gtrsim 2$; i.e., it is not possible that all of the initially captured electrons remain bound. This implies that the probabilities for initial capture of more than one electron are higher than the actually observed values. Furthermore, residual excitation of the ions prior to the capture process must be expected to reduce multiple electron capture probabilities by a substantial amount.

Multiple capture cross sections with $n>2$ have not been reported for ions heavier than argon although one should expect these processes to occur with small probabilities provided that the target contains atoms or molecules with at least n electrons. Experimental difficulties in measuring a small cross section $\sigma(q_i, q_i-n)$ via nonequilibrium charge state distributions arise when the direct transition rate $\sigma(q_i, q_i-n)Y(q_i)$ due to the ions incident with charge q becomes much smaller than second-order rates such as $\sigma(q_i-n+1, q_i-n)\times Y(q_i-n+1)$. Additional complications may be bothersome when residual ion excitation becomes influential

(see Sec. III.2). These difficulties are generally more severe for heavy than for light ions and are partly responsible for the lack of data on $\sigma(q, q-n)$ with $n>2$.

c. Single-Electron Loss

Experimental cross sections $\sigma(q, q+1)$ for the loss of a single electron by heavy ions in collisions with target atoms are contained in Table IV.1, and selected cases are shown graphically in Figs. 4.1–4.5, 4.7, and 4.8. Most of the data has been obtained for bromine and iodine ions passing through hydrogen, helium, nitrogen, and argon at energies which were usually below $\sim$65 MeV, except in a few cases of 110- and 162-MeV iodine ions. The accuracy of the reported cross sections is often close to $\sim$10%, except when $\sigma(q, q+1)$ becomes relatively small, i.e., when $q \gg \bar{q}$.

The probability $\sigma(q, q+1)$ decreases when the ions are in higher charge states. Figures 4.1–4.5 illustrate this trend for bromine and iodine ions. It appears that $\sigma(q, q+1)$ decreases more steeply in light targets than in heavy ones, especially when $q \gg \bar{q}$. The rate of decrease varies with q and a simple power function $\sigma(q, q+1) \propto q^{-a_l}$, Eq. (2.17), or an exponential function $\sigma(q, q+1) \propto \exp(-\alpha_l q)$, Eq. (2.10), are good approximations only within limited ranges of charge states. When q is close to $\bar{q}$, a_l is in general of comparable but somewhat smaller magnitude than the corresponding exponent a_c for single capture cross sections. Möller *et al.* (1968) find that a_l is only slightly larger than unity (Fig. 4.5)—in contrast to Bohr and Lindhard's theoretical estimate $a_l=3$, Eq. (4.10). There is no obvious systematic variation of a_l with the ion velocity which is clearly outside the experimental errors; however, the data are too limited to allow further generalizations to be made on a simple basis.

No striking shell effects have been observed in the loss cross sections though slight indications for a possible influence of the ions shell structure have been discussed by Betz *et al.* (1971a), and Betz and Wittkower (1972a). In many cases in which the accuracy of the experimental cross section values was better than $\sim$10%, $\sigma(q, q+1)$ exhibits a step structure such that $\sigma(4, 5)$ and $\sigma(6, 7)$ of bromine and iodine ions are somewhat larger than a smoothed trend would suggest. Since initial charge states 4+ and 6+ correspond in both cases, and for both ion species, to ion configurations with a single electron outside a closed shell, the enhancement of the loss cross sections appears plausible. A stronger shell effect can hardly be expected because a large number of outer electrons contribute to the loss cross section per ion, thereby diluting the influence of particular electrons.

Figures 4.7 and 4.8 illustrate a typical velocity dependence of single-electron loss cross sections. In the velocity ranges investigated for bromine and iodine ions, $\sigma(q, q+1; v)$ shows a broad maximum whenever the velocity of the most weakly bound ionic electron, approximated by $u_q=(2I_q/m_e)^{1/2}$, approaches the ion velocity. Though the experimental data for heavy ions allows only an approximate estimate of the location of these maxima to be made, it is evident that they are shifted to velocities u_m which lie noticeably above u. It has been noted in Sec. IV.1.d that the theoretical expectation $u_m \simeq u_q$ is based on a simple adiabatic criterion. The experimentally observed deviations from that rule, sometimes as large as $u_m/u_q \simeq 2$ even for nitrogen ions, are most likely a consequence of the approximate character of the criterion. In particular, it is not clear what kind of orbital electron velocities one should use. For example, as has been noted before and will be elaborated in Sec. V.2.c, the expectation value of the kinetic energy may be much larger than the binding energy of an electron in a multielectron atom or ion. On this basis, one could often argue that the relevant velocity u_q is significantly larger than the one discussed above. Furthermore, effects of differing target atoms and of the contributions of more tightly bound inner electrons in the ion to the single-electron loss probability per ion have been disregarded. In addition, a serious question has arisen due to the discrepancy of Massey's criterion and experimental results with Bohr and Lindhard's prediction Eq. (4.10). On the one hand, $\sigma(q, q+1; v)$ is expected to show a maximum near $v=u_q$; on the other hand, Eq. (4.10) predicts a dependence $\sigma_l \propto v^2$ in this velocity range, i.e., in the range where according to Sec. IV.1.a, Sec. V.1.a, and Sec. V.2.c the charge q is close to $\bar{q}$ and, thus, $\sigma_c(q) \simeq \sigma_l(q)$. In view of the data, it must be concluded that neither theoretical approach is strictly applicable though it must be stressed that the adiabatic criterion is at least qualitatively of considerable usefulness.

The data in Table IV.1, Figs. 4.7, and 4.8 show that σ_l generally increases with Z_T, but the differences among various targets depend on both q and v. For example, σ_l of iodine ions stripped in hydrogen and oxygen differ substantially for higher charge states, but are very close to each other for low-charge states. Dmitriev (1962a) studied single-electron loss by ions in the range $2 \leq Z \leq 18$ and $Z=36$ with velocities between 2.6 and 12×10^8 cm/sec. The results are in reasonable qualitative agreement with the above. These authors and, in a later review, Nikolaev (1965) work out a close relation between $\sigma_l(q)$ and the number of electrons in the outer shell of the ions which lose an electron in a single collision. This concept, however, is not readily applied in the case of heavy ions where inner electrons contribute significantly to the single loss cross section.

d. Multiple-Electron Loss

The probabilities for loss of several electrons as a result of a single collision of a heavy ion with a target atom or molecule are very interesting quantities which receive appreciable attention, and not only from those investigators who are primarily concerned with phenomena of charge exchange. Bohr (1948) and Bohr and Lindhard (1954) assumed, as has been discussed in

Sec. IV.1.a and Sec. IV.1.c, that the maximum energy transfer in an ion–atom collision is given by $2m_e v^2$, corresponding to classical impact of a heavy target core and an electron in an ion with the relative velocity v. Thus, in their calculation of single-electron loss cross sections, only those ion electrons are assumed to contribute to the total loss which have orbital velocities $u \leq 2v$. Consequently, multiple electron loss is severely hindered. Nevertheless, Bohr and Lindhard state that there is considerable probability that several electrons are lost or captured by the ion, though they do not give further estimates—neither do other authors.

Experimental results on cross sections $\sigma(q, q+n)$ of heavy ions have shown that simultaneous loss of n electrons occurs with extremely high probabilities even when n is large. Systematic measurements have been performed by the groups at Heidelberg (Betz *et al.*, 1966; Möller *et al.*, 1968), Oak Ridge (Moak *et al.*, 1968; Datz *et al.*, 1970), and Burlington-Cambridge (Betz *et al.*, 1971a; Betz and Wittkower, 1972a) with energetic beams of arsenic, bromine, and iodine. These and other results are listed in Table IV.1, and are partly shown in Figs. 4.1–4.4, 4.9, and 4.10. The ratio k_2 between double and single loss of iodine ions is often as large as $\sim 60\%$ in heavy targets ($Z_T \gg 7$), $\sim 50\%$ in helium, and $\sim 25\%$ in hydrogen (Fig. 4.10). In general, k_2 increases with both Z and Z_T, but decreases when v is increased. The dependence on q is mostly weak though no clear-cut trend has been observed (compare Figs. 4.1–4.4, and 4.9). As regards k_n especially for $n > 2$, there is a dramatic difference between light and heavy targets. In hydrogen and helium, k_n decreases rapidly with increasing n, but in heavier gases such as nitrogen, oxygen, or argon, k_n decreases slowly with n. For example, Fig. 4.10 illustrates that the probability of simultaneous loss of eight electrons by 15-MeV iodine ions of initial charge 5+ in oxygen amounts to almost 6% of the single loss cross section $\sigma(5, 6)$. Likewise, Moak *et al.* (1968) found $k_8 \simeq 4\%$ for 110-MeV iodine ions with initial charge 12+ in argon. Although multiple-loss cross sections have not been measured directly for $n > 8$, it is known that the maximum number of loss electrons can be much higher; for example, 12-MeV iodine ions with initial charge 5+ may lose as many as 27 electrons in a single encounter with a xenon atom (Kessel, 1970). The large probabilities for multiple-electron loss result (in the absence of equivalent multiple capture cross sections) in pronounced asymmetries of equilibrium charge state distributions; this can be explained on simple mathematical grounds (Sec. II.3) and agrees well with experimental evidence (Sec. V.4.c).

There is little doubt about a qualitative explanation of the observed effects. Following the discussion by Dmitriev *et al.* (1962b), we distinguish two basically different processes: (i) direct ionization and (ii) quasi-molecular collisions. As regards (i), individual electrons in an ion are lost via a direct interaction with atoms of the medium. In particular, the loss of an individual electron occurs independent of the presence of other electrons in the ion. Obviously, this mechanism applies primarily to the loss of electrons from outer shells and is the only relevant mechanism of electron loss by light ions or, more generally, by ions which contain very few electrons. Furthermore, this mechanism is not likely to give rise to exceedingly large multiple-electron loss cross sections and, in fact, light ions show relatively modest values of k_n (Dmitriev *et al.*, 1962b). As regards (ii), it is now well established that heavy ions in collisions with heavy targets form pseudomolecular states and emerge—immediately after the collision—in highly excited states, often with vacancies in inner shells (see, for example, Fano and Lichten, 1965; Lichten, 1967). Thus, loss of many electrons ($n \gg 1$) proceeds through the promotion and level crossing mechanism. This mode of excitation (and ionization) has also been referred to as Pauli excitation (Brandt and Laubert, 1970). In addition, rearrangement processes such as the decay of inner-shell vacancies via Anger processes lead to further ionization. Incidentally, it has been argued that extremely high-charge states of fast heavy ions are already present *before* such inner shell vacancies decay (Betz *et al.*, 1972). In this light, it is understandable that k_n remains small in light targets which can not produce sufficient shell overlap in collisions with heavy ions. Since processes (i) and (ii) are dominant for low and high values of n, respectively, one may speculate that the region of overlap of the two processes is just that range of n in which k_n shows a decrease with n which is significantly weaker than for both lower and higher values of n. This effect is clearly visible near $n = 5$ in Fig. 4.10. Further evidence for multiple ionization events is discussed in Sec. V.4.e. Incidentally, the scattering of heavy ions which results from close collisions with heavy targets is not necessarily much larger than the divergence of the ion beam; for example, when 12-MeV iodine ions collide with xenon with an impact parameter such that the L shell overlap ($2r_0 \simeq 10^{-9}$ cm), as many as 25 electrons may be finally lost but the ion is scattered by no more than approximately one degree.

Finally, we note that the hard collisions which involve inner-shell penetration cannot be described when either collision partner is treated as a point charge. It is also interesting to point out that multiple-electron loss and capture are based on essentially different processes. In particular, high excitation of ions in collisions reduces multiple capture but enhances multiple loss. Little is known about the times which are necessary to complete the rearrangement processes of ions initially highly excited. When these times are longer than the actual collision time, implications will arise with regard to stripping in large molecules or solids (see Sec. VI.2.b). Given the qualitative understanding of multiple-electron loss, one may hope that more satisfactory theories can be worked out in the future.

e. Nonadditivity of Charge-Changing Cross Sections in Molecular Targets

It has sometimes been suggested that it may be possible to predict electron capture and loss cross sections in complex molecules simply by adding together the individual cross sections for each atom in the molecule. For example, Toburen *et al.* (1968) and Dagnac *et al.* (1970) have employed such a rule quite successfully for some electron capture and loss cross sections of hydrogen projectiles passing through a variety of gases. As theoretical justification of that rule, it has been argued that at high enough velocities of the incident particle, the target molecule appears as an assembly of individual atoms whereby the molecular forces are negligible. Wittkower and Betz (1971b) measured charge-changing cross sections $\sigma(5, q)$ for 12-MeV iodine ions passing through H_2, N_2, O_2, CO_2, N_2O, CH_4, and C_3H_6O and found that no simple rule can accurately describe the cross sections for the complex molecules on the basis of cross sections for the single atoms (compare Table IV.1). In particular, they found no evidence for a general additive rule. For example, the cross sections obtained for C_3H_6O are significantly smaller than any possible addition of cross sections for its components, and the single capture or loss cross sections for C differ substantially when determined from $\sigma(CO_2)-\sigma(O_2)$ and $\sigma(CH_4)-2\sigma(H_2)$. On the other hand, it appears that the use of the additive rule for hydrogen projectiles is too successful to be fortuitous; the divergent results point out the difference of the charge exchange mechanism in these two cases.

Tuan and Gerjuoy (1960) showed in a theoretical paper that an additive rule is incorrect even in the case of electron capture by fast protons in mono- and diatomic hydrogen. However, the available experimental results with protons prove these differences to be fairly small. On the basis of the results shown in Sec. IV.1 it must be assumed that the relatively small binding in molecular targets is easily overcome by heavy ions which have a high charge and travel with high speed. Nevertheless, one must conclude from the failure of the additive rule that a collision between heavy ions and a complex molecular target cannot be treated as a sequence of successive collisions with the individual target atoms. A convincing explanation has not yet been given. Wittkower and Betz argue that collisions of heavy ions and protons differ in many aspects. For example, it is possible for more than one electron in heavy projectiles to interact with the target at the same time, and ion excitation may play an important role. Still, the nature of these complex collisions is not sufficiently understood, and we cannot yet predict heavy-ion cross sections in molecular targets even if we know the cross sections for all of their components. Finally, it is interesting to note that an additive rule, the so-called Bragg rule, appears to hold reasonably well for a description of the energy loss of heavy ions in molecular targets (Northcliffe and Schilling, 1970). This may be understood when one takes into account that energy loss is a more statistical quantity as compared to a specific charge changing probability, and contains averages of the influence of many different collision processes.

V. AVERAGE EQUILIBRIUM CHARGE STATES AND EQUILIBRIUM CHARGE STATE DISTRIBUTIONS

In this section we present a detailed discussion of the average equilibrium charge, $\bar{q}$, of heavy ions stripped in gaseous ($\bar{q}_G$) and solid ($\bar{q}_S$) targets, and of the actual distribution, $F(q)$, of charge states which are centered around the mean. On the one hand, these quantities are of great theoretical interest and their understanding requires thorough knowledge of atomic collision phenomena. On the other hand, the composition of charge states in a heavy-ion beam is of decisive importance for many practical purposes. Increasing activity in heavy-ion work makes it desirable to have extensive and accurate information about charge state distributions. This is vital, for example, for the design of charge converters (strippers), heavy-ion accelerating systems, and for the detection of heavy ions emerging from equilibrium targets. Limited theoretical calculations have been performed in order to obtain $\bar{q}$ for heavy ions penetrating through dilute gases. Qualitatively, the calculated results are sometimes in fair agreement with experimental ones, but none of these theories, all of which were published prior to 1953, allows the prediction of $\bar{q}$ both with sufficient accuracy and over large ranges of projectile species and velocities. However, it will be shown that a proper application of the well-known criterion by Lamb (1940) and Bohr (1940, 1941) is quite useful for the calculation of average charge states in gaseous targets.

No quantitative theory is available for average equilibrium charge states which are produced by solid targets. For very light ions, $\bar{q}_S$ differs very little from $\bar{q}_G$, but for heavy ions, $\bar{q}_S$ exceeds $\bar{q}_G$ often by more than a factor of 2. Interestingly, the mechanism of that effect has not yet been completely explained, and it is still being disputed whether the large increase is produced *inside* or *outside* the solid. This lack of understanding points out the great complexity of heavy-ion charge-changing collisions.

During the past 20 years, considerable efforts have been made to investigate $\bar{q}$ and $F(q)$ experimentally for a great variety of ions and targets. Especially for $\bar{q}$, quite representative experimental data has now been accumulated. Based on observed regularities and on simple theoretical grounds, many investigators were able to develop useful semiempirical techniques. Thus, it became possible to interpolate and, to some extent, extrapolate existing data on $\bar{q}$. It is far more difficult to systematize the existing experimental results on $F(q)$. Width and asymmetry of the distributions are sensitive

parameters, and more measurements need to be done in order to allow the desired generalizations to be worked out.

1. Theoretical Calculations of Average Equilibrium Charge States in Diluted Gases

The first theoretical estimates for average charge states were given by Bohr (1940, 1941), Lamb (1940), Knipp and Teller (1941), and Brunings, Knipp, and Teller (1941). These authors attempted primarily to calculate the energy loss of uranium fission fragments which was believed to vary approximately with the root mean square value of the actual charges carried by the fragments during the slowing down process. In order to obtain these charge states, it is necessary, in principle, to perform very detailed calculations of the probabilities for electron capture and loss by the fast fragments. However, since it has been realized that such an undertaking is far too difficult to be readily carried out in practice, all of the authors named above based their estimates for average charge states on general grounds rather than on calculations of individual charge changing cross sections. For the sake of clarity, it should also be noted that in the following only those parts of the cited references which deal with the direct calculation of the average ionization will be discussed, while those parts which connect $\bar{q}$ with the energy loss or, in turn, deduce $\bar{q}$ from results of energy loss measurements, will be disregarded. Some remarks on that latter vital question can be found in Sec. V.5.

a. Bohr's Criterion

Bohr presented pioneering contributions concerning the problem of average charge states of fission fragments. His ideas were first indicated in two brief notes (Bohr, 1940, 1941), and are described in greater detail in a comprehensive article on atomic collisions (Bohr 1948), and in a paper dealing exclusively with electron capture and loss by heavy ions (Bohr and Lindhard 1954). As regards the average charge, Bohr assumes that a fast heavy ion penetrating through rarified gases retains all of its electrons which have orbital velocities which are greater than the velocity of the ion. The electrons with smaller velocities are torn off by collisions, whereas the removal of electrons of higher velocity is very improbable since for such electrons the collision is adiabatic (compare Sec. IV.1.a). This physically reasonable criterion serves as a most important basis for many further theoretical and semi-empirical treatments. Its approximate validity has been proven well enough so that one can conclude that, in a first-order approximation, it reduces the problem of calculating $\bar{q}(Z, v)$ to a calculation of orbital velocities of electrons in ions, $u(Z, q)$. In an attempt to derive an analytical expression for that dependence, Bohr introduces the electronic velocity $u=Z^*v_0/\nu^*$, where Z^* is a measure of the strength of the field in the region in which the electron is bound, as compared with the field of a hydrogen nucleus, and ν^* is the so-called effective quantum number. According to Bohr, Z^* approximately represents the number of electrons with velocities smaller than u. Consequently, $Z^*\simeq\bar{q}$, and, with $u=v$, he arrives at

$$\bar{q}=\nu^*v/v_0. \tag{5.1}$$

Furthermore, Bohr argues that for the most loosely bound electron in the ground state of an ion, over a large intermediate region of q, ν^* will have a flat maximum corresponding to values close to $Z^{1/3}$, a result which is in conformity with the analysis of the electron binding by the Thomas–Fermi statistical method. For $\bar{q}$ close to, but not larger than $Z/2$, this yields the well-known formula

$$\bar{q}/Z=v/(v_0Z^{2/3}), \qquad (1<v/v_0<Z^{2/3}). \tag{5.2}$$

When this equation is used, it should be kept in mind that its range of validity is restricted. Bohr emphasizes that ν^* naturally decreases when q becomes larger or much smaller than $Z/2$. In the extreme cases of ionizations close to zero or Z, the values of ν^* approach unity. Since Eq. (5.2) does not take into account that decrease of ν^*, it overestimates $\bar{q}$ in most cases. Let us consider the example of iodine ions for which Bohr's estimate is $\nu^*=3.75$. It is possible to re-evaluate ν^* according to its definition $\nu^*=qv_0/u$, where u denotes the velocity of the most weakly bound electron in the ion. In as much as u can be computed from the relevant ionization potential (see Sec. V.2.c), one obtains for, say, $q=20$, the much smaller value $\nu^*=2.95$. But even in the range where $\bar{q}/Z$ is close to and somewhat smaller than $Z/2$, Eq. (5.2) leads to values which are 20%–30% too high. In view of the approximations for Z^* and ν^*, better agreement can hardly be expected.

The above discussion shows that, in agreement with Bohr's expectations, Eq. (5.2) is useful only for rough approximations. But it is important to emphasize that Eq. (5.2) does not reflect the full content of Bohr's criterion. It will be shown in Sec. V.2.c that a more accurate application of the criterion allows much closer estimates to be made for average charge states, provided that the relevant orbital velocities u can be computed with sufficient accuracy. Incidentally, it is interesting to apply Bohr's criterion to the extreme cases where $\bar{q}$ approaches Z: one would then expect that ions become almost fully stripped at velocities $v\simeq Zv_0$. Within the expectations, this has been verified experimentally for many light ions with $Z\leq 18$ (see, for example, Heckmann *et al.*, 1960, 1963) and is also generally accepted for heavy ions, though it must be realized that, especially for these extreme cases, the criterion can not be claimed to be a rigorous one.

Before more sophisticated calculations of $\bar{q}$ are discussed, it is essential to note that Bohr's criterion could be defined precisely only when ions were present in a single charge state. Then, in its simplest interpretation,

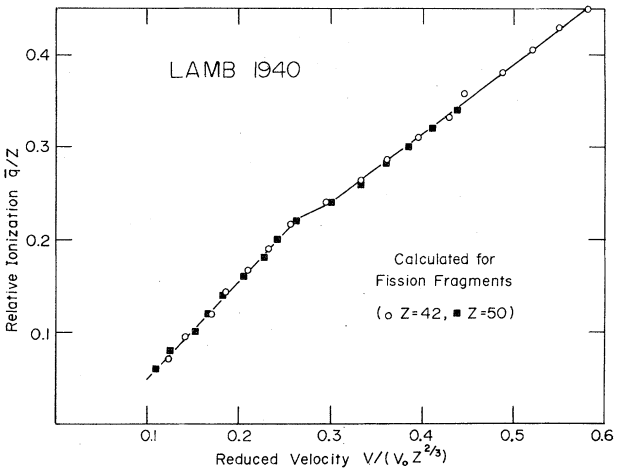

FIG. 5.1. Average relative equilibrium ionization of ions of nuclear charge 42 and 50 calculated by Lamb (1940) for a dilute gas stripper, plotted as a function of the reduced ion velocity $v/(v_0Z^{2/3})$.

the condition that, on the average, electrons with $u>v$ remain bound, defines a step function $\bar{q}(v)$ which jumps up by one unit of charge whenever v increases to the value equal to the velocity of the next inner electron. However, in practical cases where ions penetrate through a target at a given velocity, one has to deal with a distribution of charge states. Then, $\bar{q}$ becomes a continuous function of v so that Bohr's criterion can be satisfied only on the average, and the question arises how the original step function should be smoothed. This problem is particularly critical when the charge distribution extends across two different principal atomic shells.

It may be added that no new information about average charges is obtained when one equates Bohr's cross sections for electron capture and loss, Eqs. (4.10) and (4.11). The reason for that is that σ_l contains the effective charge of the target atoms which Bohr estimates directly from his criterion on average charge states. Thus, in his cursory estimates, Eq. (5.2) is introduced into the formula for σ_l rather than following from σ_l and σ_c.

b. Lamb's Approach

Independent of Bohr's work, Lamb (1940) determined the average charge $\bar{q}(v)$ of fission fragments by energetic considerations. He assumes that the fragments will be stripped down until the ionization potential of the next stage of ionization is greater than the kinetic energy of electrons which, relative to the ion, bombard the fragment with a velocity v. As in Bohr's derivation, this means essentially the neglect of the binding of the target electrons and of any specific effects from the target atoms. In his calculations for $Z=42$ and $Z=50$, Lamb estimates the required successive ionization potentials of these elements by the Thomas–Fermi method. However, since, as is to be expected, the statistical model gives too low ionization potentials for the first few charge states, he takes semiempirical values for $q\lesssim 6$. In order to compare his tabulated results for the two ions with results from other investigators, it is convenient to plot the relative ionization $\bar{q}/Z$ as a function of the reduced velocity $v_r=v/(v_0Z^{2/3})$. Figure 5.1 shows that his results conform well with such a dependence. Knipp and Teller (1941) pointed out an apparent weakness of Lamb's arguments: on the one hand, target electrons cannot rigorously be considered as free, and on the other hand, collisions with free electrons must not necessarily lead to ionization when Lamb's condition is fulfilled. However, as also stated by Knipp and Teller, the main justification of Lamb's assumption may be seen in its particular relation to Bohr's criterion. Theoretically, Lamb's method of treatment would be identical with the one by Bohr if all electrons would move in a Coulomb field, i.e., if the virial theorem could be applied to each electron in the ion. The latter theorem, however, is valid only with regard to the total ion (Löwdin, 1959) and, thus, one must expect certain differences between Bohr's and Lamb's methods. It will be shown in Sec. V.2.c that these differences are very decisive, and that Lamb's approach yields results which are in good agreement with experiment.

c. Statistical Method of Knipp, Teller, and Brunings

Knipp and Teller (1941) assume, in agreement with Bohr, that $\bar{q}$ depends primarily on the ratio of electronic to ionic velocities. As a measure of the velocity of the most loosely bound electron within the ion, they take the root mean square value, $\bar{u}$, of this velocity calculated from the Thomas–Fermi model. The statistical model allows one to represent the ionic charge q as a function of $\bar{u}$

$$q/Z=f[\bar{u}/(v_0Z^{2/3})], \tag{5.3}$$

where f has been evaluated numerically. In subsequent studies, Brunings and Knipp (1941) and Brunings, Knipp, and Teller (1941) refine the above method. They show that the universal dependence of q on $\bar{u}/Z^{2/3}$ is obtained only for large values of Z, whereas the function of f changes for smaller Z. In the cases which they present, $Z=6$ and $Z=10$, $\bar{q}/Z$ decreases by approximately 10% and 5% compared to large Z. Knipp and Teller also indicate that a transition from Eq. (5.3) to a universal relation $\bar{q}/Z=f(v/Z^{2/3})$ is not easily performed without ambiguities. In fact, when $\bar{u}=v$ is assumed, the average ion charge will lie between q and $q+1$ and may be close to $q+\frac{1}{2}$. Hence, Eq. (5.3) represents an upper envelope of Bohr's step function mentioned above, and, for a given value of $\bar{q}=q$, the corresponding value of v should be read at $q+\frac{1}{2}$ from the curve Eq. (5.3), averaged between q and $q+1$.

In a modification of Bohr's criterion, Brunings *et al.* introduce a more general relation between the chacteristic electron velocity and the ion velocity, $u=\gamma v$,

where the adjustable parameter γ serves to correct possible insufficiencies of Bohr's criterion. However, they determine values of γ from energy loss measurements; therefore, their results for γ do not allow a direct evaluation of the validity of Bohr's criterion. It should also be noted that they make the alternative supposition that the characteristic velocity is equal to the root mean square velocity of the *outermost* electron of the Thomas–Fermi distribution for the ion. The resulting ionizations are, especially for $\bar{q}/Z<0.8$, much larger than the ones obtained from Eq. (5.3) and lie mostly above Bohr's estimate Eq. (5.2). In contrast, for $\bar{q}/Z \lesssim 0.3$, their first estimate which is based on the velocity of the most weakly bound electron is substantially lower than the one by Lamb. They attribute this latter discrepancy to the apparent violation of the virial theorem in Lamb's approach (however, see Sec. V.2.c).

d. Bell's Method

A computation of the average charge of particular fission fragments which is not based directly on Bohr's criterion has been performed by Bell (1953). Using his numerical estimates for electron capture and loss cross sections (Sec. IV.1.b), he derived $\bar{q}(v)$ for the two fragments with nuclear charges 40 and 50, stripped in oxygen gas in the velocity range $2 \lesssim v/v_0 \lesssim 8$. When $\bar{q}/Z$, taken from his graphically shown results, is plotted as a function of $v/(v_0 Z^{2/3})$, one obtains almost a single curve for both fragments (Fig. 5.2). Only at relative ionizations below 0.3 do the charges for $Z=40$ fall slightly below the ones for $Z=50$. The latter trend is in qualitative agreement with the one obtained by Brunings *et al.* (1941), though Bell's values lie much higher for $\bar{q}/Z<0.3$, and are very close to Lamb's estimates.

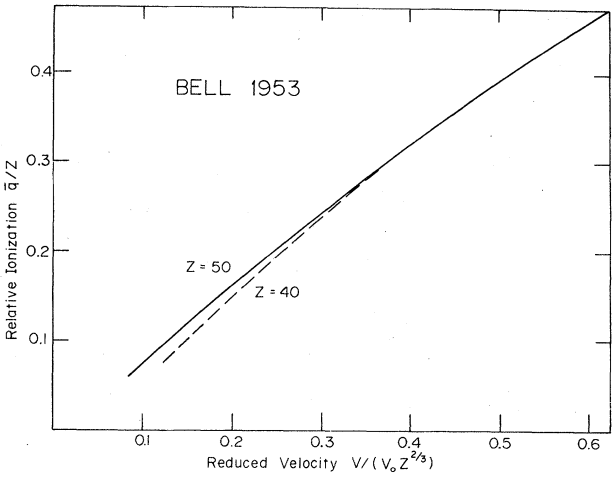

FIG. 5.2. Average relative equilibrium ionization of ions of nuclear charge 40 and 50, calculated by Bell (1953) for a low-density oxygen target, plotted as a function of the reduced ion velocity $v/(v_0 Z^{2/3})$.

2. Experimental Results and Comparison with Theory

a. Experimental Data

A complete tabulation of experimental results on equilibrium charge state distributions of ions with $3 \leq Z \leq 92$ has been prepared by Wittkower and Betz (1972a). Their Tables list $F(q)$ as well as $\bar{q}$, d, and s. The extensive results obtained by the groups at Oak Ridge have been reported by Moak *et al.* (1968) and Datz *et al.* (1971). Table V.1 lists the major portion of the available data on average equilibrium charges of ions with $Z \geq 16$, stripped in gases and solids with intermediate atomic numbers at energies up to 180 MeV. The data measured by the groups at Burlington and Cambridge (Ref. i, k, l, and m) has been measured using a short target cell ($L=2.83$ and 3.65 cm) and is influenced by the density effect (see Sec. VI), whereas the other data refer to longer collision chambers in which charge state equilibrium is reached at a lower gas density, and which better fulfill the condition for "dilute" target gases. Most of the data has been taken from the original data tables. In a few cases, apart from experimental uncertainties, the listed data could be slightly ambiguous due to one or more of the following circumstances: data was read off small graphs; the projectile mass was not specified (the mass was then assumed to be that of the most abundant isotope); it was not noted whether the projectile energy referred to the initial or to the final beam (the former possibility was then adopted); it was not indicated whether the condition for charge equilibrium had been verified; the influence of the density of target gases was not taken into account; and finally, it may be possible that mainly due to the technical difficulties in early heavy-ion experiments, the identification of the projectile ions and exact determination of the ion energy remained somewhat uncertain.

b. Comparison with Theory

In Fig. 5.3, the relative equilibrium ionization $\bar{q}/Z$ in gaseous strippers, taken from Table V.1, is plotted as a function of the reduced velocity $v_r=v/(v_0 Z^{2/3})$. Also shown are the various theoretical estimates discussed above.

As is to be expected from the Thomas–Fermi model, all of the data are roughly approximated by a universal function which depends only on v_r. A function $f(v_r)$ could be chosen such that it reproduces the data shown in Fig. 5.3 within $\pm 12\%$. However, as has been indicated by Brunings *et al.* (1941), there is the systematic trend that, for a given v_r, $\bar{q}/Z$ is smaller when Z decreases, i.e., rather than with a universal function, the data seems to be represented much better when a group of distinct functions $f_Z(v_r)$ which have decreasing values when Z becomes smaller is introduced.

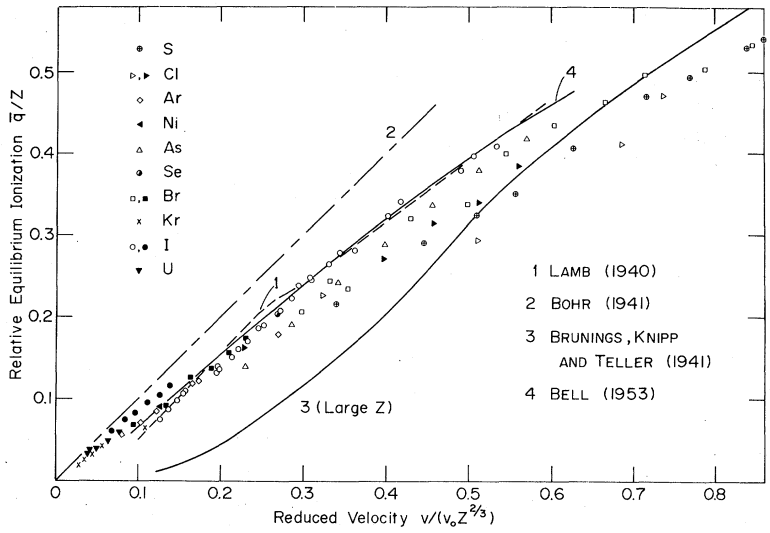

FIG. 5.3. Theoretical and experimental results for the average relative equilibrium ionization of heavy ions passing through gaseous targets, plotted as a function of the reduced ion velocity $v/(v_0 Z^{2/3})$. Theoretical curves: 1, Lamb (1940); 2, Bohr (1941); 3, Brunings, Knipp, and Teller (1941); 4, Bell (1953). Curve 3 is the result for large Z (fission fragments) which has been calculated under the assumption that the characteristic electron velocity in Bohr's criterion is the one of the most weakly bound electron in the ion. Experimental results for ions with nuclear charges in the range $16 \leq Z \leq 92$, stripped in nitrogen, oxygen, and air are taken from Table V.1. The full symbols refer to experiments in which a dense gas target has been used, and the open symbols refer to data which has been obtained in more dilute gas strippers.

The theoretical curves of Lamb and Bell for fission fragments, $Z=40$, 42, and 50, agree very well with the data for iodine ions, whereas the curve derived by Brunings *et al.* for large values of Z—the case which includes the heavy group of fission fragments—significantly underestimates $\bar{q}/Z$ below $v_r=0.7$, and probably overestimates $\bar{q}/Z$ above $v_r \simeq 0.8$. Moreover, it turns out that the observed spread of the functions $f_Z(v_r)$ is much larger than indicated by Brunings *et al.* Of course, Brunings *et al.* state that their first estimate which is shown in Fig. 5.3 and which is based on the average Thomas–Fermi velocity of the most loosely bound electron should be regarded as providing only a lower limit, whereas their second extreme assumption which is apparently less realistic than the first one, is based on the velocity of the outermost electron in the ion and is considered to give an upper limit. Still, one should expect better agreement between the data and the results from their first assumption, especially since Lamb's surprisingly accurate results are closely connected with the velocity of the most loosely bound electron derived from experimental ionization potentials and supposedly also from Thomas–Fermi potentials. The success of Lamb's approach suggests that indeed the binding energy of an electron bears great significance for the stripping process. His method of calculating u and subsequent application of Bohr's criterion provide a simple and efficient technique for the estimate of average charge states, whereas the use of actual kinetic energies is less satisfactory (see Sec. V.2.c). Bloom and Sauter (1971)[5] attempted to improve Knipp and Teller's Thomas–Fermi calculations of $\bar{q}$ in connection with a phenomenological approach to represent the electronic stopping power of heavy ions as a function of $\bar{q}$. However, since they calculate characteristic electron velocities from kinetic energies, their procedure can hardly yield substantial improvements of $\bar{q}$. It has not yet been explored whether a refined Thomas–Fermi calculation of ionization potentials which includes corrections for exchange and correlation effects is of practical advantage.

Bell's technique which was successful for $Z=40$ and 50 could probably also be applied to the calculation of charge states for other heavy ions. It has the additional advantage of being the only theoretical method thus far developed which explicitly takes into account the nature of the target atoms. However, as has been pointed out before, Bell's computation of electron capture and loss cross sections, which are necessary for a calculation of the average charge, is somewhat cumbersome, and not completely free of uncertain assumptions and over-simplifications.

The full symbols in Fig. 5.3 represent the data obtained in dense gases. It is obvious that these values lie systematically above the trend established by the measurements in more dilute gases. This reveals a density effect which influences $\bar{q}$ especially at low ionizations; a detailed discussion of the phenomenon is given in Sec. VI.1.

c. Re-examination of the Criterion of Lamb and Bohr

The results shown in Fig. 5.3 clearly indicate that Bohr's cursory estimate Eq. (5.2) gives too high charge states, whereas Lamb's approach yields almost perfect agreement with experiment. However, as has been emphasized before, Eq. (5.2) can hardly be regarded as the best quantitative representation of Bohr's criterion. We conclude, therefore, that Bohr's criterion remains essentially valid, but that the relevant electron velocities u must be computed by means of Lamb's criterion, i.e., from ionization potentials rather than from kinetic energies. As has been noted above, this distinction

[5] Bloom and Sauter compare their new formula for $f(v_r)$ graphically with the one obtained by Brunings *et al.*; however, the curve which they reproduce from Brunings *et al.* differs significantly from the original curve presented by Brunings *et al.*

becomes important due to the pronounced deviations of atomic potentials from a Coulomb potential, which Bohr, in his crude model, has not accounted for. In the following, we examine the combination of the approaches by Lamb and Bohr (LB criterion) in more detail.

In order to illustrate the success of the LB criterion, Fig. 5.4 displays the ionization potential, I_q, and, for comparison, the kinetic energy of the most weakly bound electron, T_q, for ionine ions of charge q. The values of I_q have been calculated by Carlson *et al.* (1970)[6] with an accuracy of approximately $\pm 5\%$, and T_q has been obtained from relativistic (Dirac–Fock–Slater) self-consistent field calculations with the program developed by Desclaux (1972). It is clear that T_q is much larger than I_q, especially for low charge states. For example, I_0 and T_0 amount to 10.6 and 66.9 eV, respectively. These differences result from the fact that the virial theorem is not valid for individual electrons in a multielectron atom. According to Lamb, the characteristic velocity of the most weakly bound electron in a ground-state ion may be determined for all charge states from the relation $u=(2I_q/m_e)^{1/2}$. When u is interpreted as the velocity which is relevant for the application of Bohr's criterion, one obtains, according to the procedure discussed earlier in this section, a step function for the average equilibrium charge which is shown in Fig. 5.5 (heavy line). The smooth-solid line in Fig. 5.5 reflects an attempt to average this function, but it is of little meaning other than that. On the one hand, all the experimental average charges for iodine ions listed in Table V.1 follow closely the theoretical curve. For charge states below 19, all data points lie approximately one charge state above the prediction, whereas the few points between charge states 20 and 22 fall slightly below it. Provided that the experimental uncertainty of the latter points does not exceed $\Delta\bar{q}\simeq\pm 1$, their smaller magnitude may be attributed to the transition from the N to the M shell which occurs at $q=25$. On the other hand, when one derives the characteristic electron velocities from actual kinetic energies according to $u'=(2T_q/m_e)^{1/2}$ and applies Bohr's criterion, one obtains a relation for $\bar{q}(v)$ which disagrees strongly with experimental results (light line in Fig. 5.5). This comparison reveals that the binding energy of electrons bears much more significance for charge stripping processes than does their kinetic energy. Particular evidence for that conclusion may be seen in the fact that a shell effect for I^{7+} is much more pronounced in T_q than in both I_q and the experimental results for $\bar{q}$.

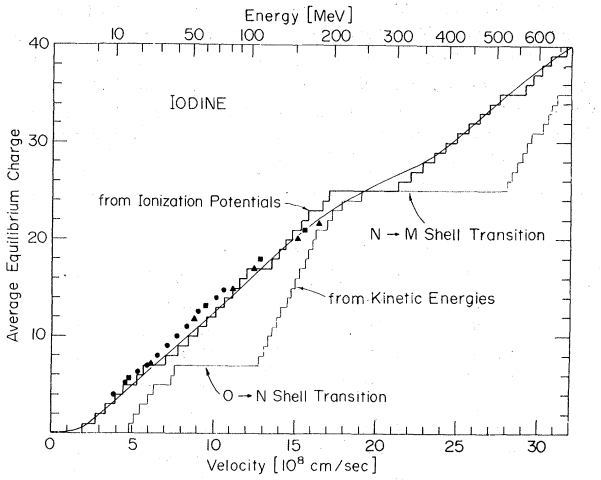

FIG. 5.5. Average equilibrium charge of iodine ions passing through dilute gases, plotted as a function of the ion velocity. Experimental points refer to nitrogen, oxygen, and air, and have been taken from Table V.1. The step functions have been calculated from Bohr's criterion under the assumption that the relevant characteristic electron velocity can be taken from ionization potentials (upper, heavy curve) or, according to Lamb's criterion, from the kinetic energy of the most weakly bound electron in the iodine ion (lower, light curve). The solid line represents an attempt to smooth the upper step function.

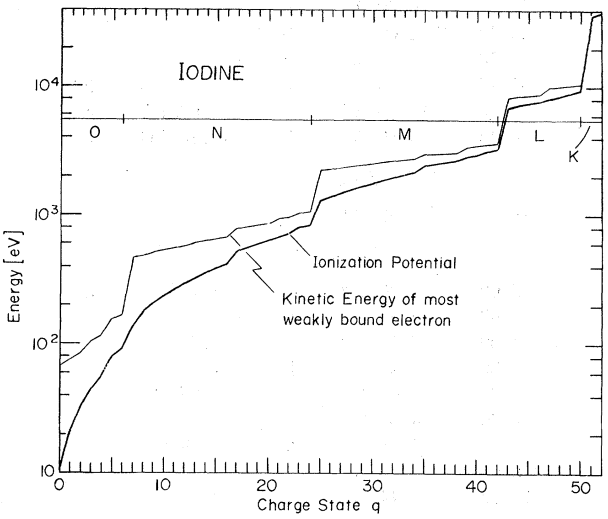

FIG. 5.4. Kinetic energy of the most weakly bound electron (upper, light curve) and single ionization potentials (lower, heavy curve) for iodine ions as a function of initial charge state. Ionization potentials have been taken from Carlson *et al.* (1970), and kinetic energies have been calculated with the program developed by Desclaux (1972).

The LB criterion can be utilized better than early statistical models to predict $\bar{q}$ as a function of Z for any given ion velocity v. In the past, it has been generally assumed that $\bar{q}$ increases slowly with Z. For example, Bohr's estimate Eq. (5.2) yields $\bar{q}\propto Z^{1/3}$, and later empirical relations use $\bar{q}\propto Z^{1/2}$. However, when we employ the LB criterion to calculate $\bar{q}$ as a function of Z for any fixed velocity, we obtain an oscillating function. For example, near velocities $v\simeq 4v_0$, $\bar{q}$ drops by almost two units of charge when Z increases from 59 to 78. It is very interesting to note that Petrov

[6] Carlson *et al.* use an approximate method based on a spherical shell solution for neutral atoms. Comparison with results from exact relativistic self-consistent field methods of Hartree and Fock shows that systematic errors of Carlson's values are such that shell effects are smoothed to a small extent.

TABLE V.1. Experimental average equilibrium charge states of heavy ions with nuclear charges in the range $16 \leq Z \leq 92$, stripped in gaseous and solid targets with intermediate atomic numbers, as a function of the projectile energy. Column 1 gives the energy in units of MeV. Columns 2 and 5 present the average charge in gases ($\bar{q}_G$) and in solids ($\bar{q}_S$), respectively. Columns 3 and 6 specify the target (Gases: AI, air; N2, nitrogen; O2, oxygen; CO, carbon dioxide; AR, argon; Solids: C, carbon; CE, celluloid; FO, formvar). Columns 4 and 7 show reference numbers which identify the source of the data and which are explained at the bottom of the Table.

E	$\bar{q}_G$	Ref.	$\bar{q}_S$	Ref.
	$Z=16$ $M=32$			
3.70	3.45 AI	b	5.85 C	b
6.40	4.65 AI	b	6.85 C	b
8.40	5.16 AI	b	7.45 C	b
10.00	5.60 AI	b	7.80 C	b
12.70	6.50 AI	b	8.45 C	b
17.00	7.50 AI	b	9.09 C	b
19.10	7.90 AI	b	9.35 C	b
20.00	8.06 AI	b	9.45 C	b
22.70	8.50 AI	b	9.71 C	b
23.80	8.65 AI	b	9.87 C	b
26.40	8.90 AI	b	10.14 C	b
27.20	8.80 AI	b	10.25 C	b
29.90	9.28 AI	b	10.46 C	b
32.60	9.58 AI	b	10.66 C	b
38.10	9.95 AI	b	11.05 C	b
43.10	10.32 AI	b	11.40 C	b
52.00	10.70 AI	b	11.87 C	b
	$Z=17$ $M=35$			
1.00	2.03 N2	k	3.41 C	k
1.00	2.07 O2	k		
2.00	2.76 N2	k	4.61 C	k
2.00	2.78 O2	k		
4.00	3.86 N2	k	6.06 C	k
4.00	3.74 O2	k		
6.00	4.60 N2	k	6.69 C	k
6.00	4.46 O2	k		
8.00	5.34 N2	k	7.56 C	k
8.00	5.18 O2	k	7.50 C	a
10.00	5.77 N2	11	8.09 C	k
10.00	5.60 O2	11		
10.00	5.00 O2	6		
12.00	6.54 N2	11	8.53 C	k
12.00	6.33 O2	11	8.60 C	a
18.00	7.00 O2	6		
20.70	8.00 O2	6		
21.00			10.00 C	a
31.00			10.80 C	a
	$Z=18$ $M=40$			
0.18			1.12 C	e
0.26			1.54 C	e
0.30	1.00 AR	8		
0.35			1.83 C	e
0.37			1.85 C	j
0.45			2.10 C	e
0.47			2.13 C	j
0.50	1.28 AR	8		
0.57			2.31 C	j
0.70	1.51 AR	8		
0.76			2.71 C	j
0.90	1.73 AR	8		
0.96			3.08 C	j
1.10	1.95 AR	8		
1.16			3.37 C	j
1.30	2.15 AR	8		
1.41	2.20 N2	7	3.70 CE	g
1.45			3.73 C	j
3.43	3.20 N2	7	5.50 CE	g
	$Z=26$ $M=56$			
0.19			0.84 C	j
0.29			1.13 C	j
0.39			1.41 C	j
0.47			1.64 C	j
0.66			2.29 C	j
0.76			2.53 C	j
0.96			3.12 C	j
1.15			3.64 C	j
1.45			4.20 C	j
	$Z=28$ $M=58$			
1.00	1.82 N2	m		
2.00	2.48 N2	m		
2.00	2.59 O2	m		
	$Z=33$ $M=75$			
10.30	4.60 AI	b		
16.10	6.30 AI	b		
23.20	8.00 AI	b		
31.50	9.50 AI	b		
41.20	11.10 AI	b	15.70 FO	b
52.00	12.50 AI	b	17.00 FO	b
64.40	13.80 AI	b	18.40 FO	b
	$Z=34$ $M=80$			
16.00	7.00 O2	q		
	$Z=35$ $M=79$			
2.00	2.20 N2	k	5.74 C	k
2.00	2.42 O2	k		
4.00	3.10 N2	k	7.73 C	k
4.00	3.27 O2	k		
6.00	4.08 N2	k	8.95 C	k
6.00	4.06 O2	k		
8.00	4.85 N2	k	9.69 C	k
8.00	4.80 O2	k		
10.00	5.44 N2	k	10.40 C	k
10.00	5.45 O2	k		
12.00	6.03 N2	k	11.20 C	k
12.00	6.09 O2	k	11.00 C	c
14.00	6.44 N2	k		
14.00	6.58 O2	k		
14.20			11.00 C	a
15.00			11.40 C	c
20.00	7.20 N2	c		
21.00			12.90 C	a
25.00	8.52 N2	c	13.80 C	c

TABLE V.1 (*Continued*)

E	$\bar{q}_G$	Ref.	$\bar{q}_S$	Ref.
28.40	8.20 O2	d	14.50 C	d
33.00			15.20 C	a
36.00			14.60 C	c
41.67	11.20 N2	c	15.60 C	c
54.00			17.20 C	c
56.00	11.80 O2	d	17.20 C	d
67.00	14.00 O2	d		
81.60			19.10 C	d
82.20	15.20 O2	d		
91.30			20.20 C	d
100.00	16.20 N2	c	20.70 C	c
106.00			20.60 C	d
115.00	17.40 O2	d	21.80 C	d
140.00	17.60 N2	c	23.40 C	c
148.00			23.60 C	d
162.00	18.70 O2	d	24.30 C	d
	$Z=36$ $M=84$			
0.20	0.72 N2	h		
0.30	0.95 N2	h		
0.40	1.10 N2	h		
0.50	1.20 N2	h		
0.60	1.34 N2	h		
0.70	1.44 N2	h		
0.80	1.50 N2	h		
2.97	2.35 N2	g	5.95 CE	g
97.40			20.60 C	p
	$Z=53$ $M=127$			
1.05	1.99 O2	i		
2.95	3.19 O2	i	6.10 C	k
4.50	3.93 O2	i		
6.00	4.39 O2	i	7.70 FO	b
8.00	5.02 O2	i		
9.50	5.05 CO	o		
10.00	5.54 O2	i	10.40 C	k
10.00	4.00 AI	b	9.50 FO	b
11.00			10.50 C	f
11.70	4.60 AI	b	10.30 FO	b
12.00	6.15 O2	i	12.10 C	k
13.70	6.11 CO	o		
13.70	5.20 AI	b	11.20 FO	b
15.00	5.66 N2	c		
15.20	5.80 AI	b	11.90 FO	b
17.00			13.00 C	f
18.60	7.22 CO	o		
19.20	6.40 AI	b	13.10 FO	b
23.80	7.00 AI	b	14.70 FO	b
24.00			13.50 C	c
24.30	7.40 AI	b	14.80 FO	b
24.40	8.40 CO	o		
24.80	7.20 O2	d	15.80 C	e
28.70	8.00 AI	b	16.00 FO	b
30.80	8.44 CO	o		
30.80	8.50 AI	b	16.40 FO	b
34.10	9.00 AI	b	17.40 FO	b
38.00	9.90 AI	b	18.20 FO	b
38.10	10.56 CO	e		
39.20			19.20 C	f
40.00	10.00 AI	b	18.60 FO	b
46.10	11.54 CO	e		
46.50	11.00 AI	b	19.70 FO	b
51.30	11.80 O2	d	20.40 C	d
54.80	12.61 CO	o		
54.80	12.60 AI	b	21.00 FO	b
60.00	13.13 N2	c	21.80 C	c
60.70	13.00 AI	b	21.90 FO	b
64.30	13.60 CO	o		
68.50	14.00 AI	b	23.10 FO	b
74.50	14.80 AI	b		
74.60	14.55 CO	o		
76.80			23.80 FO	b
78.00			24.40 C	d
82.80	14.90 O2	d		
103.80	17.10 O2	d	25.40 C	d
110.00	18.00 N2	c	25.80 C	c
126.00			26.80 C	d
150.00			28.80 C	d
152.00	20.10 O2	d		
162.00	21.00 N2	c	29.20 C	c
180.00	21.70 O2	d	29.50 C	d
	$Z=73$ $M=181$			
2.00	1.72 N2	l		
2.00	1.89 O2	l		
4.00	2.41 N2	l		
4.00	2.67 O2	l	5.86 C	l
6.00	2.90 N2	l		
6.00	3.14 O2	l	7.22 C	l
8.00	3.40 N2	l		
8.00	3.63 O2	l	8.22 C	l
10.00	3.76 N2	l		
10.00	3.97 O2	l	8.98 C	l
15.00	4.64 N2	l		
15.00	4.87 O2	l	11.10 C	l
45.00			20.70 C	d
69.00			24.50 C	d
81.00			24.70 C	d
90.00			25.40 C	d
127.00			28.20 C	d
137.00			28.20 C	d
148.00			29.00 C	d
	$Z=92$ $M=238$			
2.00	2.61 N2	l		
2.00	2.82 O2	l	3.40 C	l
4.00	3.08 N2	l		
4.00	3.34 O2	l	5.10 C	l
6.00	3.65 N2	l		
6.00	3.77 O2	l	6.50 C	l
7.20			6.10 FO	b
8.00	3.97 N2	l		
8.00	4.16 O2	l	7.90 C	l
9.90			8.10 FO	b
10.00	4.48 N2	l		
10.00	4.67 O2	l	8.90 C	l
12.90			9.80 FO	b
15.00	5.44 N2	l		

TABLE V.I (*Continued*)

E	$\bar{q}_G$	Ref.	$\bar{q}_S$	Ref.	E	$\bar{q}_G$	Ref.	$\bar{q}_S$	Ref.
15.00	5.54 O2	l	10.80 C	l	51.90			21.00 FO	b
16.40			11.00 FO	b	58.30			22.50 FO	b
20.30			12.50 FO	b	60.00			24.00 C	d
24.40			13.90 FO	b	65.70			23.60 FO	b
29.20			16.30 C	n	70.00			26.00 C	d
29.20			15.40 FO	b	80.00			27.00 C	d
30.00			17.00 C	d	90.00			27.50 C	d
34.00			16.60 FO	b	100.00			27.90 C	d
39.80			18.20 FO	b	110.00			29.10 C	d
40.00			19.00 C	d	120.00			30.50 C	d
45.60			19.40 FO	b	130.00			31.00 C	d
45.70			21.80 C	n	140.00			30.60 C	d
50.00			21.00 C	d	150.00			31.90 C	d

[a] Almqvist *et al.* (1962).
[b] Betz *et al.* (1966).
[c] Datz *et al.* (1971), and Moak *et al.* (1968).
[d] Grodzins *et al.* (1967).
[e] Hvelplund *et al.* (1970).
[f] Litherland *et al.* (1963).
[g] Nikolaev *et al.* (1960).
[h] Pivovar *et al.* (1965a).
[i] Ryding *et al.* (1969b).
[j] Smith *et al.* (1969).
[k] Wittkower and Ryding (1971).
[l] Wittkower and Betz (1972b).
[m] Kulcinsky *et al.* (1971).
[n] Brown (1972).
[o] Franzke *et al.* (1972).
[p] Baron (1972).
[q] Ryding *et al.* (1971b).

et al. (1970) observed precisely such an effect for ions with nuclear charges between 58 and 78. More recently, Hvelplund *et al.* (1972) reported a systematic investigation of equilibrium charge state distributions of all ions with $Z \leq 18$ (except $Z=4$ and 14) stripped in helium at energies between 100 and 400 keV. They find that $\bar{q}$ fluctuates considerably with Z for fixed v. Again, utilization of the LB criterion allows one to reproduce their results surprisingly well. These experimental findings must be regarded as giving extremely strong support for the applicability of the LB criterion.

In view of the results shown in Fig. 5.5, it may be concluded that the above simple interpretation of the LB criterion allows close estimates to be made on average charge states. However, the limitations of the criterion and of such a procedure are evident. The effects of the target species are disregarded, though it is known that $\bar{q}$ may differ significantly in various gaseous strippers. This has been demonstrated, for example, by Datz *et al.* (1971) and is elaborated in the following section. In addition, the large cross sections for multiple-electron loss in single collisions lead to a shift of $\bar{q}$ to values above that charge for which, according to Bohr's criterion, the cross sections for capture and loss of a single electron are of equal magnitude, $\sigma_c(q)=\sigma_l(q)$. Another question arises because of the presence of several adjacent charge states around the mean value $\bar{q}$; it appears that it is a crude approximation to restrict the consideration to a single electron in each case, namely to the most weakly bound one. Finally, the existence of shell effects in the dependence $\bar{q}(v)$, which cannot always be ignored, makes the precise definition of characteristic velocities particularly difficult.

It must be concluded that a more detailed calculation of average charge states is extremely complex, and that attempts to refine the application of the LB criterion should be viewed with suspicion. Incidentally, even when a very sophisticated Thomas–Fermi model is used, one calculates in essence somewhat different characteristic electron velocities u, but the problems outlined above, especially the one of relating u to v are not solved, except that the dependence of $\bar{q}$ on the atomic shell structure is smoothed, at the expense that all shell effects disappear.

Wolke (1968) examined the effects of shell structures in terms of the LB criterion for highly stripped ions with $Z \leq 10$. He applies the LB criterion to ions of particular velocities $\hat{u}_q$ at which the charge states in an assumed two-component system are of equal magnitude, $F_q=F_{q+1}$. This corresponds to the condition $\sigma_l(q)=\sigma_c(q+1)$ and leads to a half-integer average $\bar{q}=q+\frac{1}{2}$. A comparison of the energy $E_q=m_e\hat{u}_q^2/2$ with the ionization potential I_q reveals the influence of shell structures on the average charge. It can be seen from Fig. 5.5, for example, that E_q differs from I_q when the experimental curve for $\bar{q}(v)$ does not intersect the LB step function at half-integer values of q. Obviously, $E_q \neq I_q$ is to be expected especially in the vicinity of shell transitions. Wolke showed that the relative effect $(E_q-I_q)/I_q$ at the K–L transition is similar for all of the ions which he investigated. Such regularities could perhaps be utilized in order to smooth the step function $\bar{q}(v)$

obtained from ionization potentials. However, these results are not readily extrapolated to higher Z, and it appears necessary to have more experimental data on $\bar{q}$ near shell transitions in heavier ions.

In view of the increasing interest in superheavy elements with nuclear charges $Z \gtrsim 110$, it is of some importance to have information on the average equilibrium charge of these ions. Based on Bohr's criterion and theoretical ionization potentials (Carlson *et al.*, 1971) $\bar{q}$ can be readily estimated in the way indicated above. Figure 5.6 shows the resulting LB model step function for element $Z=114$, along with semiempirical estimates which are discussed in the following section.

3. Semiempirical Relationships for the Average Charge

For several reasons, considerable attention has been devoted to the development of semiempirical methods which allow approximate predictions to be made for average equilibrium charge states without requiring a calculation of charge-changing cross sections. On the one hand, there is growing practical need for such information. On the other hand, such relations are of theoretical significance and, since the results from early statistical calculations indicate striking regularities in the dependence of $\bar{q}$ on Z and v, one should expect that it would not be too difficult to find simple but useful relations for $\bar{q}$. The first systematic measurements with light ions confirmed that theoretical expectation

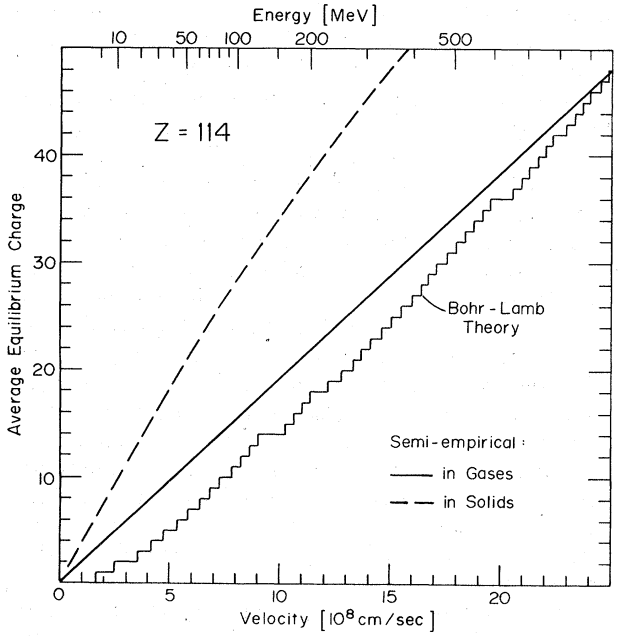

FIG. 5.6. Average equilibrium charge of superheavy ions with nuclear charge $Z=114$. The step function has been calculated for gaseous targets from the criterion by Lamb and Bohr using single ionization potentials. Also shown are extrapolated semiempirical estimates: —, in gases, Eq. (5.5); - - -, in solids, Eq. (5.8).

TABLE V.2. List of parameters for the semiempirical formula Eq. (5.4) by Dmitriev and Nikolaev (1964).

Medium	α_1	α_2	m_1	n_1
H_2	0.4	0.3	1.2	4.0
He			1.3	4.5
N_2, Ar			0.9	7.0
solid	0.1	0.6	1.2	5.0

and have given great impetus to the search for generalized relations; comparatively little data for heavy ions sufficed to develop quite universal formulas for average charge states which satisfy most practical needs in large ranges of Z and v.

a. Semiempirical Relations

Papineau (1956), in connection with studies of ranges in nuclear emulsions, estimated mean charge states for ions with $Z \leq 10$ on the basis of the statistical model in which the relative charge is a function of the Thomas–Fermi velocity, $\bar{q}/Z=f(vZ^{-2/3})$. According to that prescription, he plotted a very few experimental average charge states for nitrogen, oxygen, and neon stripped in gases and solids, and obtained a single quite definite curve for these cases. But his results cannot be extended to heavier ions without considerable loss of accuracy as is evident, for example, from Fig. 5.3.

A more sophisticated approach has been suggested by Dmitriev (1957). He assumes that the probability P for removal of an electron in an ion is a function only of v/u_i, where u_i is the velocity of the electron being considered, and can be taken from ionization potentials. Thus, he determines P from stripping experiments with hydrogen projectiles, and obtains the mean charge for an ion simply by summing P for all electrons in the ion, $\bar{q}=\sum_i P(v/u_i)$. Using that technique, he is able to produce mean charge states for nitrogen, oxygen, and fluorine ions with reasonable accuracy. It can be argued that a modification of this approach could be useful for heavy ions, especially since the simultaneous use of successive ionization potentials would lead to a much smoother relation $\bar{q}(v)$ than the previously discussed direct application of Lamb's and Bohr's criterion. No such efforts have yet been reported.

Heckmann *et al.* (1963) displayed both their data for ions with $Z \leq 18$ stripped in solids at high velocities, $E/m \lesssim 10$ MeV/amu, and similar data obtained by other investigators at lower velocities. They find that $\bar{q}/Z$ is well approximated by a function $f(vZ^{\epsilon})$, where ϵ ranges between 0.55 and 0.58. It is obvious from Fig. 5.3, and will be specified later, that the choice of $\epsilon < \frac{2}{3}$ is also of some advantage for heavier ions. Furthermore, the plot by Heckmann *et al.* indicates that, for their data below $\bar{q}/Z \approx 0.9$, $lg(1-\bar{q}/Z)$ may be approximated by a linear function of $vZ^{-0.55}$. It will be shown below that a similar quite universal dependence can be

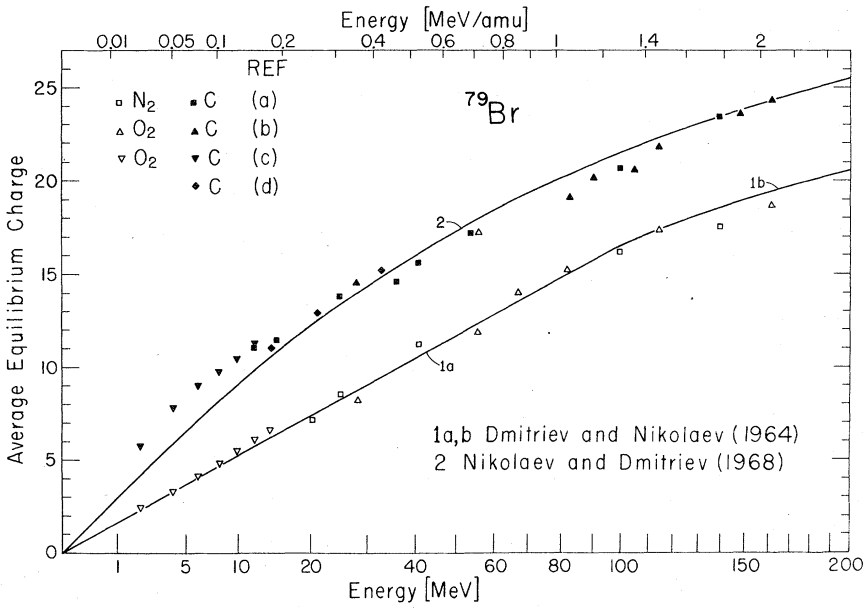

FIG. 5.7. Average equilibrium charge of bromine ions stripped in nitrogen and oxygen gas (open symbols), and in carbon foils (full symbols), plotted as a function of the projectile energy. Experimental results are taken from Table V.1: (a) Moak *et al.* (1968) and Datz *et al.* (1971); (b) Grodzins *et al.* (1967); (c) Wittkower and Ryding (1971); (d) Almqvist *et al.* (1962). Semiempirical estimates: 1a, b, Dmitriev and Nikolaev (1964), Eqs. (5.4) and (5.5); 2, Nikolaev and Dmitriev (1968), Eq. (5.8).

successfully used for heavier ions. For ionizations $\bar{q}/Z>0.9$, where the ions considered by Heckmann *et al.* are almost fully stripped, their data shows a different trend. Since this may reflect a shell effect, it is questionable whether this part of their relation for $\bar{q}/Z$ can be easily extended to heavier ions.

The first analytical semiempirical relationship for $\bar{q}$ was given by Dmitriev and Nikolaev (1964). They relied on a generalization of the result from the Thomas–Fermi theory and assumed $u\approx Z^{\alpha}f(\bar{q}/Z)$. Applying Bohr's criterion, $u=v$, and utilizing the limited data available at that time, they were able to derive an explicit expression for the relative mean charge in gases

$$\bar{q}/Z=lg(v/m_1Z^{\alpha_1})/lg(n_1Z^{\alpha_2}) \qquad (0.3\lesssim\bar{q}/Z\lesssim 0.9). \tag{5.4}$$

The four parameters α_1, α_2, m_1, and n_1 have been evaluated from experimental data for ions with $Z\leq 10$ and for fission fragments, and are listed in Table V.2. If we use these parameters, Eq. (5.4) reproduces that data within 5% as a rule. The usefulness of the formula for heavier ions may be estimated from a comparison with more recent data. In Figs. 5.7 and 5.8, the predictions according to Eq. (5.4) are shown for bromine (curve 1b) and for iodine ions (curve 3b), together with the experimental results. Although the restriction to ionizations $\bar{q}/Z\gtrsim 0.3$ allows a comparison to be made only for the smaller part of the data, it appears that Eq. (5.4) predicts the experimental values almost within their error limits. For the range $\bar{q}/Z<0.3$, Dmitriev and Nikolaev give a different empirical relation

$$\bar{q}/Z=AvZ^{-1/2} \qquad (\bar{q}/Z<0.3), \tag{5.5}$$

where the parameter A is equal to approximately 0.18 in nitrogen and argon strippers. That prediction is also shown in Figs. 5.7 and 5.8 for bromine and iodine (curves 1*a* and 3*a*), as well as in Fig. 5.9 for uranium ions. In the region of overlap between Eqs. (5.4) and (5.5) the approximate character of the empirical parameters leads to some ambiguity as to which equation should be preferred. In the case of iodine ions, for example, the two formulas give charge states at $\bar{q}/Z\approx 0.3$ which differ by one unit of charge. It can be seen that Eq. (5.5) agrees quite well with the data, though some systematic deviations are evident. Provided that the target gas is sufficiently dilute so that any residual ion excitation can be disregarded, it is observed that the mean charge increases at low-ion velocities less rapidly than is predicted by the linear relation Eq. (5.5). This may be explained by applying Bohr's criterion to the actual ionization potentials. For example, Fig. 5.5 illustrates that the very first electron is relatively difficult to ionize, and that the next few electrons have binding energies which lie relatively closer together. This would suggest that the curve $\bar{q}(v)$ has a slope which is close to zero at very small velocities, in contradiction to Eq. (5.5). In this connection, it is interesting to point out the different behavior of mean charges obtained in dense target gases. Figure 5.8, for example, shows that the mean charges measured for iodine ions by Ryding *et al.* (1969b) in dense oxygen not only lie systematically above the trend established by Betz *et al.* (1966) in air at lower densities, but are much more closely approximated by a linear relationship of the form Eq. (5.5).

With a different set of parameters, which is also listed in Table V.2, formula (5.4) can be used to predict average charge states obtained from solid strippers. This case will be discussed later in connection with an improved formula for $\bar{q}$ which has been given by the same authors. No value for A in Eq. (5.5) has

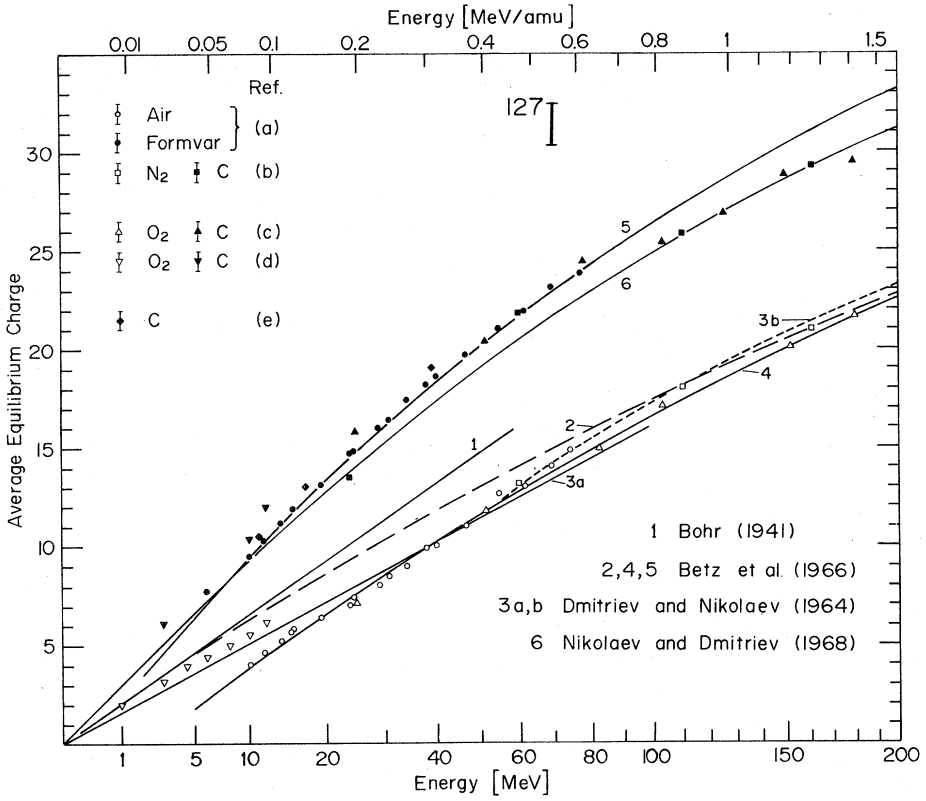

FIG. 5.8. Average equilibrium charge of iodine ions stripped in nitrogen, oxygen, and air (open symbols), and in carbon and formvar foils (full symbols), plotted as a function of the projectile energy. Experimental results are taken from Table V.1: (a) Betz *et al.* (1966); (b) Moak *et al.* (1968) and Datz *et al.* (1971); (c) Grodzins *et al.* (1967); (d) Ryding *et al.* (1969b), and Wittkower and Betz (1972a); (e) Litherland *et al.* (1963). Theoretical and semiempirical estimates: 1, Bohr (1941); 2, Betz *et al.* (1966), Eq. (5.6) with $C=1$ and $\gamma=2/3$; 3a, b, Dmitriev and Nikolaev (1964), Eqs. (5.4) and (5.5); 4, 5, Betz *et al.* (1966), Eq. (5.7); 6, Nikolaev and Dmitriev (1968), Eq. (5.8).

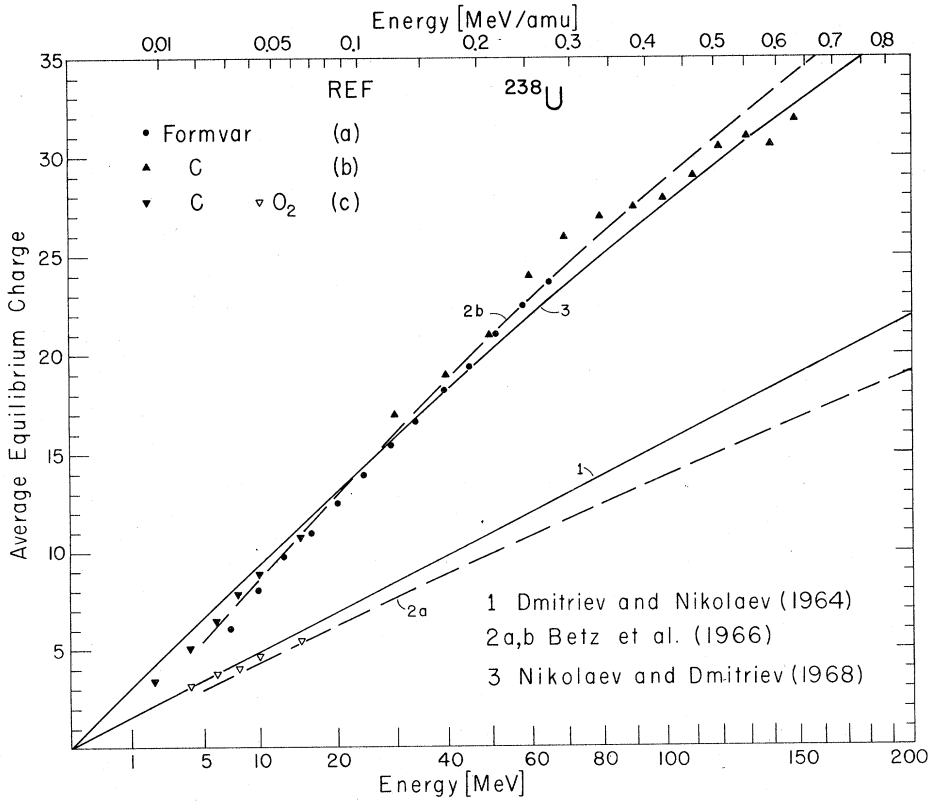

FIG. 5.9. Average equilibrium charge of uranium ions stripped in oxygen (open symbols), and in carbon and formvar foils (full symbols), plotted as a function of the projectile energy. Experimental results are taken from Table V.1: (a) Betz *et al.* (1966); (b) Grodzins *et al.* (1967); (c) Wittkower and Betz (1972b). Semiempirical estimates: 1, Dmitriev and Nikolaev (1964), Eq. (5.5); 2, 4, 5, Betz *et al.* (1966), Eq. (5.7); 3, Nikolaev and Dmitriev (1968), Eq. (5.8).

TABLE V.3. List of parameters for the semiempirical formulas Eqs. (5.6) and (5.7) by Betz *et al.* (1966).

	Air stripper		Formvar foil stripper	
Ion	C	γ	C	γ
S	1.135	0.663	1.083	0.604
As	1.117	0.628	(1.098)[a]	(0.538)[a]
I	1.065	0.641	1.030	0.518
U	...	...	1.030	0.510

[a] These values may be slightly in error because of some uncertainty in the identification of the projectile.

been estimated for solid targets. In view of the most recent data, it is believed that $A=0.33$ renders Eq. (5.5) useful for approximating mean charge states for heavy ions stripped in carbon foils in the range $\bar{q}/Z<0.3$.

Extensive experimental data on sulphur, arsenic, iodine, and uranium ions stripped in air and in formvar foils at energies between 5 and 80 MeV has been used by Betz *et al.* (1966) to derive a semiempirical relation for average charge states

$$\bar{q}/Z=1-C\exp[-v/(v_0Z^\gamma)] \qquad (v\gtrsim v_0), \quad (5.6)$$

where the two parameters C and γ are to be determined empirically for each ion and target. With the values for C and γ given in Table V.3 the data could be fitted in practically all cases within the experimental errors of ± 0.5 charge states. Since $\bar{q}$ does not increase linearly with v at low-ion velocities, C is not equal though close to unity and depends slightly on Z. As has been mentioned above, this fact may be related to the ionization potentials. Of course, with $C=1$, the use of Eq. (5.6) must be restricted to velocities $v\gtrsim v_0$. Small variation of γ with Z is to be expected on the basis of the theoretical studies of Brunings *et al.* (1941), and is also evident from the illustration of the data in Fig. 5.3. When Eq. (5.6) is used for ions other than the ones investigated by Betz *et al.*, it is necessary to interpolate mainly γ and, to a lesser extent, the parameter C for the desired Z. For gaseous targets, the choice of constant values $C=1$ and $\gamma=\frac{2}{3}$ gives reasonable estimates for $\bar{q}$ which differ in general less than ~ 2 units of charge from the experimental results for any ion species stripped in nitrogen, oxygen, air, or argon, although the calculated values are overestimates, especially for lower ionizations. In solid targets, γ is clearly a decreasing function of Z. Using a rough estimate for $\gamma(Z)$, Betz *et al.* generalized Eq. (5.6) to

$$\bar{q}/Z=1-C(0.71Z^a)^{v/v_0}, \qquad (10\leq Z\lesssim 92;\ v\gtrsim v_0), \quad (5.7)$$

where $a=0.053$ for formvar foil strippers, and C is the parameter from Eq. (5.6). With $a=0.067$ for stripping in air, the new relation Eq. (5.7) is in good agreement with all experimental results on $\bar{q}$ obtained by Betz *et al.* However, due to limitations of the available data and correlations between the parameters C and γ, the particular dependence $\gamma(Z)$ chosen by Betz *et al.* is not completely satisfactory. As a consequence, Eq. (5.7) is not as general as one might have hoped. For example, it underestimates $\bar{q}$ considerably in gaseous strippers for $Z\gtrsim 70$, especially at very high-ion velocities, and underestimates $\bar{q}$ to a lesser extent in solid strippers for $Z\lesssim 35$ at low velocities. Still, as is illustrated in Figs. 5.8 and 5.9 for the case of iodine and uranium ions stripped in gases and in solids, most of the available data can be approximated by means of Eq. (5.7).

Taking into account experimental data at energies above 100 MeV, Nikolaev and Dmitriev (1968) developed another universal expression for average charge states produced in solid targets,

$$\bar{q}/Z=[1+(Z^{-\alpha}v/v')^{-1/k}]^{-k} \qquad (Z\gtrsim 16), \quad (5.8)$$

where $v'=3.6\times 10^8$ cm/sec, $\alpha=0.45$, and $k=0.6$. In the range of overlap with the earlier formula Eq. (5.4), the new formula is in somewhat better agreement with the data, though the difference amounts in most cases to less than one charge state. The usefulness of Eq. (5.8) is evident from Figs. 5.7, 5.8, and 5.9. To further illustrate the universal character of Eq. (5.8), Fig. 5.10 shows $\bar{q}/Z$ as a function of the reduced velocity $v/(v'Z^{0.45})$ for all the data in solids which are listed in Table V.1. The solid line represents Eq. (5.8). Most of the data falls within a narrow band, and the scattering of the data points is often less for different Z that it is for a particular value of Z. The curve according to Eq. (5.8) agrees well with the data though it appears that a slight modification of the function would, on the average, result in an even better fit.

The question may be raised as to whether a similar unified description is possible for mean charges obtained in gaseous targets. Following the suggestion by Heckmann *et al.* (1963), the relative equilibrium charge $\bar{q}/Z$, as obtained from Table V.1, is plotted in Fig. 5.11 as a function of the reduced velocity $v/(v_0Z^{0.55})$. It is found that for the greater part of the data such a representation is as effective as the corresponding one for solids shown in Fig. 5.10. Due to the scattering of the data points, the exponent can hardly be chosen without considerable uncertainty and the value 0.55 may not necessarily be the best choice. Still, a comparison between Figs. 5.3 and 5.11 shows that a value close to two-thirds appears to be somewhat too high. This means that, in the velocity range of present interest, the classical Thomas–Fermi velocity, $v/(v_0Z^{2/3})$, is perhaps not as close to the relevant characteristic velocity as one had hoped.

It may be concluded from the above discussion that it is possible to predict mean equilibrium charge states for heavy ions from semiempirical relationships with an average uncertainty of approximately ± 1 units of charge for both gaseous and solid targets. It should be kept in mind, however, that despite the generally

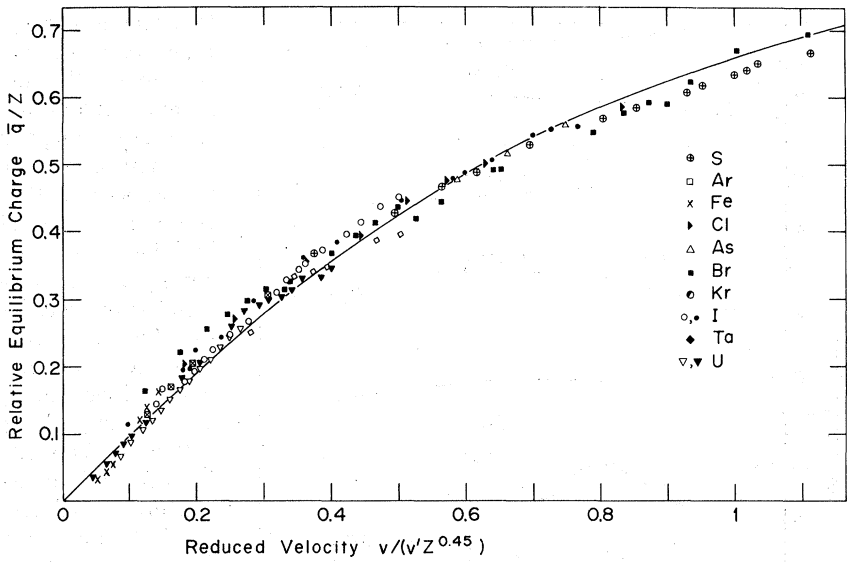

FIG. 5.10. Average relative equilibrium ionization of heavy ions passing through carbon (full symbols) and other light foils (open symbols), plotted as a function of the reduced ion velocity, $v/(v'Z^{0.45})$, with $v'=3.6\times10^8$ cm/sec. The experimental data has been taken from Table V.1. The solid line represents the semiempirical estimate by Nikolaev and Dmitriev (1968), Eq. (5.8).

smooth behavior of $\bar{q}$, all these semiempirical estimates are useful mainly for interpolation purposes, and that extrapolations beyond the investigated ranges of both Z and v must still be regarded as risky. Shell effects are one of the reasons why smoothly extrapolated predictions may significantly deviate from actual data. In Fig. 5.8, for example, such an effect occurs for iodine ions stripped in solids at energies above 80 MeV. When charge 25+ is reached, all electrons have already been stripped from the N shell, and further stripping requires that those M electrons which are more tightly bound be removed. The pronounced increase of the ionization potential at charge 26+ (Fig. 5.4) obviously results in a less steep increase of $\bar{q}(v)$. Thus, an extrapolation of Eq. (5.7) which is based on data obtained below 80 MeV, overestimates $\bar{q}$ at, say, 160 MeV by almost two units of charge, whereas Eq. (5.8), which fits the data above 80 MeV, underestimates $\bar{q}$ by approximately one charge state in the range where $\bar{q}<25$.

b. Influence of the Target Species

In the above discussion, primarily those targets have been considered which have a nuclear charge not too far from seven. This restriction has been made not only to facilitate comparisons of experimental data but also because those targets have been studied most fre-

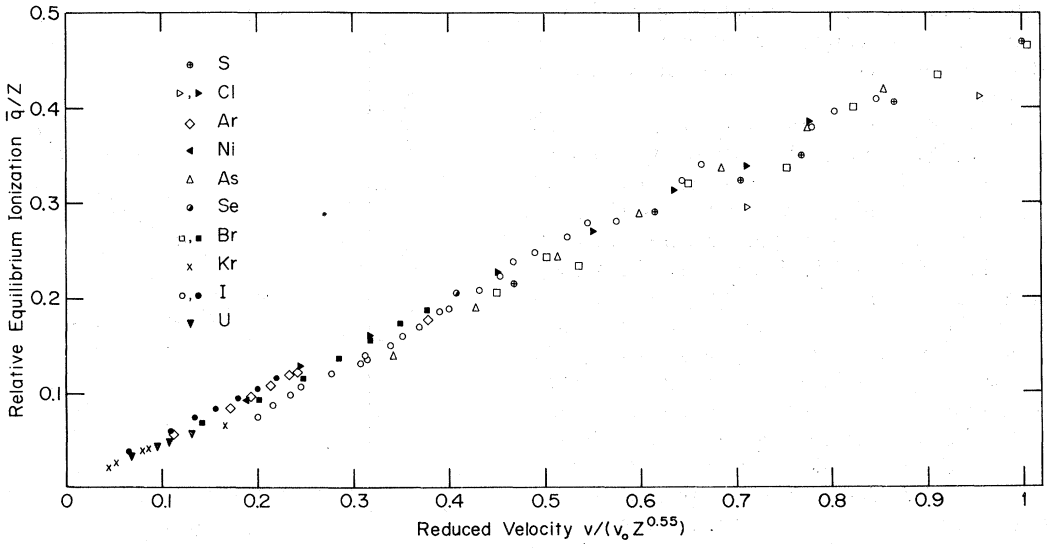

FIG. 5.11. Average relative equilibrium ionization of heavy ions passing through gaseous targets of nitrogen, oxygen, and air, plotted as a function of the reduced ion velocity $v/(v_0Z^{0.55})$. All data points are taken from Table V.1. The full and open symbols refer to dense and more diluted gas targets, respectively.

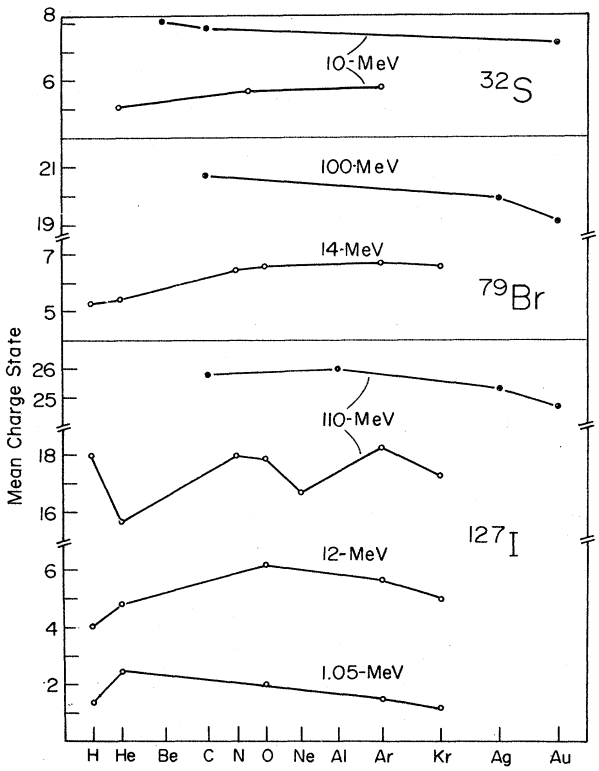

FIG. 5.12. Average equilibrium charge for sulphur, bromine, and iodine ions as a function of the target species. Open and full symbols refer to gaseous and solid strippers, respectively. The ion energy is indicated at each curve (in units of MeV); from Betz *et al.* (1966), Datz *et al.* (1971), Ryding *et al.* (1969b), and Wittkower and Ryding (1971).

quently. Nevertheless, a significant portion of the data has been taken in other gases and solid targets, and some general trends could be revealed. Still, these results on the mean charge as a function of Z_T do not seem to be consistent enough to allow very precise quantitative predictions to be made on a simple empirical basis.

Essentially all of the experiments which have yielded information on $\bar{q}(Z_T)$ confirm the early results obtained by Lassen (1951a) for the light and heavy group of fission fragments. Excluding hydrogen targets which are discussed below, one finds a quite general trend illustrated in Figs. 5.12 and 5.13. In gases, the highest mean charge is obtained for nitrogen, oxygen, and argon, with the differences among these strippers generally small. In heavier gases, $\bar{q}$ decreases slightly with increasing Z_T. Similarly, $\bar{q}$ decreases in solids almost continuously with increasing Z_T. Beryllium seems to be the most efficient solid target, whereas gold is one of the least efficient strippers. Quantitatively, the general evidence from the present data is that the maximum difference of $\bar{q}$ produced either by different gases or by different solids reaches at most approximately two units of charge. Theoretically, Bell (1953) and also Bohr and Lindhard (1954) estimate that, for example, the average charge in other gases than oxygen but of comparable atomic number is about the same as that in oxygen, i.e. that for a large range of atomic weights of stripping gases, the mean charge is essentially independent of the stripping gas.

A hydrogen target behaves differently depending on the velocity of the ions. At low velocities, it produces comparatively small mean charge states, but at very high-ion velocities it becomes as efficient as nitrogen or argon, and is substantially better than helium. This trend is evident for iodine ions from a comparison of, say, Figs. 5.17 and Fig. 5.20. Likewise, Martin (1965) found an anomalously high average charge for carbon ions stripped in hydrogen at velocities in the range $9 \leq v/v_0 \leq 20$, corresponding to energies between 24 and 120 MeV. This effect can be qualitatively understood by taking into account the probability for electron capture in hydrogen, which has been discussed by Bell and Bohr and Lindhard (see Sec. IV.1). The electrons in a hydrogen molecule, or in a hydrogen atom, are bound loosely enough to be readily liberated by an approaching highly charged ion. Due to their high escape probability, they have little chance of being captured by the ion and, thus, the balance between electron capture and loss is shifted towards higher mean charge states. Incidentally, one may expect on those grounds that the stripping efficiency of hydrogen becomes systematically better when the ion velocity is increased further. Bell has calculated average charge states of fission fragments in hydrogen targets, but his estimates are far too high especially for high fragment velocities and, thus, are of little use for practical purposes.

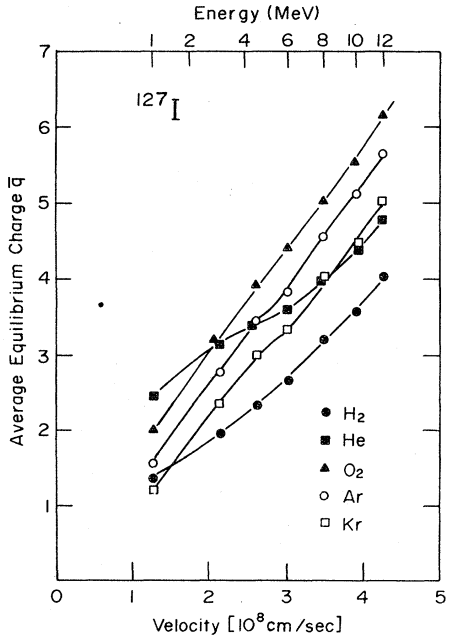

FIG. 5.13. Average equilibrium charge for iodine ions stripped in various gases, as a function of the projectile velocity; from Ryding *et al.* (1969b).

In most rare gases, and especially in helium targets, the average equilibrium charge of slow ions shows an unusual behavior. For example, Wittkower and Betz (1972b) observed for tantalum and uranium ions at velocities $v \lesssim v_0$, that $\bar{q}$ in helium is not only higher but also less sensitive to the ion velocity than in all other gases. As a further result they find that 2-MeV uranium ions attain a value of $\bar{q}$ which is as large as the one in a carbon foil, and at even lower energies it must be expected that helium will give the highest $\bar{q}$ among all gaseous and solid strippers, despite the presence of the density effect (Sec. VI.2). To a lesser extent, this trend of $\bar{q}$ is evident from Fig. 5.13 for iodine ions. Incidentally, comparison of experimental charge fraction results by many different authors reveal that $\bar{q}$ is always exceptionally high in helium targets, provided that v is sufficiently small. Quick comparison of these results can be made by using the extensive compilation by Wittkower and Betz (1972a) of all existing charge state data. Finally, we note that when helium gives for light projectile ions the highest values of $\bar{q}$ among gases, it is not particularly surprising that these values may then also exceed the ones obtained from solid stripper targets. The reason for this lies in the small magnitude of the density effect for light ions. For high ion velocities, the anomalous effect disappears and helium becomes the least efficient stripper. This trend can be understood when the behavior of the capture cross sections $\sigma_c(v)$ is taken into account (see Sec. IV.2.a).

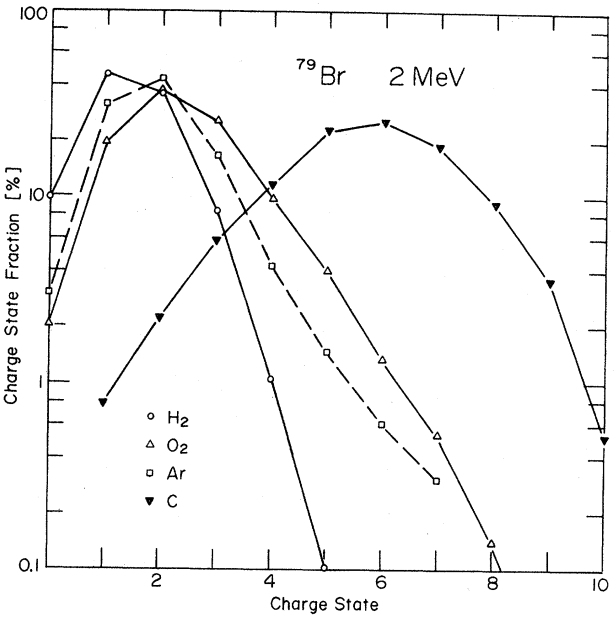

FIG. 5.14. Equilibrium charge state distributions for 2-MeV bromine ions, stripped in gases of hydrogen, oxygen, and argon, and in a carbon foil. All distributions are influenced by density effects; from Wittkower and Ryding (1971).

4. Equilibrium Charge State Distributions

For a comprehensive description of the charge states in an ion beam passing through thin sheets of matter it is necessary to consider not only the mean charge but also the actual distribution of charge states around the mean, i.e., the relative intensity $F(q)$ of the various charge states which are present in the emerging beam. The existence of such charge distributions demonstrates that Bohr's criterion (see Sec. V.1.a) can, of course, be satified only for the *average* charge, and gives no information for other neighboring charge states. Especially when q is not too close to $\bar{q}$, equilibrium fractions $F(q)$ obtained for a given q in different strippers may differ by many orders of magnitude, even though the mean charges may lie closely together. According to Sec. III, equilibrium charge distributions are a direct result of the competition between electron capture and loss processes. In principle, therefore, $F(q)$ could be calculated from charge-changing cross sections. However, as has been explained in Sec. IV, these cross sections are not known well enough even in the case of rarified gases, not to mention dense gases or solids, so that theoretical estimates of $F(q)$ cannot yet be made with good accuracy, if at all. It must be pointed out that a calculation of equilibrium fractions is particularly difficult for heavy ions because the number of influential cross sections is very large; incidentally, the number of relevant charge states is much larger than in the case of light ions and, as important, cross sections for simultaneous loss of several electrons in single collisions are usually so large that they can no longer be neglected. In view of the complexity of the situation, it is not surprising that all major attempts to predict charge state distributions have been based on empirical or on semiempirical considerations, thereby relying on regularities which have been observed in numerous experiments. The following discussion, therefore, will to a considerable extent be concentrated on the phenomenological description of extensive experimental results, and on simple procedures which facilitate interpolations of existing data.

a. Experimental Distributions

Some typical equilibrium charge distributions are displayed for bromine ions at energies between 2 and 140 MeV in Figs. 5.14–5.16, and for iodine ions between 12 and 183 MeV in Figs. 5.17–5.21, stripped in various gases, vapors, and solids. Apart from the large difference in the mean charge which is produced by gaseous and solid strippers, it is evident that the distributions in both of these target groups also depend significantly on the target sepecies. Figures 5.14, 5.15, 5.17, and 5.19 are typical in that very light targets, especially hydrogen, produce distributions which are much narrower and more symmetrical than the ones obtained in heavier gases with $Z_T \gtrsim 7$. In solids, the distributions are as broad as in a heavy gas, but they are generally less asymmetrical. The most intense charge fractions are

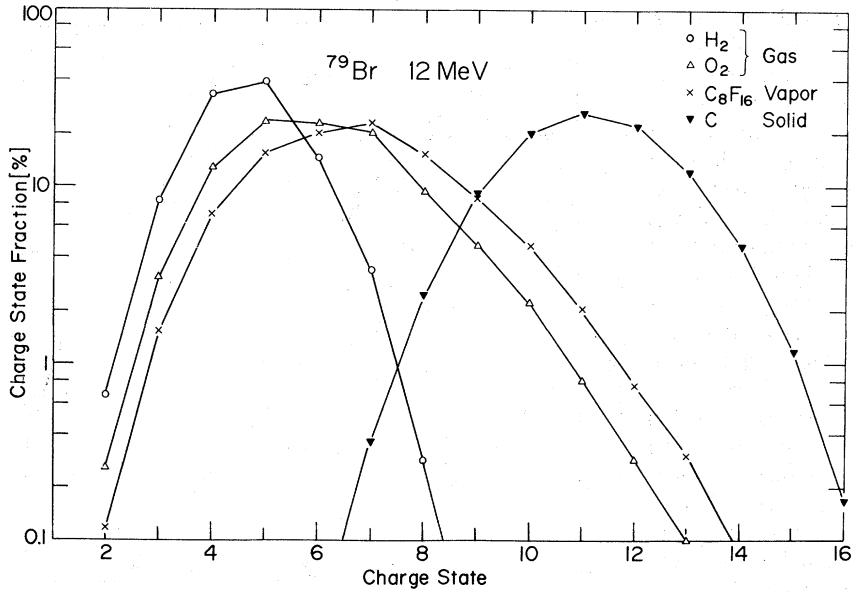

FIG. 5.15. Equilibrium charge state distributions for 12-MeV bromine ions, stripped in gases of hydrogen and oxygen, in a fluorocarbon vapor (C_8F_{16}), and in a carbon foil. All distributions are influenced by density effects; from Wittkower and Ryding (1971).

closely approximated by a Gaussian distribution Eq. (2.11). Thus, when average charge and distribution width are known, Eq. (2.11) allows reasonable estimates to be made in many cases for charge fractions with intensities of, say $>1\%$.

Of course, the limitations of Eq. (2.11) are all too obvious. Significant deviations from the Gaussian shape are often pronounced either as a systematic enhancement of fractions with $q>\bar{q}$, or due to a direct influence of the atomic shell structure. A good example for the latter case, which has been found by Moak *et al.* (1967), is shown in Fig. 5.16. The equilibrium distribution of 140-MeV bromine ions stripped in carbon shows an unusual decrease of charge fractions F_q with $q>25$. However, Fig. 5.21 illustrates that for iodine ions stripped in argon at 162- and 183 MeV no such pronounced break occurs near $q=25$ where the transition from the N to the M shell takes place. This different behavior may result from several causes. Firstly, the stripping mechanism in solids differs markedly from that in gases. Secondly, the number of electrons in the next inner shell plays an important role and, accordingly, the 18 M electrons in iodine may smooth out shell effects more effectively than the 8 L electrons in bromine. Furthermore, the increase in the ionization potential at $q=25$ is steeper for bromine than for iodine. The ratio I_{25}/I_{24} amounts to 2.16 for bromine, but only 1.56 for iodine. Thus, one may understand the smoothness of the distribution for iodine, and one may argue that the observed distortion of the distribution for bromine in carbon is largely caused by the difficulty of exciting and removing electrons from the L shell of the ions. Incidentally, measurement of charge-changing cross sections for bromine and iodine ions revealed no excessive decrease of σ_l at the M–N and N–O shell transition, where I_7/I_6 amounts to 1.68 and 1.56, respectively. Instead, $\sigma_c(7, 6)$ showed a distinctive reduction which causes the fraction $F(6)$ to decrease much more than $F(8)$ to a value which is clearly below the trend established by the neighboring charge fractions. This effect is visible in Figs. 5.15 and 5.17, and has also been discussed by Datz *et al.* (1970). Probably for the same reason, the distribution for 183-MeV iodine, shown in Fig. 5.21, exhibits a noticeable decrease of $F(24)$. The distribution at 162 MeV shows

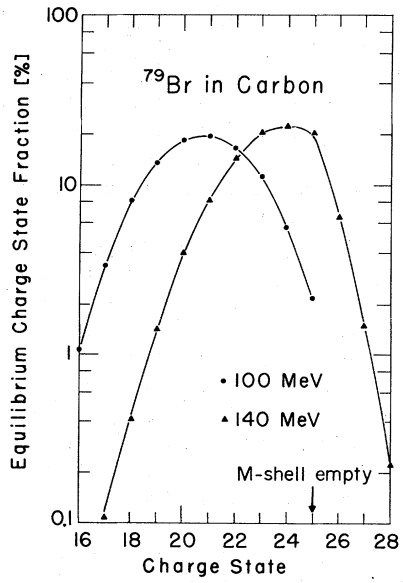

FIG. 5.16. Equilibrium charge state distributions for bromine ions, stripped in a carbon foil at 100 and 140 MeV; from Moak *et al.* (1967, 1968).

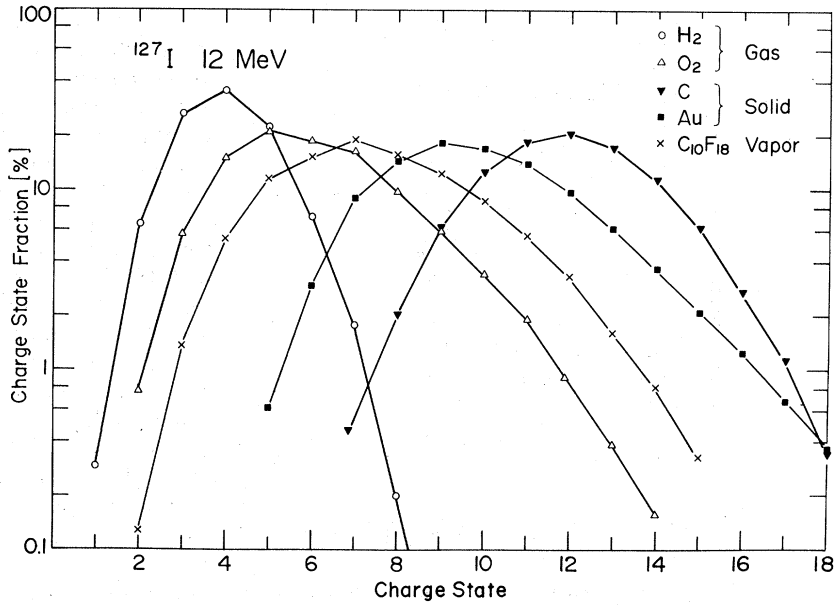

FIG. 5.17. Equilibrium charge state distributions for 12-MeV iodine ions, stripped in gases of hydrogen and oxygen, in a fluorocarbon vapor ($C_{10}F_{18}$), and in gold and carbon foils. All distributions are influenced by density effects; from Ryding *et al.* (1969b) and Wittkower and Ryding (1971).

a similar dip, but it is not clear why it occurs at charge state 23 rather than at 24.[7]

b. Distribution Width

In wide ranges of both Z and v, the distribution widths show great regularity and can, thus, be approximated by semiempirical relations. Dmitriev and Nikolaev (1964) derived the estimate

$$d = d_1 Z^w, \tag{5.9}$$

where the parameters d_1 and w have been determined semiempirically via the mean charge and amount to 0.32 and 0.45 in nitrogen or argon, and to 0.38 and 0.40 in solids, respectively. The data obtained by Betz *et al.* (1966) and Betz and Schmelzer (1967) for heavy ions up to uranium at energies below 80 MeV indicated that the choice

$$d = 0.27 Z^{1/2} \tag{5.10}$$

agrees satisfactorily with the experimentally observed widths, measured in air and in formvar foils. Figure 5.18 illustrates the constancy of d for iodine ions stripped in formvar in the energy range between 18.6 and 54.7 MeV. In view of more recent data, Nikolaev and Dmitriev (1968) presented a new estimate for solid strippers,

$$d = d_2\{\bar{q}[1-(\bar{q}/Z)^{1/k}]\}^{1/2}, \tag{5.11}$$

where $d_2 = 0.5$ and $k = 0.6$. The results by Ryding *et al.* (1969b) and by Wittkower and Ryding (1971) confirm the usefulness of the simple approximation Eq. (5.10) for a variety of heavy ions with $Z \leq 92$, stripped in oxygen gas and in carbon foils at energies below 20 MeV. Part of these results are shown in Fig. 5.22. It is a common observation that the widths are, in wide ranges of ion velocities, practically independent of v, except at very low and most likely also at very high velocities, where d becomes much smaller. This later effect is clearly visible in Fig. 5.22; especially for iodine ions, d seems still to increase at $v \simeq 4.4 \times 10^8$ cm/sec (12 MeV), but it has been found by Betz *et al.* (1966) that the plateau value is reached at velocities close to 5.5×10^8 cm/sec (20 MeV). Consequently, expressions of the type Eq. (5.9) and Eq. (5.10) describe only a maximum value of d, whereas Eq. (5.11) is claimed to be valid also beyond that maximum.

It is not easy to assess the general significance of the above semiempirical predictions on d. In many cases, calculated maximum widths deviate less than 20% from the experimental ones. However, the data often scatters considerably, and the influence of shell effects

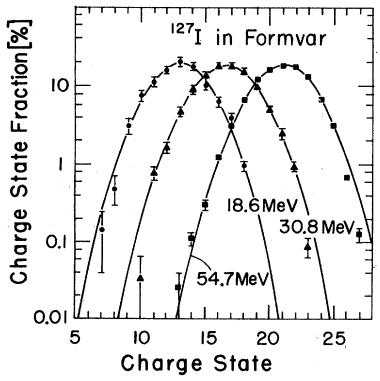

FIG. 5.18. Equilibrium charge state distributions for iodine ions at 18.6, 30.8, and 54.7 MeV, stripped in formvar foils; from Betz *et al.* (1966).

[7] The fractions shown in Fig. 5.21 for 162-MeV iodine ions in argon have been taken from the original data table by Datz *et al.* (1971); the top of that distribution is not as flat as one would assume from the graphs shown by Moak *et al.* (1968) and Datz *et al.* (1971).

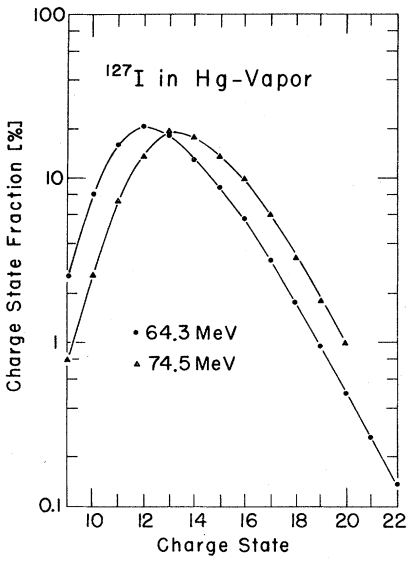

FIG. 5.19. Equilibrium charge state distribution for iodine ions at 64.3 MeV and 74.5 MeV, stripped in a supersonic jet of mercury vapor; from Franzke *et al.* (1967).

and asymmetries of distributions presents additional complications. Furthermore, it is likely that d increases again at higher ion velocities to values which lie significantly above the well established plateau Eq. (5.10). For example, the widths for iodine ions are close to $d=2.5$ at 162 and 183 MeV (Fig. 5.21), and close to 2.7 at 150 MeV in a C_7F_{14} stripper (Franzke *et al.*, 1972), whereas the predictions from Eq. (5.9) and Eq. (5.10) are all below 2.0. In the velocity range in which the experimental widths increase, Eq. (5.11) gives fair agreement only for ions with $Z \lesssim 35$. In these cases, however, the absolute variation of d is very small and does not allow a definite proof to be given for the velocity dependence which is suggested in Eq. (5.11). When heavier ions are considered, $Z>35$, Eq. (5.11) gives generally unsatisfactory results. For iodine and uranium, for example, the energy where d reaches its maximum is predicted to be close to 100 MeV and above 200 MeV, respectively, but plateaus have been found at approximately 20 and 50 MeV, respectively. Consequently, Eq. (5.11) predicts for 12-MeV iodine and 15-MeV uranium the low values 1.53 and 1.66, respectively whereas the experimental values are 1.93 and 2.1 for carbon, and 2.33 and 2.3 for gold foils, respectively. This example also demonstrates that for both solids and gases the influence of the target species can not always be disregarded. Further evidence for that can be found in the data compilations by Moak *et al.* (1971) and Wittkower and Betz (1972a). Figure 5.23 shows some results for iodine, stripped in various gases at energies below 12 MeV, where d has not yet reached the broad maximum. It can be seen that d depends significantly on Z_T, even when only the heavier gases are considered. This latter result does not change very much in the range where d becomes less dependent on the energy. The larger width in heavy gases compared with hydrogen and helium must be attributed to multiple-electron loss processes which are much less important in light targets than in heavier ones [see Eq. (2.16) and Sec. IV.2.d].

c. Asymmetries

Equilibrium charge state distributions obtained in hydrogen and helium show a remarkable symmetry and may well be described by a Gaussian distribution Eq. (2.11). However, heavier gases produce, especially at lower energies, very pronounced asymmetries even

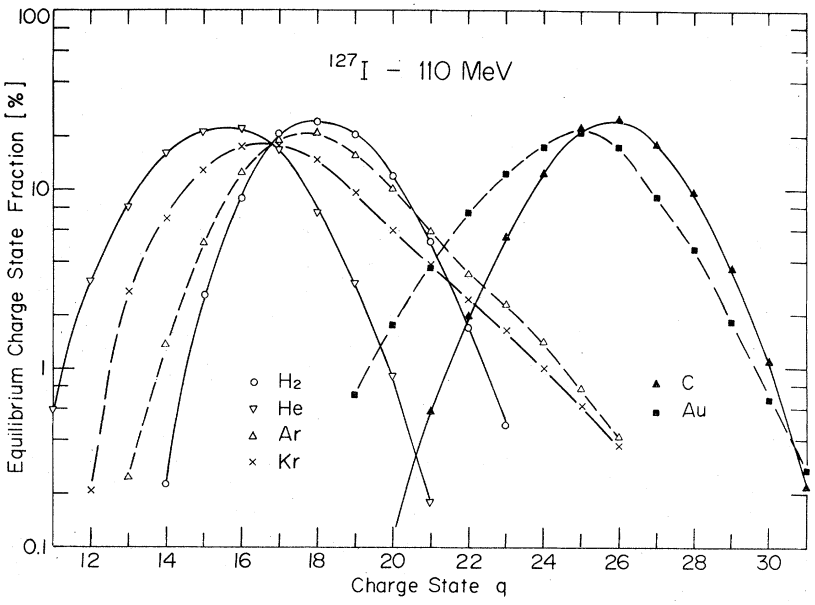

FIG. 5.20. Equilibrium charge state distributions for 110-MeV iodine ions, stripped in gases of hydrogen, helium, argon and krypton, and in carbon and gold foils; from Datz *et al.* (1971).

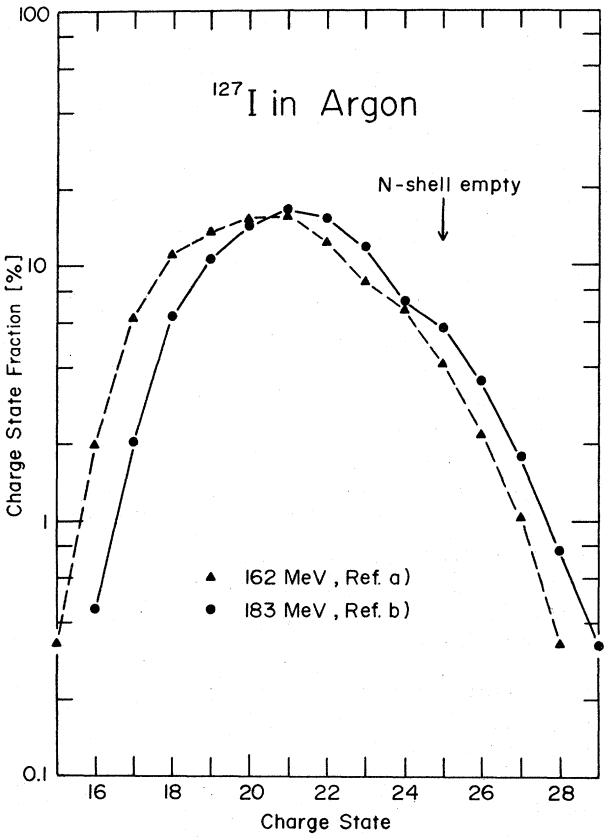

FIG. 5.21. Equilibrium charge state distributions for iodine ions, stripped in argon gas at 162 MeV and at 183 MeV; from (a) Datz *et al.* (1971); (b) Grodzins *et al.* (1967). See also Footnote 7.

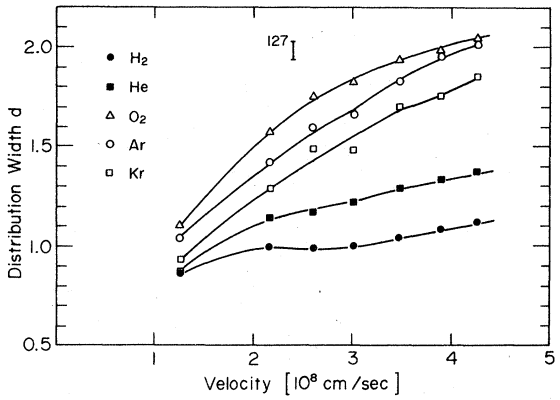

FIG. 5.23. Width d of equilibrium charge state distributions of iodine ions passing through various gases, plotted as a function of the projectile velocity; from Ryding *et al.* (1969b).

for charge fractions $>0.1\%$ (Figs. 5.14, 5.16, 5.17, 5.19, 5.20); in most cases, fractions F_q with $q>\bar{q}$ show a much slower decrease than the fractions on the low charge state tail. In view of the fundamental relations between cross sections and equilibrium distributions (Sec. II.3) and the experimental results on charge-changing cross sections (Sec. IV.2), it must be concluded that the observed asymmetries are largely a consequence of cross sections for multiple-electron loss which are relatively small in light targets, but are very large in heavier targets. Furthermore, the broadening factor $\bar{k}$ which describes the increase of the width of distributions obtained from heavy and light targets is in reasonable agreement with the measured increase of relative multiple-electron loss probabilities. Since the functional dependence of cross sections for capture and loss of a single electron on the initial charge of the ions is not very sensitive to the target species (Sec. IV.2.a), $\bar{k}$ may be approximated by means of Eq. (2.16). Incidentally, the associated shift of charge distributions towards higher charge states which is associated with the large cross sections for multiple-electron loss in heavy targets is not necessarily the only cause for a higher mean charge of ions stripped in heavy gases compared with light gases. The absolute values of the cross sections for capture and loss of a single electron are in general affected differently when different target gases are being used and, thus, lead to an additional shift of $\bar{q}$. Other sources which contribute to production of asymmetric charge distributions may be found (i) in cross sections $\sigma(q)$ which show a basically different dependence on q that the one given by Eqs. (2.10), (2.14), or (2.17), and (ii) in density effects which lead to preferential excitation of higher charge states. The

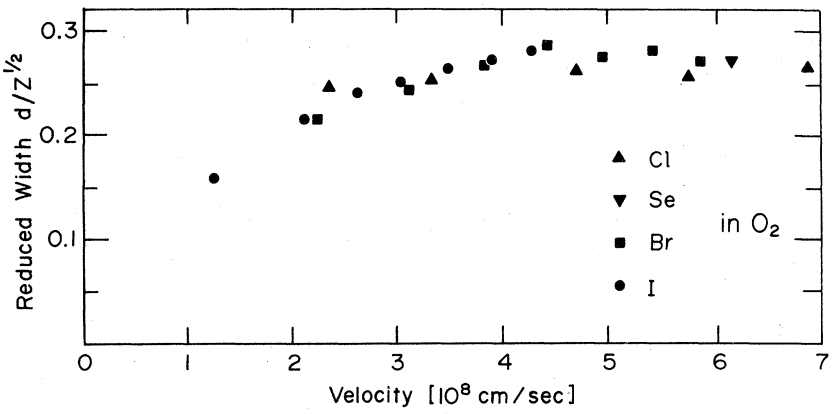

FIG. 5.22. Reduced width $dZ^{-1/2}$ of equilibrium charge state distributions for chlorine, selenium, bromine, and argon ions passing through oxygen, plotted as a function of the projectile velocity; from Ryding *et al.* (1969b) and Wittkower and Ryding (1971).

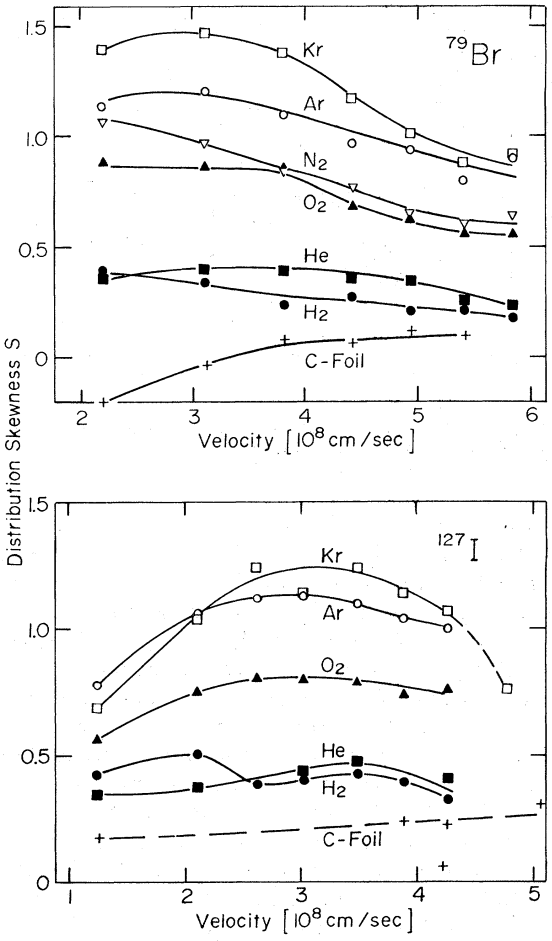

FIG. 5.24. Skewness s of equilibrium charge state distributions of bromine and iodine ions passing through various gases and a carbon foil, plotted as a function of the projectile velocity; from Wittkower and Ryding (1971).

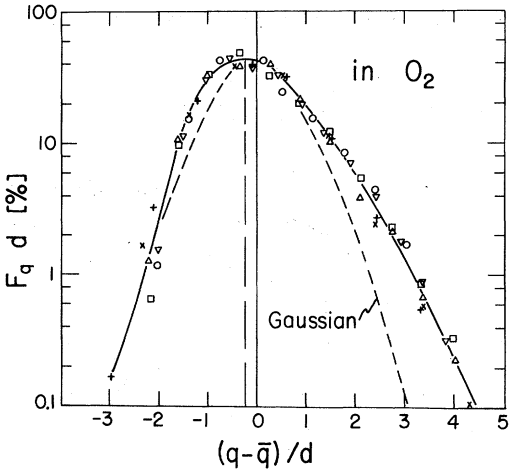

FIG. 5.26. Reduced equilibrium charge state fractions $F_q d$ of heavy ions stripped in oxygen gas, plotted as a function of $(q-\bar{q})/d$; Chlorine: ×, 3.3 MeV; +, 12 MeV; Bromine: □, 7.45 MeV; △, 14 MeV; Iodine: ○, 3 MeV; ▽, 12 MeV; from Ryding *et al.* (1969b) and Wittkower and Ryding (1971). The dashed vertical line indicates the location of the maximum of the charge distribution and, for comparison, the dashed curve shows a pure Gaussian distribution.

relative importance of these two possibilities is probably small, though difficult to evaluate, especially because there is not yet a single case in which *all* cross sections $\sigma(q, q')$ of heavy ions stripped in a heavy target have been determined with reasonable accuracy within the full range of charge states in which the equilibrium fractions have been measured.

The asymmetry parameter s defined in Eq. (2.9) is shown in Fig. 5.24 for bromine and iodine ions at various velocities, stripped in gases and in carbon. It can be seen that the highest asymmetries result from heavy gas strippers and at low or intermediate ion velocities.

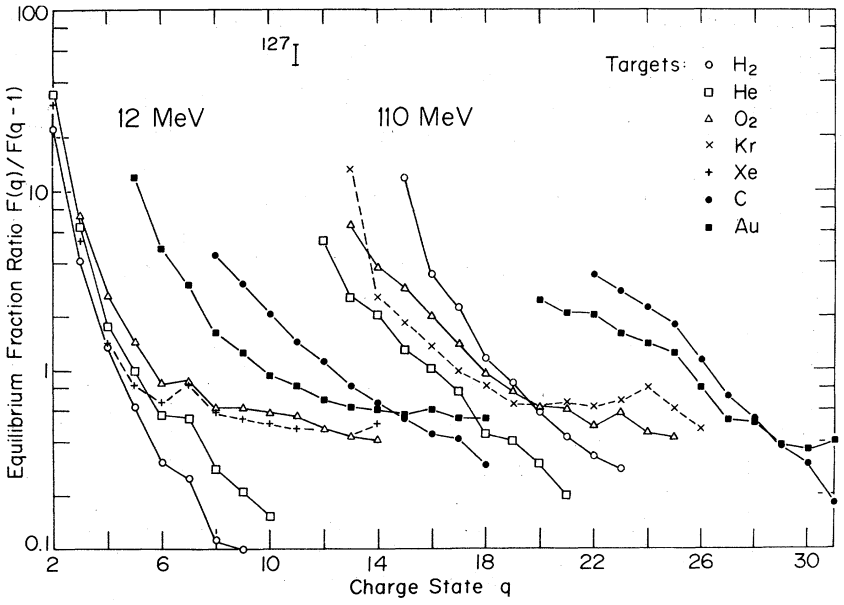

FIG. 5.25. Equilibrium charge state fraction ratios, $F(q)/F(q-1)$, of 12- and 110-MeV iodine ions stripped in gases and solids; from Ryding *et al.* (1969b) and Datz *et al.* (1971).

With increasing velocity, s tends to decrease. However, distributions for iodine at 64.3 and 74.5 MeV (Fig. 5.19), and even at 110 MeV (Fig. 5.20) still deviate strongly from a symmetrical shape. A value of s close to zero indicates near symmetry. Incidentally, the negative value of s shown in Fig. 5.24 for carbon and low bromine velocities indicates an unusual case where the fractions on the left side of the distribution are enhanced rather than the ones on the right side. Figure 5.25 presents a more sensitive test of some distribution shapes. For 12- and 110-MeV iodine ions, the ratio of adjacent equilibrium fractions, $F(q)/F(q-1)$, is plotted as a function of q. Again, it becomes obvious that hydrogen, helium, and carbon targets yield quite steadily decreasing fraction ratios (symmetrical distributions), whereas heavier targets exhibit a distinctly slower decrease for $q>\bar{q}$ (asymmetrical distributions). It is also interesting to point out the shell effect at $q=7$. The fraction ratios $F(7)/F(6)$ are enhanced in all targets; this has been attributed to the $O\rightarrow N$ shell transition which occurs for iodine at $q=7$ (see Sec. V.1.a).

Finally, Fig. 5.26 shows the similarity of equilibrium distributions for chlorine, bromine, and iodine ions, stripped in oxygen at energies between 3.3 and 14 MeV, taken from Ryding *et al.* (1969b) and Wittkower and Ryding (1971). In that generalized representation, $dF(q)$ is plotted versus $(q-\bar{q})/d$, and interestingly, all fractions fall closely on a universal but asymmetrical curve. The trend of that curve is in agreement with observations by Nikolaev (1965) on ions of sodium, phosphorus, and argon passing through nitrogen at $v=2.6\times10^8$ cm/sec.

It is evident from a comparison of Figs. 5.14–5.21 and (especially Figs. 5.24 and 5.25) that solid strippers produce more symmetrical distributions than comparable gases at least within the range of the most intensive charge state fractions. Since multiple-electron loss is

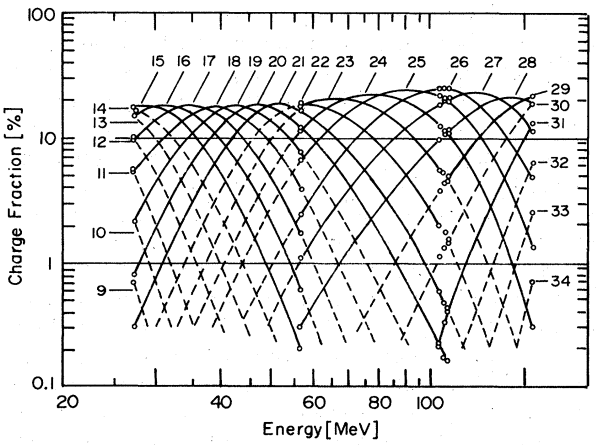

FIG. 5.27. Interpolation graph for equilibrium charge state distributions of iodine ions, stripped in carbon, plotted as a function of the projectile energy; from Moak *et al.* (1967) and Datz *et al.* (1971).

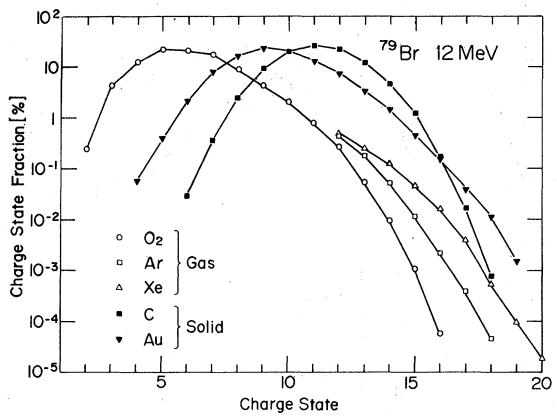

FIG. 5.28. Charge state distributions and high charge state tails of 12-MeV bromine ions, stripped in gases of oxygen, argon, and xenon, and in carbon and gold foils; from Ryding *et al.* (1971b). The high charge state tails in the gaseous targets probably do not reflect charge state equilibrium.

expected to be significant in collisions of heavy ions with, say, carbon atoms, the absence of striking asymmetries may be regarded as an indication of the fundamental differences of stripping heavy ions in solid and gaseous targets. A tentative explanation of that effect is given in Sec. VI.

d. Charge State Interpolation

Unknown asymmetries and uncertainties in the distribution widths usually rule out the use of the Gaussian approximation Eq. (2.11) for accurate calculation of individual charge fractions, especially of fractions not too close to $\bar{q}$. In many cases, however, the measurement of equilibrium distributions at even a very few energies allows satisfactory interpolations to be made on a purely empirical basis. Frequent use has been made of the possibility of plotting the fractions F_q as a function of the ion velocity. Figure 5.27 gives an example for iodine ions, stripped in carbon foils (Datz *et al.* 1971). Essentially, only four different energies have been investigated, but it is obvious that the intrinsic regularities in the dependence $F_q(v)$ allow the connection of the data points by smooth lines which can be readily drawn by hand. The accuracy of the fractions interpolated in this way for intermediate energies satisfies most practical needs. Even the shell effect near $q=25$ is well incorporated. Unfortunately, extrapolations beyond the investigated velocity range, and to other ions, remain risky. For example, the curves $F_q(v)$ show an extremely anomalous behavior for tantalum and uranium ions passing through helium (Wittkower and Betz, 1972b). Secondary maxima appear at low velocities, $v\lesssim v_0$, and for low charge states which make it impossible to extrapolate charge fractions on the basis of data from ion velocities $v>v_0$. This effect appears to occur in all rare gases (see the discussion in Secs. IV.2.a and V.3.b). There is plenty of experimental evidence for the anomalous behavior of

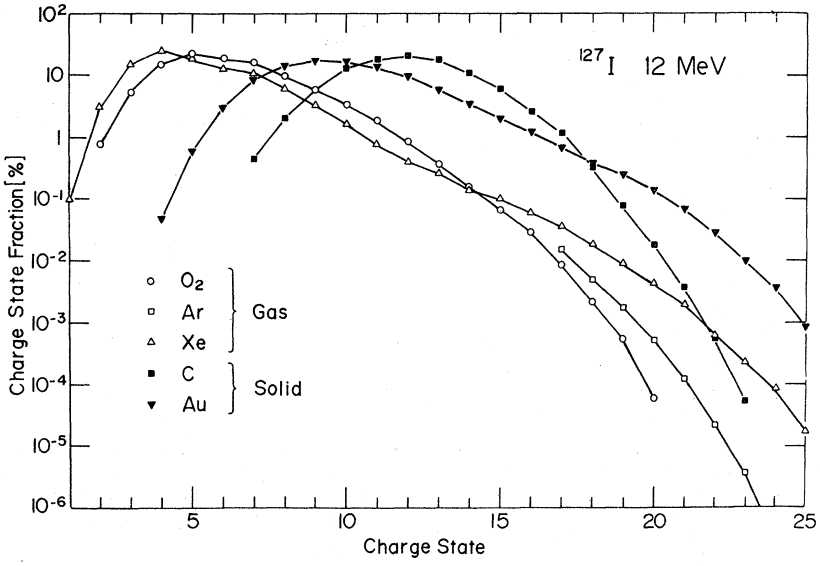

FIG. 5.29. Charge state distributions and high charge state tails of 12-MeV iodine ions, stripped in gases of oxygen, argon, and xenon, and in carbon and gold foils; from Ryding *et al.* (1971b). The high charge state tails in the gaseous targets probably do not reflect charge state equilibrium.

the particular charge fraction F_0 in the data by Stier *et al.* (1954), Pivovar *et al.* (1965a), Wittkower and Gilbody (1967), Pivovar and Nikolaichuk (1970), and Hvelplund *et al.* (1972). Though the above authors do not discuss the effect, it is evident that in the specified cases F_0 decreases with decreasing ion velocity rather than showing a monotonous approach towards unity for $v \rightarrow 0$.

e. High Charge State Tails

Most investigators have studied equilibrium charge state distributions for those fractions which showed a relative intensity of more than $\sim 0.1\%$. Though only the most intense charge fractions are generally of practical importance, it is quite interesting to study the abundance of charge states far above the mean charge. Ryding *et al.* (1971b) investigated these smaller fractions in the intensity range $10^{-1}\%$–$10^{-6}\%$ for bromine, selenium, and iodine ions between 6 and 18 MeV, stripped in gases and solids. Results are shown in Fig. 5.28 for bromine, and in Fig. 5.29 for iodine ions at 12 MeV. The fractions above $\sim 0.1\%$ were taken from their earlier work performed with the apparatus shown in Fig. 3.2, whereas the fractions below $\sim 0.1\%$ were detected with a modified apparatus, essentially by using an additional magnetic analyzer with higher resolving power. The results show that the high-charge states have intensities which decrease very slowly with increasing charge, and that, for example, charge states as high as 25+ can be detected without difficulties in cases where the mean charge is only 5+.

Ryding *et al.* argue that these highly stripped ions are formed mainly in single violent collisions with the target atoms, i.e., in encounters in which one or more inner shell electrons are removed from the ion so that readjustment of the ion excitation occurs via an ionization cascade. Evidence of the importance of these inner shell excitation processes for the production of high-charge states in heavy-ion collisions can be found, for example, from the work of Pivovar (1967b) on argon and krypton ions below 1.7 MeV, and Kessel (1970) on iodine in xenon between 1.5 and 12 MeV. It is well established that due to the larger energy transfer in close collisions, the charge of the ions increases significantly with increasing scattering angle. Kessel's experiments show, for example, that 12-MeV iodine ions of initial charge 5+ emerge at 2.5 deg from single collisions with xenon atoms in a most probable charge state $q=23$. In such encounters, the L shells of the colliding ions interpenetrate and an energy of the order of ~ 10 keV is transferred to the ion sufficient for the removal of a large number of electrons, including up to two L electrons. Since the apparatus used by Ryding *et al.* (1969b) allows the detection of an ion beam with a divergence of at least ± 20 mrad, it is not difficult to understand that, for example, a fraction of 12-MeV iodine ions is measured in xenon which amounts to $10^{-5}\%$ for charge state $q=25$ (Fig. 5.29). As is to be expected the fractions with $q>15$ exhibit, especially for iodine ions, a distinct "hollow beam" characteristic. Further support for the single collision formation mechanism may be seen in the observation that the target thickness required for the production of the very high-charge states was substantially less than the one required to equilibrate the most probable charge. Furthermore, on the basis of the single collision processes, it is possible to explain that for $q \gg \bar{q}$ the highest charge state fractions are produced by the heaviest targets. For example, xenon gas gives a lower average charge than oxygen or carbon, but it produces fractions of 12-MeV iodine ions which exceed the ones in oxygen for $q>14$, and the ones in a carbon foil for $q>22$ (Fig. 5.29).

The above argument implies that the cross sections

for multiple electron loss $\sigma(q, q+n)$ are influential even when n reaches extremely large values; in the above example, the cross section $\sigma(5, 25)$ should effect the formation of charge fraction $F(25)$. However, it is not clear to what extent the high-charge state tails of the distributions measured by Ryding *et al.* (1971b) in gases reflect charge state equilibrium. Since the target thicknesses were of the order of $\sim 1.5\times 10^{15}$ molecules/cm^2, one should expect that the tails are influenced both by direct multiple-electron loss processes proceeding from the incident ions and by competition between electron capture and loss by the heavy ions.

5. Effective Charge and Energy Loss

The particular relation between charge states and energy loss of fast heavy ions penetrating through matter deserves some brief comments. Rather than attempting a full description of that complex question, we outline the approach which has been adopted most frequently, and indicate typical experimental results and some of its implications.

Bohr (1941, 1948) argues that a calculation of the energy loss of fission fragments requires that a certain effective charge, $\bar{q}_{\text{eff}}$, which characterizes the ionic charge of the fragments, must be known for all velocities during the slowing down process. Then, in its simplest interpretation, the stopping cross section, S, of a partially stripped heavy ion is related to the stopping cross section, S_p, of protons at the same velocity and in the same stopping material by

$$S=\bar{q}_{\text{eff}}^2(v)\,S_p(v).^8 \qquad (5.12)$$

Bohr assumes that the classical approximation on which Eq. (5.12) is based is valid over almost the entire range of fission fragments. Furthermore, he suggests that the effective charge does not differ practically from the rms value of the charges actually carried by the ions, and that the width of the actual charge distribution is small, $d_0^2 \ll \bar{q}^2$. Hence, he finds

$$\bar{q}_{\text{eff}}^2 \simeq \overline{q^2} \simeq (\bar{q}^2). \qquad (5.13)$$

Among many authors, this concept has been discussed by Bethe and Ashkin (1953), Northcliffe (1963), and Northcliffe and Schilling (1970), and served as an important though largely semiempirical basis for subsequent investigations of charge states and energy loss of fast heavy ions. For example, Brunings *et al.* (1941) utilized Eqs. (5.12) and (5.13) to deduce characteristic electron velocities which, in turn, are essential for the calculation of $\bar{q}$ on the basis of Bohr's and Lamb's criterion (see Sec. V.1). Heckmann *et al.* (1960) inferred effective charge states from experimental range-energy relations of ions with $Z\leq 18$, stopped in nuclear-track emulsion. Essentially the same procedure has been applied, for example, by Roll and Steigert (1960a, b), Northcliffe (1960), Martin and Northcliffe (1962), Teplova *et al.* (1962), and Bethge *et al.* (1966) for ions with atomic numbers $Z\leq 18$ and, in a few cases, $Z\leq 36$, stopped in a variety of solid and gaseous materials. Energy loss and effective charge states of heavier ions up to uranium have been investigated by Booth and Grant (1965), Cumming and Crespo (1967), Pierce and Blann (1968), Kalish *et al.* (1969), and Brown and Moak (1972). All of the authors named above found that, in essence, Eq. (5.12) can be regarded as a practical prescription for systematizing experimental data measured at ion velocities $v \gtrsim v_0$, and for obtaining interpolations and extrapolations of energy loss and ranges of heavy ions. In addition, the values of $\bar{q}_{\text{eff}}$ deduced from Eq. (5.12) are in reasonable agreement with certain average charge states $\bar{q}$ and, thus, seem to justify Eq. (5.13). Roll and Steigert (1960a) report no significant differences in $\bar{q}_{\text{eff}}$ for ions with $Z\leq 10$ when stopped in gaseous and solid media, but in a more careful analysis of more extensive data, Roll and Steigert (1960b) find that for fluorine ions solid stopping materials lead to distinctly higher values of $\bar{q}_{\text{eff}}$ than gaseous ones. They attribute this difference to the density effect[9] (see Sec. VI). Teplova *et al.* (1962) report the same trend for ions with $Z\leq 36$ and observe that $\bar{q}_{\text{eff}}$ is 10%–20% larger than $\bar{q}_G$, but significantly smaller than $\bar{q}_s$ provided that $Z\gtrsim 18$. Cumming and Crespo (1967) determine $\bar{q}_{\text{eff}}$ in solid targets from their data on fission fragments ($Z\lesssim 66$) and from the data by Moak and Brown (1966) on bromine and iodine ions and find also that $\bar{q}_{\text{eff}}$ is substantially smaller than the values of $\bar{q}_S$ which have been measured directly from stripping experiments in solids. Pierce and Blann (1968) study $\bar{q}_{\text{eff}}$ for ions with $Z\leq 53$ in gaseous and solid stopping materials; they confirm Teplova's and Cumming and Crespo's observations and, moreover, find (i) that $\bar{q}_{\text{eff}}$ does not, in fact, depend significantly on whether the stopping material is a gas or a solid and (ii) that $\bar{q}_{\text{eff}}$ is very close to $\bar{q}_G$ obtained directly from gaseous strippers. Kalish *et al.* (1969) confirmed the latter trend for the case of tantalum ions stopped in solids.

A comprehensive analysis of $\bar{q}_{\text{eff}}$ has been reported by Brown and Moak (1972). They measured stopping cross sections for uranium ions in various solids and used this data as well as earlier results on bromine and iodine ions with energies up to ~ 180 MeV in solids (Moak and Brown, 1966; Bridwell *et al.*, 1967) to calculate $\bar{q}_{\text{eff}}$ from Eq. (5.12). Corrections of S due to nuclear stopping (Lindhard *et al.*, 1963) and due to the "effective" charge of protons at low velocities as defined by Hall (1950) and Booth and Grant (1965) have been taken into account. The values of $S_p(v)$ have been

[8] At velocities below $\sim 2v_0$, one has to take into account the "effective" charge of the proton as discussed by Hall (1950) and Booth and Grant (1965).

[9] Roll and Steigert (1960b) confuse the density effect in solids with the one in gases (see Sec. VI). Since the density effect in solids is not pronounced for light ions, the interpretation of Roll and Steigert is doubtful.

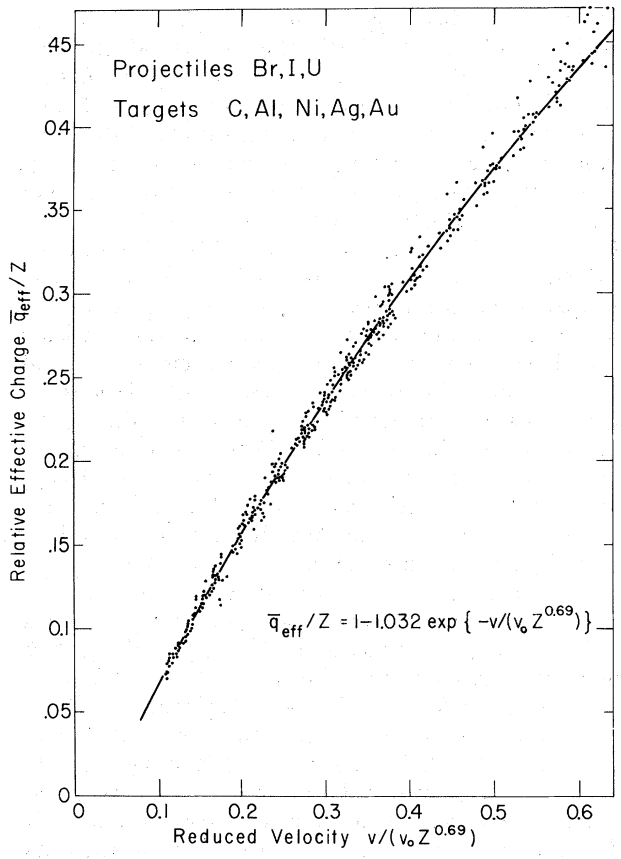

FIG. 5.30. Relative effective charge, $\bar{q}_{eff}/Z$, of bromine, iodine, and uranium ions, deduced from measurements of the energy loss of these ions in various solid targets, plotted as a function of a reduced ion velocity $v_R = v/(v_0 Z^{\gamma})$, where $v_0 = e^2/\hbar$, and $\gamma = 0.690$. The solid line represents a least-squares fit and coincides with Eq. (5.6) for $C = 1.032$ and $\gamma = 0.690$; from Brown and Moak (1972).

interpolated from the semiempirical data tables by Northcliffe and Schilling (1970). Figure 5.30 shows the resulting values of $\bar{q}_{eff}/Z$, plotted as a function of a reduced ion velocity. It turns out that the data is approximated with remarkable accuracy by Eq. (5.6), provided that $C = 1.032$ and $\gamma = 0.690$ (solid line in Fig. 5.30). This result is in close agreement with earlier estimates by Barkas (1963) and Pierce and Blann (1968) who used the same formula with $C = 1$ and $\gamma = \frac{2}{3}$, but replaced the Thomas–Fermi velocity, $v_r = v/(v_0 Z^{2/3})$, by the modified reduced velocity $0.91 v_r$ and $0.95 v_r$, respectively. Interestingly, Brown's well substantiated function for $\bar{q}_{eff}/Z$ almost coincidences with the semiempirical relation for $\bar{q}_G/Z$ of Betz *et al.* (1966). It is worth noting that according to Brown's results and in contrast to expectations based on the theory by Lindhard *et al.* (1963), neither $\bar{q}_{eff}$ nor S vary strictly proportionally with v in any wide range of ion velocities.

Another significant result on $\bar{q}_{eff}$ has been reported by Petrov *et al.* (1970). They investigated both $\bar{q}_G$ and $\bar{q}_{eff}$ for ions in the range $36 \leq Z \leq 74$ at velocities near $v/v_0 \simeq 4$ in air and helium. They find that not only $\bar{q}(Z)$ but also $\bar{q}_{eff}(Z)$ show an anomalous decrease when Z increases from ~ 60 to 74. While the effect for $\bar{q}_G$ is understandable as has been discussed in Sec. V.2.c, the observation that $\bar{q}_{eff}$ behaves like $\bar{q}_G$ even in such a particular situation points out again the deep correlation between $\bar{q}_G$ and $\bar{q}_{eff}$.

When it first became evident that $\bar{q}$ differs substantially depending on whether heavy ions are stripped in gases or in solids, one expected, according to Eq. (5.12), a significant difference in corresponding stopping powers.[10] The fact that this expectation could not be verified experimentally resulted in considerable speculation on possible screening of the high-charge states of ions inside solids, or of surface effects of the stripping foils, etc. The recent conclusion by Betz and Grodzins (1970) that the charge states of heavy ions *inside* solids differ little from those in gaseous strippers—which has been worked out independent of considerations of stopping powers—resolves many of the discrepancies though a satisfactory understanding of the states of heavy ions inside solids still has not been reached (see Sec. VI.2).

A problem of great theoretical importance arises from the argument that essential assumptions which lead to Eq. (5.12) may not be fulfilled for the case of partially stripped heavy ions. This has been clearly realized by most of the investigators. Nevertheless, Eq. (5.12) has been shown to represent a useful semiempirical concept, and it remains to be proven whether the general and close agreement between $\bar{q}_{eff}$ and $\bar{q}_G$ is more than a fortuitous coincidence. Of course, it must be realized that $\bar{q}_{eff}$ can hardly be identical with $\bar{q}_G$; for example, $\bar{q}_{eff}$ has been found to be much more independent on the target material than $\bar{q}_G$. Finally, it is worth mentioning that the formula for the stopping cross section S by Lindhard *et al.* (1963) is completely independent of the density of the stopping medium, i.e., is intended to apply to both gaseous and solid media and does not explicitly contain an effective charge. In view of a comparison of this formulation with Eq. (5.12), we note that the ionic charge is not a free variable inside a target but assumes certain velocity-dependent equilibrium values. Utilizing this well-defined dependence $\bar{q}_G(v)$, the charge dependence can be eliminated from Eq. (5.12).

VI. DENSITY EFFECTS IN HEAVY-ION STRIPPING

Since the earliest theoretical studies of the phenomena of heavy-ion charge exchange in atomic collisions, it has been realized that the state of excitation of the projectile ions may significantly influence the probabilities for electron capture and loss by the heavy ions. Lamb (1940), in his investigation of the slowing down process of uranium fission fragments, explicitly

[10] See the remark in the paper by Bohr and Lindhard (1954) on pp. 29–30.

notes that his calculations of the average ionic charge can be valid only when the target is an ideally rarified gas. He argues that only in that case is the time between impacts great enough so that the ions always have time to return to their ground state before the next collision. Under these circumstances one can be certain that the fragments are not stripped further than to the extent implied by assuming a dilute target gas. The first conclusive experimental evidence for density effects was found in connection with systematic studies of the ionic charge carried by fission fragments. Lassen (1951a) showed very clearly that the average equilibrium charges obtained in solids are significantly higher than the ones produced in gaseous targets. He also found that the mean charge in gases increases slightly but noticeably when the gas pressure is sufficiently increased (Lassen 1951a, b). In an important paper, Bohr and Lindhard (1954) presented a quite detailed explanation for the density effect which occurs in gases, and a qualtitative theory for the density effect which is produced by solid targets. These two theoretical models, to which we refer hereafter as the BL models, have generally been accepted though no convincing experimental proof has ever been given. In the course of time, several investigators confirmed Lassen's basic observations for heavy ions other than uranium fission fragments, thereby establishing the existence of a general influence of ionic excitation on charge-changing collisions involving heavy particles. Additional contributions, however, which helped to enlighten the mechanism of the density effects, were not made until direct measurements of cross sections for electron capture and loss as a function of the degree of residual ion excitation were performed (Ryding *et al.*, 1970c). The results, for the first time, revealed that the BL model for the density effect in gases is not completely correct and needs substantial refinement (Betz, 1970). Partly based on these results, it was possible to develop a basic modification of the BL model for the density effect in solids, which leads to a result quantitatively opposite to the predictions of the BL model (Betz and Grodzins, 1970). Still, much uncertainty prevails and more work needs to be done before a full and quantitatively satisfactory understanding of both density effects will be attained. It is important to note that the study of ionic excitation produced in charge-changing collisions yields not only information which is useful for many practical purposes, but which must also be regarded as a powerful technique for investigating many of the basic phenomena associated with ion–atom collisions.

1. Density Effect in Gases

a. Bohr and Lindhard Model

The first basic assumption in the BL theory for the density effect in gases is that an excited electron can be stripped from a heavy ion more easily than an electron which is bound in the ground state. In a dense target, the most weakly bound electron in colliding ions is considered to have an average residual excitation $\bar{\epsilon}I$ where I denotes the ground state ionization potential for that electron. It is expected that the cross section for loss of such an excited electron increases substantially when $\bar{\epsilon}$ increases. As a second decisive process, the BL model takes into account that capture by an already excited ion may lead to a state in which the total excitation energy exceeds the binding energy of the most loosely bound electron. In these cases, an electron will be ejected by a rapid Auger process within a time ($\sim 10^{-15}$ sec) which is short compared to the average time between two successive charge-changing collisions. As a consequence, the electron capture cross section appears to be reduced.

Bohr and Lindhard base their quantitative estimates on a simple linear expansion of Eqs. (4.10) and (4.11) of the cross sections per atom for loss and capture of a single electron by ground state ions of charge q. Provided that q is not too far from $\bar{q}$, they assume

$$\sigma_l(q) = \sigma_0[1+\alpha_l(\bar{q}-q)], \tag{6.1a}$$

$$\sigma_c(q) = \sigma_0[1-\alpha_c(\bar{q}-q)], \tag{6.1b}$$

where $\bar{q}$ denotes the average charge for which, in this simplified description, the cross sections for loss and capture are of equal magnitude, $\sigma_l(\bar{q}) = \sigma_c(\bar{q}) = \sigma_0$. The parameters α_l and α_c are approximated by $3/\bar{q}$ and $2/\bar{q}$. In a cursory estimate, the cross sections per atom for excited heavy ions are assumed as follows:

$$\sigma_l^*(q) = \sigma_l(q)+\sigma_0\beta_l\bar{\epsilon}, \tag{6.2a}$$

$$\sigma_c^*(q) = \sigma_c(q)-\sigma_0\beta_c\bar{\epsilon}, \tag{6.2b}$$

where β_l and β_c are correction factors close to unity. Equating σ_l^* with σ_c^*, one can derive the shift of the mean charge $\bar{q}$ in the equilibrium charge state distribution which results from the influence of residual ion excitation,

$$\Delta\bar{q} = \bar{\epsilon}(\beta_l+\beta_c)/(\alpha_l+\alpha_c). \tag{6.3}$$

The residual excitation in which an ion is left after having lost a single electron is expected to be, on the average, about $\frac{1}{2}I$, whereas the average excitation of an electron after being captured by a ground state ion is believed to be about $\frac{2}{3}I$ in heavy targets, but higher in light targets such as hydrogen or helium. On these grounds, Bohr and Lindhard approximate $\bar{\epsilon} \simeq \frac{1}{2}$ for heavy target gases at densities which are sufficiently high so that deexcitation between two successive collisions can be neglected. Then, with $\beta_l \simeq \beta_c \simeq 1$, Eq. (6.3) yields their final estimate for the maximum of the density effect

$$\Delta\bar{q} = \bar{q}/5. \tag{6.4}$$

In light targets, especially for very fast ions in which, under charge equilibrium conditions, the outer electrons are in states of considerably higher binding energies

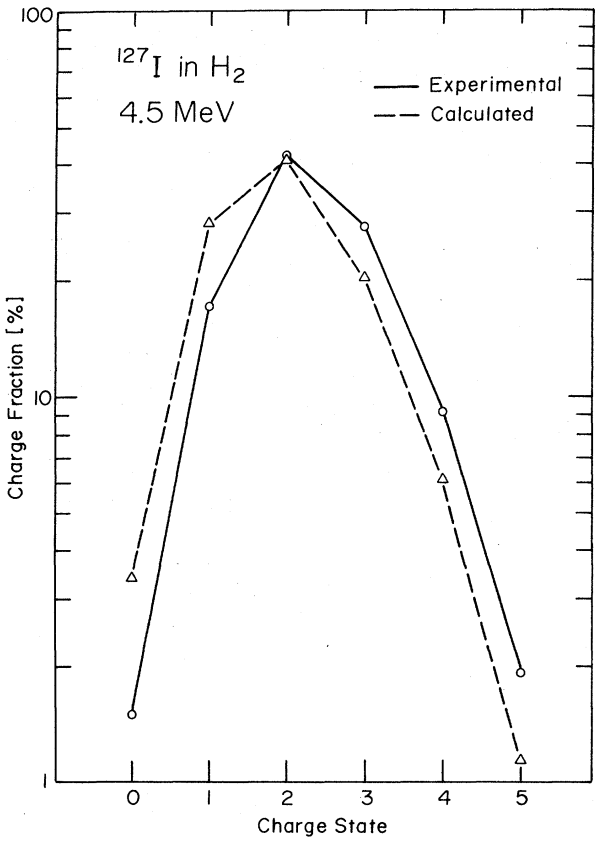

FIG. 6.1. Density effect in equilibrium charge state distributions of 4.5-MeV iodine ions passing through hydrogen: - - -, calculated from ground state cross sections for electron capture and loss; —, measured in dense hydrogen (~0.5 Torr); from Ryding *et al.* (1969a).

than the electrons in the target atoms, Bohr and Lindhard expect values of $\Delta\bar{q}$ which are larger than one would deduce from Eq. (6.4).

b. Experimental Results

Although experiments with fission fragments have well proven the existence of density effects, more thorough investigations were not reported until 1963. Nikolaev *et al.* (1963) measured nonequilibrium charge distributions of 4.9-MeV nitrogen ions passing through nitrogen gas at pressures between 4.5×10^{-5} and 5×10^{-2} Torr. They also calculated the distribution from the relevant experimental cross sections which had been determined in their earlier work [Nikolaev *et al.* (1961a) and Dmitriev *et al.* (1962a)], and observed small deviations of the experimental distribution from the calculated one; in particular, the average charge increased by 0.23 units of charge (~6%) when the gas pressure was increased from 10^{-3} to 10^{-2} Torr. They concluded that in the case investigated the density effect has already occured in that pressure range, though, as they state, the large uncertainties in the experimental cross sections (~15%) do not allow a unique interpretation of their data. At energies below 0.15 MeV where $\bar{q}\lesssim1$, Pivovar *et al.* (1967a) found that charge fractions of lithium, sodium, and potassium ions after passage through vapors of magnesium and cadmium changed by at most a few tens of percent when the pressure of the target gas was increased to as much as 0.7 Torr.

A marked effect was reported by Franzke *et al.* (1967). They measured nonequilibrium charge state distributions for iodine ions stripped in a mercury vapor jet at energies between 18 and 86 MeV and found an anomalous behavior of the mean charge. Using incident ions with charge states slightly higher than the expected mean charge, they observed that $\bar{q}$ first decreased with increasing density of the target, but that at pressures of ~0.15 Torr, $\bar{q}$ reached a minimum value and then increased until equilibrium was established. With a total variation of $\bar{q}$ which amounted to approximately 0.3 units of charge (~3%), the effect is outside the experimental errors. Since nonequilibrium charge state distributions $Y(q;x)$ generally give a monotonous change of $\bar{q}(x)$ towards the equilibrium value, Franzke *et al.* attribute the appearance of a minimum in $\bar{q}(x)$ to the density effect. This reasoning is probably correct though it must be realized that the presence of very large cross sections for multiple-electron loss may lead to a small minimum of $\bar{q}(x)$ even in the absence of residual ion excitation; however, as test calculations show, it appears quite unlikely that the experimentally observed effects can be quantitatively reproduced when reasonably assumed sets of charge-changing cross sections for the ground state alone are being used. Ryding *et al.* (1969a) measured both charge-changing cross sections and the equilibrium charge state distribution for 4.5-MeV iodine ions in hydrogen very accurately. The distribution which was calculated from the experimental cross sections deviated systematically from the measured one (Fig. 6.1); some charge fractions differed by a factor of ~2 and the mean charge of the experimental distribution was shifted by 0.35 units of charge (~17%) towards higher charge states. Since the effective length of the target cell was only 2.94 cm, comparatively high pressures of ~0.5 Torr were required to establish charge equilibrium. Therefore, the time between two successive collisions of an ion was, on the average, as short as $\Delta t=10^{-10}$ sec, and it is reasonable to assume that lifetimes of excited states of iodine ions with charge states $\gtrsim4^+$ can be long compared to Δt. It must be concluded that Ryding *et al.* have observed a density effect in a hydrogen target which influences the effective charge-changing cross sections but which preserves the symmetry in the equilibrium charge state distribution.

A study of the mechanism of the density effect and, thus, a test of the BL theory was performed by Ryding, Betz, and Wittkower (1970c) and Betz and Wittkower (1972b). The decisive achievement in these experiments was that the cross sections for electron capture and loss

were measured directly as a function of the density of the target gas. In that way, it was possible to determine the influence of ionic excitation on charge-changing processes. In one experiment, Ryding *et al.* (1970c) measured cross sections for 15-MeV iodine ions for the cases in which the charge incident on the target cell was produced (i) in the terminal of the accelerator which was located at a distance of ~10m from the target cell, and (ii) in a charge converter cell located about 50 cm in front of the target cell. It turned out that the capture cross section $\sigma(7, 6)$ from (ii) was ~25% smaller than the one from (i), whereas the loss cross section $\sigma(7, 8)$ did not change within the experimental errors of ~5%–10%.

In a modification of case (i), a varying amount of gas (air) was admitted into the charge converter cell, so that the residual gas pressure P increased slightly in the beam line. It was then found that $\sigma(7, 6)$ decreased continuously with increasing P from the maximum value obtained from (i) to the minimum value from (ii). Again, $\sigma(7, 8)$ was not significantly affected. In another approach, complete nonequilibrium charge state distributions have been measured for 4-MeV chlorine ions passing through hydrogen. As an example, Fig. 6.2 shows the particular distribution in which the incident ions carried the charge +4. A cross section analysis described in Sec. III.2 has been applied to several density ranges of the growth curves and yielded the effective cross sections as a function of the target gas density and, thus, of the residual ion excitation. The result is shown in Fig. 6.3. The effective capture cross

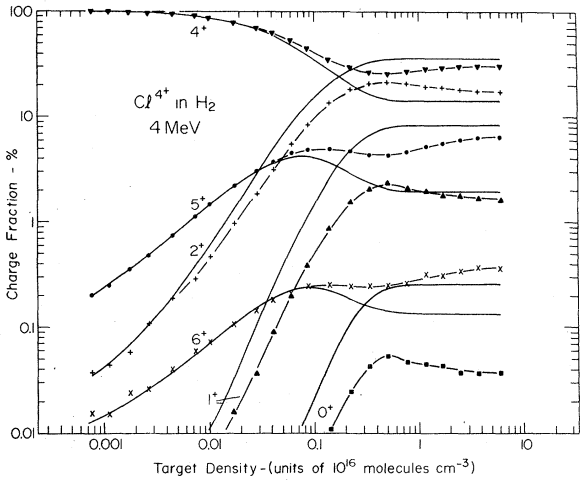

FIG. 6.2. Charge state fractions of a 4-MeV chlorine beam as a function of hydrogen target density (cell length $L=3.65$ cm). Here, 99.7% of the incident ions carried the charge +4. For simplicity, the fractions with charge +3 have been omitted from the graph. The solid lines are computed from a complete set of experimental ground state charge-changing cross sections, and the deviations from the measured fractions indicate the influence of excited states (density effect). The interrupted lines are drawn at intermediate densities to guide the eye and are computed at high densities using ground state cross sections, lifetimes, and parameters for the average residual ion excitation; from Ryding *et al.* (1970c), Betz (1970), and Betz *et al.* (1971b).

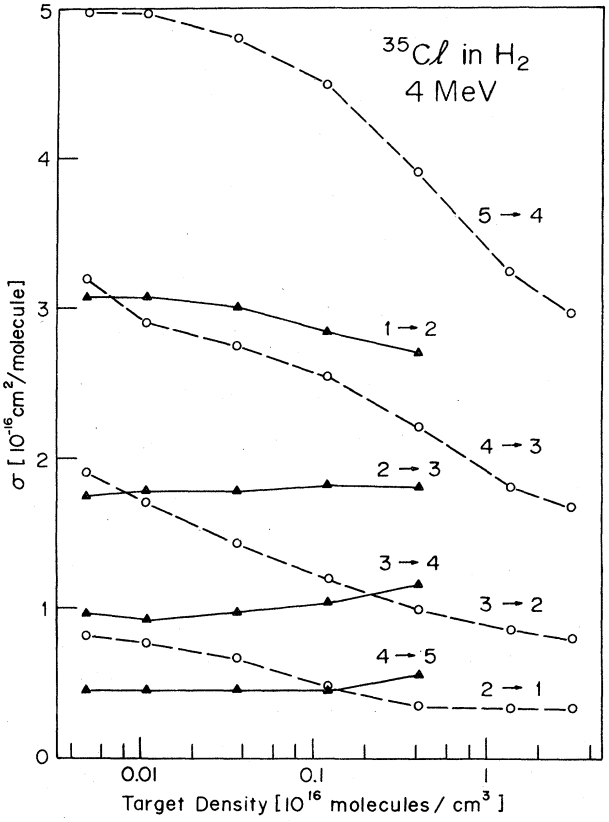

FIG. 6.3. Effective charge-changing cross sections for 4-MeV chlorine ions, determined experimentally as a function of hydrogen target density (cell length $L=3.65$ cm): ▲, single-electron loss; O, single-electron capture; from Ryding *et al.* (1970c).

sections sometimes decreased by as much as a factor of ~2, but no clear-cut change could be observed in the electron loss cross sections. Additional experiments with bromine and iodine ions at other energies and in other target gases yielded similar results (Betz and Wittkower 1972b); in some cases, the capture cross section decreased to one-third of the possible maximum value. Recently, Franzke *et al.* (1972) extended measurements of the above kind to iodine ions stripped in carbon dioxide at energies between 9.5 and 54.8 MeV and likewise found that increasing target density in all cases caused the capture cross sections to decrease significantly, whereas the loss cross sections remained constant within the experimental errors.

The effect of residual ion excitation is further illustrated in Figs. 6.4 and 6.5. In agreement with earlier results (Fig. 6.1), equilibrium charge state distributions which have been measured for bromine and iodine ions stripped in a short target cell containing helium differ systematically from the distributions which have been calculated from experimental charge changing cross sections. Figure 6.6 shows a more direct experimental proof of the density effect for 46-MeV iodine ions (Franzke *et al.*, 1972). At comparable target densities,

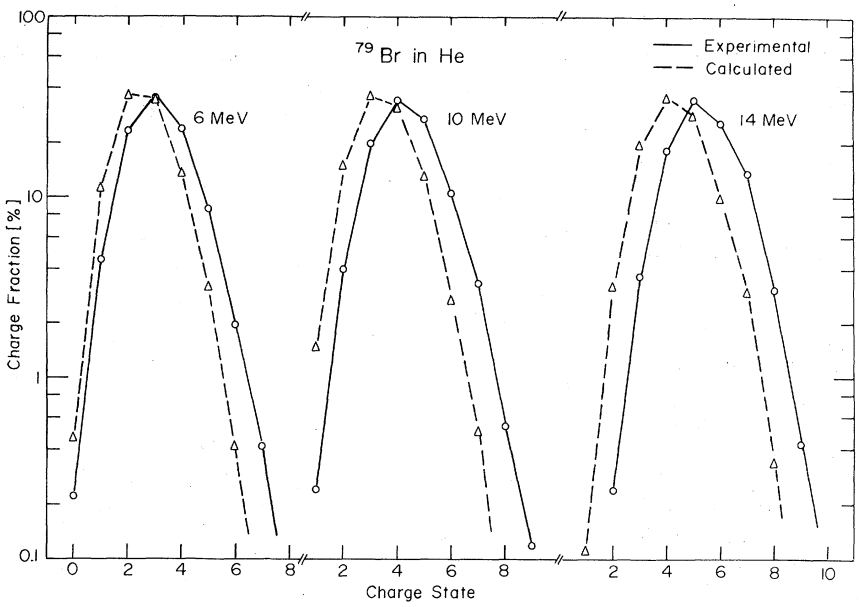

FIG. 6.4. Equilibrium charge state fractions in dilute and dense helium gas for bromine ions at 6, 10, and 14 MeV. The distributions in dilute helium (triangles) have been calculated from experimental ground state cross sections. The distributions in dense helium (circles) have been measured at target densities of approximately 3×10^{16} molecules/cm^3; from Ryding *et al.* (1969b), Betz *et al.* (1971a), and Betz and Wittkower (1972b).

carbon dioxide and nitrogen give very similar equilibrium distributions, but the distributions measured in a dense jet of carbon dioxide are shifted by $\Delta\bar{q}\simeq0.7$ towards higher charge states compared with the distribution obtained from a more dilute nitrogen target. Figure 6.7 presents the shift $\Delta\bar{q}$ of the average charge state which results for the cases shown in Figs. 6.4 and 6.5, as well as for bromine ions stripped in hydrogen and for aluminum ions stripped in nitrogen (Betz and Wittkower, 1972b). It seems that $\Delta\bar{q}$ increases somewhat with the ion velocity. Similar results were obtained by Franzke *et al.* (1971, 1972). Figure 6.8 shows their measurements of average equilibrium charge states for iodine ions stripped at energies between 10 and 75 MeV in dilute and dense gases of carbon dioxide. A maximum difference of $\Delta\bar{q}\simeq1$ is observed at the higher projectile energies.

c. *Modifications of the Bohr and Lindhard Model*

Several modifications of the theory for the density effect in gases, based on the most recent results described above, have been suggested by Betz (1970). These will be discussed below, along with interpretations of the experimental results:

(1) The most significant deficiency of the BL theory

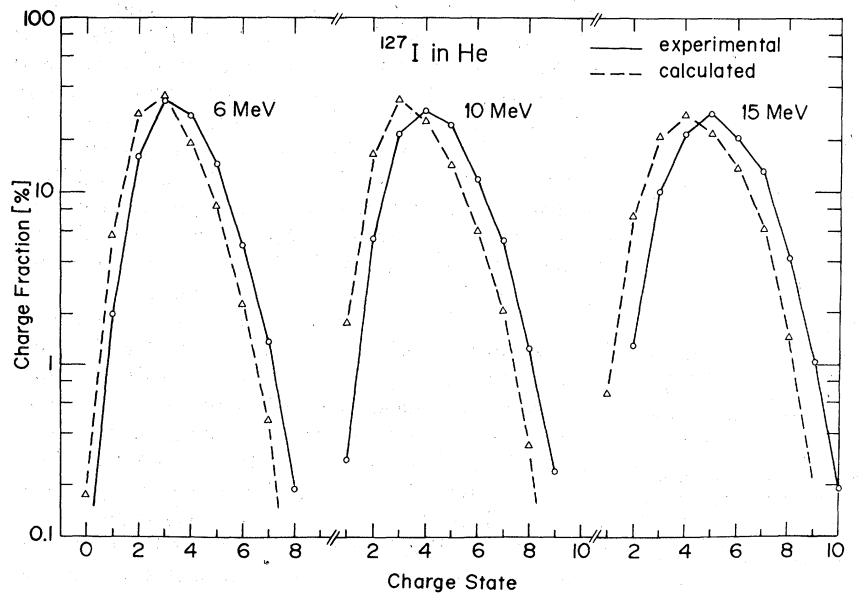

FIG. 6.5. Equilibrium charge state fractions in dilute and dense helium gas for iodine ions at 6, 10, and 15 MeV. The distributions in dilute helium (triangles) have been calculated from experimental ground state cross sections. The distributions in dense helium (circles) have been measured at target densities of approximately 3×10^{16} molecules/cm^3; from Ryding *et al.* (1969b), Betz *et al.* (1971a), and Betz and Wittkower (1972b).

is the assumption that the electron loss cross section per ion increases with the residual excitation of that ion. This prediction could not be verified in any of the experiments cited above. Instead, the cross sections for excited ions do not differ noticeably from the ones for ground state ions, and the parameter β_l in Eq. (6.2a) is close to zero so that

$$\sigma_l^*(q) \simeq \sigma_l(q). \tag{6.5a}$$

(2) The decrease which is observed in the capture cross section is too large to make Eq. (6.2b) practical. Since no strong systematic variation of the maximum decrease was observed, it seems advantageous to replace the BL estimate for σ_c, Eq. (6.2b), by the modified formula

$$\sigma_c^*(q) = \sigma_c(q)/g(q), \tag{6.5b}$$

where the parameter g may to some extent depend on q.

(3) The ground state cross sections for electron capture and loss can be approximated by $\sigma_c(q) \propto q^a$ with appropriate values of a. Rather than using the BL estimates [Eqs. (4.10) and (4.11)] we express, according to Eqs. (2.12) and (2.18), the exponents a in terms of the distribution width d which is better known from experiments. However, one must also take into account that the cross section for capture and loss of more than one electron in a single collision lead to a broadening of the distribution. Thus, according to Eq. (2.16), the reduced width d_0 must be used in Eq. (2.12) rather than the experimental width d.

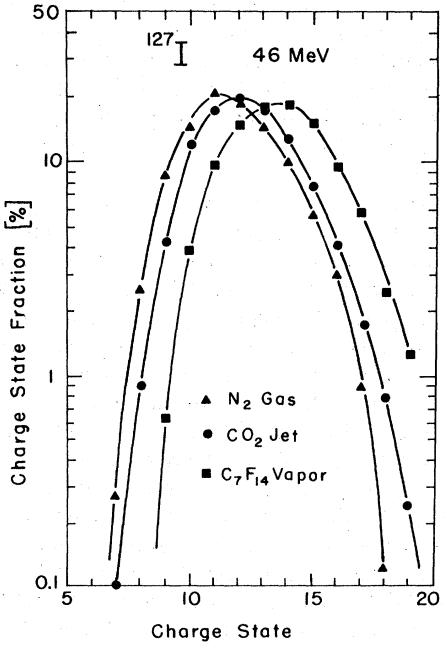

FIG. 6.6. Equilibrium charge state distributions for 46-MeV iodine ions stripped in nitrogen gas at intermediate density of $\sim 3\times 10^{14}$ molecules/cm^3, in a supersonic jet of carbon dioxide with a density of $\sim 1.5\times 10^{17}$ molecules/cm^3, and in a fluorocarbon vapor; from Franzke *et al.* (1972).

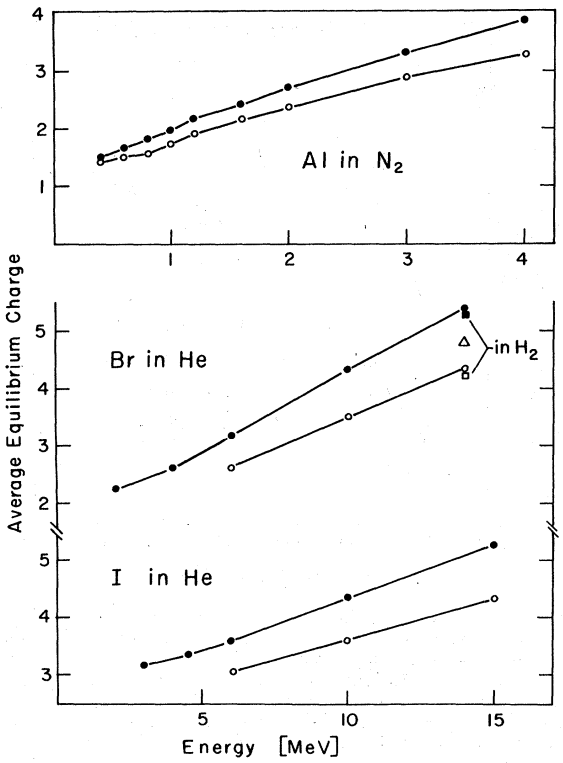

FIG. 6.7. Influence of the target gas density on the average equilibrium charge of aluminum, bromine, and iodine ions, stripped in gases of hydrogen, helium, and nitrogen, as a function of the projectile energy. The full symbols represent values which have been measured in dense gases ($\sim$0.5 Torr), and the open symbols represent values which have been calculated from ground state charge-changing cross sections; from Ryding *et al.* (1969b, 1970a, 1970b), Betz *et al.* (1971a), and Betz and Wittkower (1972b). The open triangle indicates the mean charge which has been measured by Datz *et al.* (1970) for 13.9-MeV bromine ions in helium at intermediate densities of $\sim$0.02 Torr.

If we combine all of the above, a new analytical expression is obtained for the maximum shift of the mean charge under the influence of residual excitation

$$\Delta\bar{q} = d_0^2 \ln g(\bar{\epsilon}), \tag{6.6}$$

where g is the average of $g(q)$ for all relevant charge states.

With $g \simeq 2$ and the results for d_0, Eq. (6.6) describes well the experimentally observed shift. The slight increase of $\Delta\bar{q}$ for higher ion velocities shown in Fig. 6.7 is probably related more closely to the increase in the distribution width which is observed in that velocity range, than to an increase in the residual ion excitation. The increase of $\Delta\bar{q}$ shown in Fig. 6.8 must be largely ascribed to the density effect which occurs to some extent even in the "dilute" target gas (10^{-2} Torr CO_2). It is interesting to note that Eq. (6.6) also conforms to the results shown in Figs. 6.4 and 6.5. In these cases, where most of the relevant ground state cross sections have been measured, the assumption that Eq. (6.5a) is valid, makes it possible to determiue σ_c^* solely from the

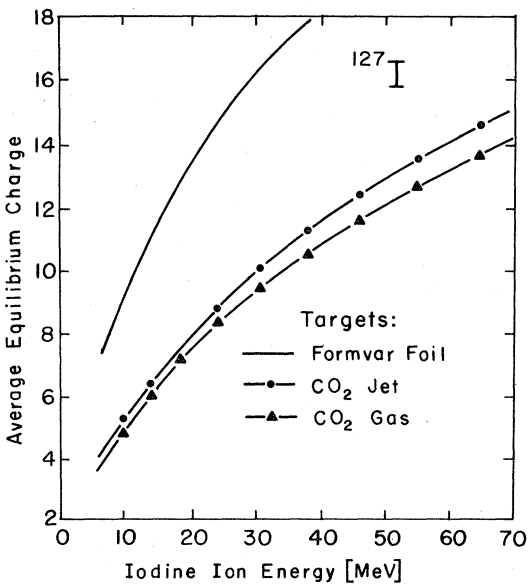

FIG. 6.8. Average equilibrium charge of iodine ions stripped in carbon dioxide at intermediate densities of $\sim 3.3\times 10^{14}$ molecules/cm^3 and in a supersonic jet of carbon dioxide at higher densities of $\sim 1.5\times 10^{17}$ molecules/cm^3, as a function of the energy of the iodine projectiles; from Franzke *et al.* (1971). For comparison, the average equilibrium charge of iodine ions is also shown for formvar foil targets; from Betz *et al.* (1966).

equilibrium distributions which have been obtained in the dense gas. The values of g determined in that way were always close to 2. In particular, it follows that a reduction of the ground state capture cross sections by $\sim 50\%$ allows the reproduction with high accuracy of the experimental distributions for the dense gases. It must be emphasized, however, that this latter procedure is successful only when most of the relevant ground state cross sections are known and is, thus, not easily applied when numerous multiple electron loss cross sections, which are difficult to measure are influential.

Discussion of electron loss. The question arises as to whether the above modifications represent a general trend. In order to throw light on that problem, the following explanation of the result Eq. (6.5a) may be attempted. First, in a heavy ion, a large number of electrons, especially the ones in the outermost shell, are in comparable quantum states and have binding energies which differ little. One would expect, therefore, that all of these electrons have similar probabilities of being removed in a collision. Second, in a dense gas, the average time between two successive collisions is still long enough to allow Auger processes to take place so that the residual ion excitation will be smaller than the ionization energy. In these cases, even though the loss cross section for a particular excited electron will increase as anticipated in the BL model, the loss cross section per ion will change very little as all the other contributing electrons are still in the ground state. That conjecture is not true, of course, when the residual excitation is extremely high so that the loss cross section for the excited electron dominates. However, such an excessive average excitation has not been observed as will be evident from the discussion of the capture cross sections below. In addition, there is some evidence that an increase of the excitation above a certain value does not lead to a further significant increase of the loss cross section for that electron; for helium ions the approximate maximum cross section is reached for the excitation which corresponds to the metastable state (Gilbody, 1971).

It must also be noted that an additional dilution of the effects of excited electrons on effective loss cross sections arises in view of the possibility that not all collision processes leave the ions in excited states; thus, a considerable fraction of ions in a beam passing through a dense gas may still be either in the ground state or close to it. Incidentally, the above explanation and the net result Eq. (6.5a) need not be substantially changed when it is assumed that the residual ion excitation is distributed among several electrons. The conjecture that many electrons in an ion contribute to the total electron loss cross section is also supported by the observation that multiple loss events are frequent even in helium targets (Datz *et al.*, 1969; Betz *et al.*, 1971a), and that cross sections for removing electrons from inner shells are more important than anticipated in the BL theory.

The argument concerning σ_l^* which we have discussed above implies that Eq. (6.5a) refers only to those ions which contain a large number of bound electrons whereas it can not apply to ions or atoms with only a few bound electrons. For example, it is well established that σ_l^* for excited helium projectiles is indeed significantly larger than for the ground state projectiles (Schlachter *et al.*, 1968; Gilbody *et al.*, 1968, 1970).

Discussion of electron capture. The experimental results on effective electron capture cross sections allow direct estimates to be made of the states into which electrons are captured by partially stripped heavy ions. This is of particular significance because no rigorous theoretical calculations of these final states have been performed. Only two estimates have been frequently considered. First, the BL model suggests that electrons are captured into states of extremely high excitation, especially in the case of swift heavy ions passing through very light gases. Second, it has often been argued that in analogy to the results for protons or other fully stripped ions, electron capture into the ground state is of dominant importance, especially for high-ion velocities (see Sec. IV.2). Neither picture, however, can be used in order to explain the particular experimental observation that effective capture cross sections of excited ions generally decrease to about half the value which is measured for ground state ions (Ryding *et al.*, 1970; Betz 1970; Betz and Wittkower, 1972b). The dis-

crepancy between these findings and the two estimates mentioned above is easily demonstrated by considering those experiments in which the capturing ion of charge q has been formed and excited itself solely by electron capture. Whenever the total excitation I_t^* of such ions immediately after the second capture event exceeds the ionization potential I_{q-1}, autoionization can occur within a relatively short time and the ionic charge will increase back to its original value; then, no contribution is given to the measured effective capture cross section. On the one hand, in the BL picture, such processes would occur with very high probability since the large excitation associated with each capture event would easily lead to $I_t^* > I_{q-1}$. As a consequence, the effective capture cross section $\sigma_c^*(q)$ would be very small compared to $\sigma_c(q)$. On the other hand, preferential capture into the ground state would not often allow the condition $I_t^* > I_{q-1}$ to be satified and σ_c^* would be very close to σ_c. On the basis of the experimental values $\sigma_c/\sigma_c^* \simeq 2$, it may be concluded that in approximately 70% of the processes electrons are captured into states of relative excitation $\epsilon_c \gtrsim \frac{1}{2}$, and that in 30% of the cases electrons are captured, directly into the ground state or into states with $\epsilon_c < \frac{1}{2}$. The lack of better theoretical understanding and the relatively sparse experimental data preclude a generalization of that conclusion though it seems likely that it represents a situation which is quite typical for partly stripped heavy ions in the velocity range which has been investigated experimentally.

In the above estimate we have neglected any influence of the residual ion excitation on the probability for capturing electrons. Of course, it can not be ruled out that an ion which is already excited captures with a somewhat smaller probability than a ground state ion. However, while such an influence would to some extent decrease the relative number of Auger electrons emitted in the cases where $I_t^* > I_{q-1}$, it would probably have no dramatic influence on the above conclusions regarding initial electron capture. The latter argument is based mainly on the large number of final states into which electrons may be captured. In a further complication, residual ion excitation may depend on the ionic charge and may be influenced by shell effects. There has been evidence that σ_c/σ_c^* increases to the larger value of $g \simeq 3$ near the $M \rightarrow N$ and $N \rightarrow 0$ shell transition for bromine and iodine ions of charge 7+, respectively (Betz and Wittkower, 1972b). Such an increase appears plausible on the grounds that I_6 is significantly smaller than I_7. Then, I_t^* is more likely to exceed I_6, and the probability for emission of an Auger electron is enhanced.

d. Average Lifetimes of Excited Heavy Ions

The density effect in gaseous targets can be utilized to study average lifetimes of heavy ions excited in collisions with the target gas atoms. Extensive knowledge of these lifetimes, in turn, allows predictions about the occurrence of the density effect. Although our present understanding of charge-changing and excitation processes is still too incomplete to serve as a basis for an accurate determination of the lifetimes involved, it is quite useful to summarize a few attempts which have been undertaken in order to elucidate this question.

Bohr and Lindhard (1954) presented a simple theoretical estimate for radiative lifetimes of excited highly ionized heavy ions:

$$\tau \cong \tau_0 \nu^{*5}/q^4 \qquad (\tau_0 = 0.9 \times 10^{-10}\ \text{sec}), \quad (6.7)$$

where q is the charge of the ion, and ν^* an effective quantum number somewhat higher than, but comparable to the quantum numbers of the most loosely bound electrons in the ground state of the ion. Bohr and Lindhard based their consideration on the probability for spontaneous emission of dipole radiation which yields the well-known formula

$$\tau \propto \Delta E^{-3} a^{-2}, \quad (6.8)$$

where ΔE and a represent the excitation energy I^* and the radius of the radiating ion. For the present case, they approximate I^* by I_q/ν^*. Expressing the ionization potential I_q in terms of the statistical velocity u of the outermost electron in the ion, $u = v_0 q/\nu^*$, and using $a = a_0 \nu^{*2}/q$, one arrives easily at Eq. (6.7). Though Eq. (6.7) has often been considered as a reasonable approximation, it may not always be directly applicable in its simplest sense to practical cases of present interest. For example, charge-changing collisions may excite states of high angular momentum which do not decay in a simple manner.

In order to explain the experimental results on the density effect obtained by Lassen (1951a, b), Bohr and Lindhard (1954) describe a simplifying model for the excitation and de-excitation of fission fragments. They derive an expression for the increase of the average equilibrium charge as a function of the target gas density

$$\Delta \bar{q} = (\beta_l + \beta_c)\tau v \sigma_t \rho / [(\alpha_l + \alpha_c)(2\tau v \sigma_t \rho + 1)], \quad (6.9)$$

where τ is the lifetime under investigation, v the ion velocity, ρ the density of the target gas, and σ_t the total charge-changing cross section which, in fact, stands for the effective excitation cross section. For large values of ρ, Eq. (6.9) becomes identical with Eq. (6.3). With their theoretical estimates of σ_t, Bohr and Lindhard compared Eq. (6.9) with the charge increases which had been observed by Lassen for fission fragments penetrating through gases at pressures above ~ 1 Torr. The lifetimes which resulted from that analysis for the light and heavy group of fission fragments were of the order of 10^{-11} sec. With slightly modified techniques, Fulmer and Cohen (1958)

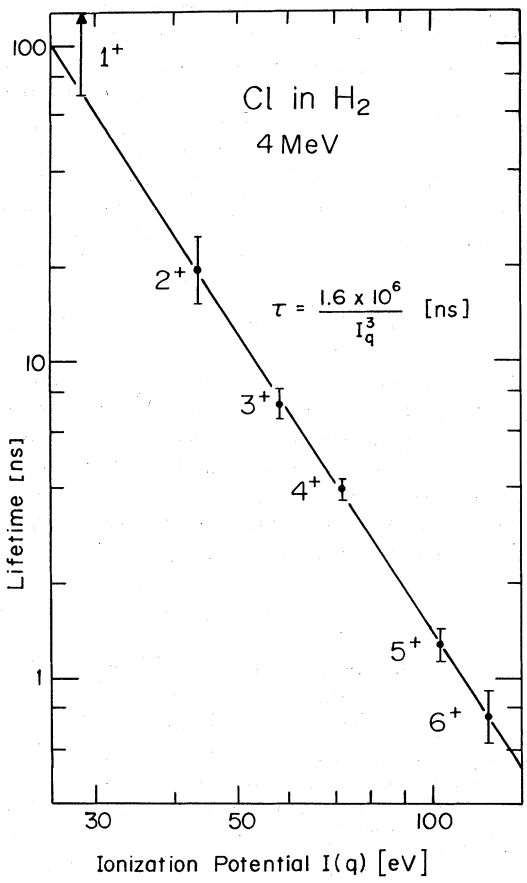

FIG. 6.9. Average effective lifetimes τ_q of 4-MeV chlorine ions excited in collisions with hydrogen atoms as a function of the ionization potential I_q of the relevant charge state; from Betz *et al.* (1971b). The potentials I_q are taken from Carlson *et al.* (1970).

repeated Lassen's experiment and Bohr and Lindhard's analysis and arrived at lifetimes of essentially the same order of magnitude.

An interpretation of these lifetimes is very complicated; they are not only averages over large ranges of ionic and nuclear charges and masses of the fission products, but are also based on quite uncertain assumptions on both charge-changing cross sections and excitation mechanisms. Nevertheless, these early results agree surprisingly well with the estimates Eq. (6.7).

A more sohpisticated technique for determining average lifetimes has been reported by Betz *et al.* (1971b). It is mainly based on the sensitivity of electron capture cross sections to the state of excitation of the capturing ion. Some advantages of that technique which is discussed below are summarized as follows: (i) resultant lifetimes are averages over only a certain number of excited states of a well-defined ion, (ii) ground state charge-changing cross sections and the relative number of excited ions are determined within the experiment rather than by theoretical estimate, and (iii) the important dependence of charge-changing cross sections on residual ion excitation is accounted for.

Betz *et al.* utilized the pressure dependence of the charge state distributions of heavy ions traversing gaseous targets (see Fig. 6.2). Though the increase of $\bar{q}$ beyond the value which would be obtained in a dilute gas remains relatively small, the individual charge state fractions may change more than by a factor of ~ 2 and, thus, show a remarkable sensitivity to residual ion excitation. A complete and thorough analysis of these charge state distributions requires a description of the build-up and decay of excitation of ions in the various charge states. This procedure, however, is too complicated to be readily carried out in practice. Therefore, Betz *et al.* restricted the lifetime analysis to those parts of the distributions for which the gas density was sufficiently high to produce equilibrium in the distribution of both charge states and excitation of these charge states. Under such circumstances, the distributions $F(q)$ reflect charge state equilibrium inasmuch as they are independent of initial conditions of the incident ion beam, but they do change with ρ, and the final equilibrium distribution is not reached until ρ is high enough so that all relevant lifetimes are small compared to the average time, Δt, which elapses between two successive charge-changing collisions.

It is possible to describe the charge state fractions for each gas density in the specified restricted range of densities by reinterpreting the well-known system of coupled linear equations Eq. (2.1) in the form

$$\sum_{q' \neq q} [\sigma^*(q', q; \rho) F(q'; \rho) - \sigma^*(q, q'; \rho) F(q; \rho)] = 0, \tag{6.10}$$

where q' and q vary between the lowest and highest relevant charge states, and σ^* stands, depending on the sign of $q'-q$, for either effective electron loss or capture cross sections. As a first approximation, it is assumed that the average initial equilibrium excitation, $\bar{\epsilon}_q$, which is produced in the collisions, decays between two successive collisions to $\bar{\epsilon}_q \exp[-\Delta t(q)/\tau(q)]$, where for each initial q, $\Delta t(q)$ is related to the total ground state charge-changing cross section by

$$\Delta t(q) = [v \sigma_t(q) \rho]^{-1}. \tag{6.11}$$

Increasing gas density will shorten Δt and increase the number of ions which remain excited until they undergo a charge-changing collision. According to the results elaborated in Sec. VI.1.c, Betz *et al.* define the parameters $g(q)$ as those fractions of ions with charge q the electron capture processes of which are followed by immediate emission of Auger electrons. Then, the effective capture cross sections become

$$\sigma_c^*(q) = \sigma_c(q) \{1 - g(q) \exp[-\Delta t(q)/\tau(q)]\}. \tag{6.12}$$

Introducing Eqs. (6.11) and Eq. (6.12) into Eq. (6.10) and utilizing the result that σ_l^* is practically very close to σ_l [Eq. (6.5a)], one can obtain the parameters $\tau(q)$ and $g(q)$ from a usual least-squares analysis in which the fractions $F(q;\rho)$ computed from Eq. (6.10) are fitted to experimental fractions which have been measured over an appropriate range of target densities. As an example, Fig. 6.9 shows results deduced for 4-MeV chlorine ions passing through hydrogen gas. The lifetimes for charge states 1+ to 6+ range from more than 65 nsec to less than 1 nsec and decrease with increasing charge. With regard to the theoretical estimate Eq. (6.8), it is interesting to point out the proportionality $\tau_q \propto I_q^{-3}$ and, since $g(q)$ is not critically dependent on q, $\tau_q \propto I_q^{*-3}$.

In the above technique, several simplifications have been made. It has been assumed that substantial excitation is mainly a result of charge exchange rather than of less violent collisions in which the ionic charge is preserved. Cross sections for multiple-electron capture have been neglected; however, usually in hydrogen targets, and especially in the case considered here, double capture amounts to less than 1% of the corresponding single capture cross section. There is also some uncertainty concerning the precise definition of $\sigma_t(q)$ in Eq. (6.11); it may be necessary to take into account some dependence on ρ. We note that a possible influence of residual ion excitation on initial electron capture, which was discussed in Sec. VI.1.c, will not affect the determination of τ. More critical is a realistic interpretation of the deduced lifetimes. In general, it can hardly be assumed that they correspond to single radiative transitions or to averages of several differing single transitions. In fact, the possibility of cascades cannot be ruled out. Evidence for that may be seen in the result that the experimental lifetimes shown in Fig. 6.9 are significantly longer than one would expect from theoretical estimates, e.g. from Eq. (6.8). It appears likely that charge-changing collisions excite states of high angular momentum which decay mostly via cascades. If only two participating intermediate levels are added, one obtains, on a classical basis, Eq. (6.8), lifetimes which are longer by almost two orders of magnitude and, thus, offer an explanation of the experimental values. If that conjecture is correct, one should observe further density effects at significantly higher target densities.

Effective lifetimes which are very long ($\tau v \gtrsim 1m$) may be investigated more directly by the following technique. The ions are excited at a distance R in front of the main target cell, and the capture cross sections for electron pickup by ions of a particular isolated charge state are measured in the main target cell. The increase of $\sigma_c^*(q)$ with increasing R allows us to determine $g(q)$ and $\tau(q)$ solely from Eq. (6.12), where $\Delta t(q)$ is to be replaced by R/v.

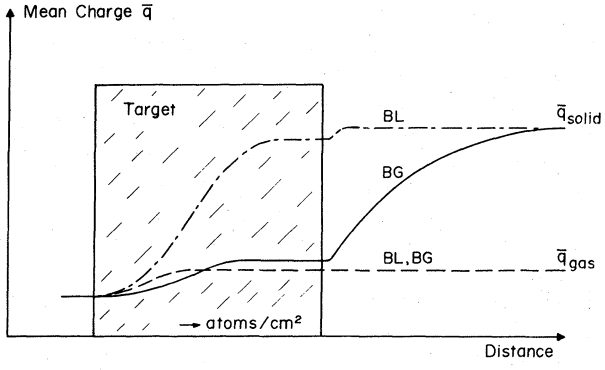

FIG. 6.10. Schematic illustration of the average charge of heavy ions passing through dense gases and solids. The slashed area represents the target. BL, theory by Bohr and Lindhard; BG, modified theory by Betz and Grodzins (1970).

2. Density Effect in Solids

a. Bohr and Lindhard Model

Bohr and Lindhard (1954) have presented a qualitative explanation for the difference $\Delta\bar{q}_s$ between the mean equilibrium charge in a solid compared with a gas stripper. In its simplest interpretation, the BL model suggests that collisions with the target atoms lead to excitation of the most loosely bound electron in the heavy ion. Due to the rapid succession of collisions, the dissipation of ion excitation by radiation can be neglected and excitation initially confined to one electron will rarely be redistributed over several electrons. Thus, the collisions constantly increase the excitation of the most weakly bound electron until it is lost. This reasoning applies consecutively to a certain number of electrons. Finally, a new equilibrium will be reached in which electron capture balances electron loss, the latter being significantly increased due to decreased binding energy of the excited electrons. In particular, an electron captured into an excited state will be lost from the same state, so that for each single-electron state there is a direct competition between electron capture and loss.

It must be concluded that the main increase of the equilibrium charge occurs inside the solid (see Footnote 10), though Bohr and Lindhard also indicate that the high excitation of the ions in solids may result in a subsequent emission of electrons from the ions immediately after their escape into vacuum, which increases the mean charge to a certain extent. Part of Fig. 6.10 illustrates this argument schematically.

In a closer discussion, it is enlightening to point out how the BL model explains the major part of the difference of the density effects in solids and gases. In view of the ratio between collision frequency and revolution frequency for the orbital motion of the ion

electrons, individual collisions in gases and solids are not treated as being basically different. Therefore, it is assumed that in both cases electrons are initially captured into states of fairly high excitation. As regards solids, this assumption is necessary in order to argue that the effective loss cross sections for these excited electrons are significantly larger than are those for the same electrons in the ground state. It may be estimated from Fig. 6.11 that the ratio σ_l^*/σ_l which is needed in order to explain the observed shifts $\Delta\bar{q}_s$ must indeed be exceptionally high (typically ~ 80). In a dense gas target, in contrast, the time between two successive collisions is still long enough to allow a redistribution of the initial excitation among several electrons so that the effective loss cross sections are much less enhanced and, thus, result in an increase of the mean equilibrium charge which is much smaller than the one for solids.

b. Modifications of the Bohr and Lindhard Model

Betz and Grodzins (1970) have shown that the BL model needs fairly substantial modifications which are partly suggested by the results obtained in connection with the density effect in gases (see Sec. VI.1.). We will first give some indirect evidence that the BL assumptions on the initial ion excitation are in disagreement with experimental observations. Then, based partly on that result and partly on general grounds, a modified theory will be described.

A consistent interpretation of the BL model requires us to assume that in both gases and solids, fast heavy ions capture electrons into states of very high excitation. The experiments which have been carried out in dense gaseous targets do not support that assumption (Sec. VI.1.b, c). Since redistribution of electron excitation does not change the excitation per ion, subsequent electron capture by such highly excited ions would most likely lead to a total excitation energy which is larger than the ionization energy for the ion in the new charge state. Consequently, an Auger electron would be ejected and the effective capture cross section for an excited ion would be extremely small as compared to a ground state ion. This could not be verified experimentally (Sec. VI.1). It must be concluded that it is unlikely that the average excitation of an ion produced in a single charge-changing collision is extremely high. This reasoning does not change when additional processes, such as electron loss processes, which also contribute to ion excitation, are taken into account. Therefore, it becomes difficult to reckon with exceedingly large ratios σ_l^*/σ_l inside solids. Such large ratios are even more questionable in view of the experimental results that effective electron loss cross sections per ion do not significantly change when the ions assume an excitation which is produced in typical single charge changing collisions (Sec. VI.1.b).

In an alternative explanation of the density effect in solids which is in better agreement with available experimental results, Betz and Grodzins (1970) suggest that (i) single charge-changing collisions produce, on the average, an excitation of single electrons which is not exceedingly high, and (ii) all electrons in outer subshells of a heavy ion are to be treated equally, i.e., a large number of electrons will significantly contribute to electron loss and ion excitation. On that basis, a heavy ion which enters a solid with a charge close to the average equilibrium charge obtained in a gas will experience collisions in which all outer electrons become preferentially excited rather than lost. Thus, under equilibrium conditions, a large number of outer electrons and, perhaps, some inner electrons will be simultaneously excited. Due to that excitation of essentially all electrons which also contribute to electron loss, the effective loss cross section per ion will increase to some extent and the average charge will be shifted by a relatively small amount, $\Delta\bar{q}_i \simeq 1-2$. As a most decisive consequence of the new model, the total excitation per ion will be large enough to allow the ejection of many Auger electrons after the ions have emerged from the solid. This latter effect is then responsible for the main increase of the charge (Fig. 6.10).

In a closer discussion of the equilibrium states of fast heavy ions inside solids, Betz and Grodzins point out that substantial simultaneous excitation of several electrons in an ion is possible because Auger processes are not fast enough to allow the ions to return to their ground state or close to it within the short time between two successive collisions in a solid. More specifically, equilibrium is maintained by competition between electron capture and loss on the one hand, and collisional excitation and Auger processes on the other hand. This means that the Auger effect serves as a readjustment process which, in competition with further excitation, contributes to maintaining the equilibrium level of excitation. The lifetimes for autoionization processes in outer shells are difficult to estimate. In general, one should expect that the relatively large overlap among wave functions will cause the lifetimes to become shorter than in cases involving inner-shell vacancies. We note that this argumentation does not hold for radiative de-excitation. For example, K vacancies decay much faster by x-ray emission than L vacancies. However, it must be realized that multiple excitations in outer shells are of an extremely complex nature. For example, Lichten (1967) points out that the excitation levels are ill-defined and that except for the case of long-lived discrete states a statistical model like the one proposed by Russek (1963) may be the only practical theoretical approach. This is in marked contrast to the case of collisions which result in inner-shell excitation with well-defined states and which can be better handled theoretically (Fano and Lichten, 1965; Lichten, 1967).

As a further consequence, the decisive difference of

the density effects in gases and solids can now be explained in a simple manner. In a solid, the collision frequency is too high to allow complete Auger de-excitation to take place between two collisions, whereas in a dense gas there is still sufficient time for rearrangement processes via emission of Auger electrons. The total residual excitation energy, therefore, will be very high inside a solid ($I_t^* \gg I_q$), but small in a dense gas ($I_t^* < I_q$).

Despite the fact that several details of the BL model can hardly be maintained, the new model by Betz and Grodzins cannot yet be regarded as a final one, especially because an experimental verification has not yet been made.[11] A quantitatively accurate estimate of the charge increase inside the solid, $\Delta\bar{q}_i$, is particularly difficult. For example, it may be possible that initial electron capture is reduced due to the large ion excitation inside solids. This would lead to a further enhancement of $\Delta\bar{q}_i$. Still, whenever the total ion excitation inside a solid is very high, the Auger effects outside the solid will contribute the major fraction to the observed density effect.

Equilibrium charge state distributions obtained from solids are, at least for fractions above $\sim 1\%$, more symmetrical than corresponding distributions in gases with, say, $Z_T \simeq 6-8$. Though the exact reason for this effect is unknown we conjecture that, on the one hand, the asymmetries inside solids are less pronounced than in comparable gases and that, on the other hand, remaining asymmetries are partly suppressed by the statistical Auger processes which occur outside the solid. As regards the first of the two possible explanations, we are faced with the fundamental question of the significance of multiple-electron loss cross sections inside solids. It has been argued in Sec. IV.2 that in addition to the one kind of collisions in which several electrons are directly knocked out of a heavy ion during an encounter, we also have another kind of collision in which the many electrons, rather than being ejected during the actual encounter, are emitted as a consequence of certain rearrangement processes. In the latter case, substantial excitation energy is transferred to the ion in a collision and it requires a certain time, Δt_R, until de-excitation and emission of all Auger electrons are essentially complete. It is not too difficult to imagine that Δt_R could be longer than the average time between two successive collisions of a heavy-ion penetrating through a solid at high speed. Under those circumstances, multiple-electron loss cross sections will to some extent change into excitation cross sections. Thus, in the balance of electron capture and loss, the influence of multiple-loss cross sections is diminished and, according to the discussion in Sec. II.3, a reduced asymmetry of the charge distribution results. Incidentally, multiple-electron capture cross sections are of somewhat increased importance in solids. Following the above argument, the condition that the total excitation energy immediately after electron capture should be smaller than the ionization potential of the ion in the new charge state must, in contrast to the situation for gases, not necessarily be fulfilled in order to count the event as a capture process inside a solid.

Finally, it is quite interesting to point out that with the closeness of the distributions of charge states inside gaseous and solid targets, it is considerably easier to understand the experimental results which have shown that the stopping power for fast heavy ions is nearly independent of whether the medium is a gas or a solid. We stress, however, that this experimentally established

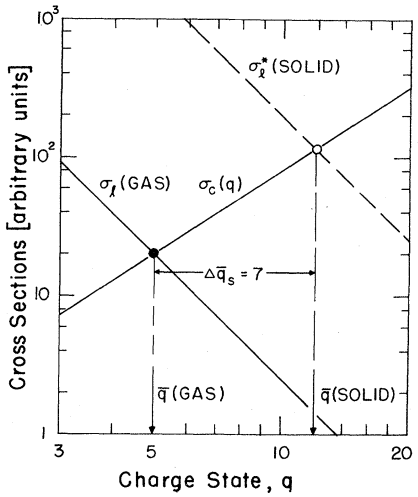

FIG. 6.11. Schematic illustration of electron loss cross sections in the Bohr and Lindhard model for the density effect in solids. In a typical example, it is demonstrated that large shifts of the mean equilibrium charge are obtained only when the effective loss cross sections of excited ions inside solids are substantially higher than the loss cross sections of ground state ions in dilute gases. Capture and loss cross sections are assumed to vary proportional to q^2 and q^{-3}, respectively. Multiple cross sections have been neglected.

[11] It is difficult to observe Auger electrons from heavy ions which emerge from solids. Many measurements are available for light ions and highly stripped ions. For example, autoionization of ions after their passage through thin carbon foils has been reported for helium atoms (Harrison and Lucas, 1971), nitrogen ions (Lucas and Harrison, 1972), and lithiumlike chlorine and argon ions (Sellin *et al.*, 1972). However, the observation of *particular* excitation states of a very small fraction of the beam ($\sim 1\%$) can not be readily utilized in order to infer the *average* excitation of all the emerging ions. In addition, results for ions which contain few electrons bear little significance for the present discussion because in these cases the density effect is known to be extremely small. Conclusions on the BL model and its modification which are based on such experimental data must be viewed with suspicion. Sellin *et al.* attempted conclusions on these lines, but partly for the above reasons, and partly because these authors misinterpret the suggested modifications of the BL model, their arguments are not convincing. Hopefully, studies of collision-induced emission of heavy-ion x-rays will provide some new evidence of the kind of excitation states of heavy ions during passage through solid targets (see, e.g., Lutz *et al.*, 1972; Betz *et al.*, 1972).

independence bears no direct significance for the above derivation of the new model for the density effect in solids.

c. *Stripping in Large Molecules*

For a long time many investigators have directed efforts towards finding a replacement for stripper foils, one which would produce higher average charge states than the gaseous targets, yet have a longer lifetime than a foil under intense heavy-ion bombardment. The search for possible materials has largely concentrated on heavy hydrocarbon molecules, but in no case were the resulting charge distributions found to be shifted to charge states higher than the ones obtained with simple mono- or diatomic gases such as nitrogen or oxygen.

Renewed interest in that search has been generated by the findings of Ryding *et al.* (1971a) who showed that fluorocarbon vapors indeed give a substantial effect. They investigated equilibrium fractions of bromine and iodine ions at energies between 3 and 12 MeV, stripped in three fluorocarbon vapors, C_7F_{14}, C_8F_{16}, and $C_{10}F_{18}$.[12] The resulting effect is also shown in Figs. 5.15, 5.17, and 6.6. It is evident that the fluorocarbons are more effective than simple gases but do not reach the high charge states obtained from solids.

In an attempt to explain the expected and observed effect, it is generally assumed that the large molecules act like small parts of a foil and produce to some extent the density effect known from solids. This implies that a single encounter of the ions with a large molecule is sufficient to produce the entire effect, provided that the incident charge is not too far from the equilibrium value. Experimental observation by Ryding *et al.* (1971a) support that conclusion; they found that very little vapor was required to produce charge state equilibrium. It is worth noting that the small equilibrium thicknesses are of advantage for practical applications because particle losses due to scattering are no worse than with the more standard stripping gases and are appreciably smaller than in foils.

It is not known exactly why the effect could be observed in fluorocarbons but not in other large molecules. Ryding *et al.* speculate that the effectiveness of the fluorocarbons is due to absence of hydrogen in these molecules. There is little doubt that collisions with hydrogen atoms lead to less substantial excitation of the ions than collisions with heavier atoms; however, the role of individual atoms within a target molecule in charge exchange collisions is poorly understood (see Sec. IV.2). A decisive quality of fluorocarbons must probably be seen in their approximately spherical form which enhances the probability that ions during a single encounter interact strongly with more than one or two of the atoms in the large molecules.

It must be expected that fluorocarbons become less effective when the particle energy increases. Since the cross sections $\sigma(q, q'; v)$ are decreasing functions of v for charge states $q \simeq \bar{q}(v)$, the number of collisions, n_{coll}, within a single molecule which lead to excitation and charge-changing processes decreases with v. Evidently, n_{coll} is not large enough in any of the investigated materials to produce the full density effect even in the region where σ is large. A further reduction of n_{coll} will then suppress the density effect to a larger extent. Recent observations by Franzke *et al.* (1972) seem to support that expectation. They find that iodine ions attain an average equilibrium charge in fluorocarbons (C_7F_{14}) which exceeds the one measured in nitrogen as much as by $\Delta\bar{q} \simeq 3$ at 50 MeV, but only by $\Delta\bar{q} \lesssim 1$ at 150 MeV. In addition, they observe that multiple-electron loss probabilities $\sigma(q, q+n)$ are anomalously large for $n \simeq 5$. To a lesser extent, this effect is visible in Fig. 4.10. In a tentative explanation of the increase of that effect in C_7F_{14} compared to an oxygen target, we may argue that relatively soft collisions which are likely to result only in single-electron loss are very similar in both targets, whereas harder collisions lead to an interaction—excitation and multiple electron loss—which is more extensive in the core of the large molecule than in an oxygen molecule. Further investigation of these and related complex processes and mechanisms in heavy ion–atom collisions are likely to reveal effects of far-reaching practical significance and to give results of great interest to our theoretical understanding of these collision phenomena.

GLOSSARY

The following is a brief list of the most important symbols which have been consistently used, with little exception, throughout all sections of this article.

a_c, a_l	Exponents in the power law approximation of cross sections for capture and loss, Eq. (2.17)
a_0	Bohr radius ($\hbar^2/(m_e e^2) = 5.291 \times 10^{-9}$ cm)
b	Collision diameter
d	Charge state distribution width, Eq. (2.7)
d_0	Charge state distribution width due to single-electron capture and loss
E	Projectile energy
$\bar{\epsilon}$	Relative average excitation of an ion, I^*/I
$F(q)$	Normalized equilibrium charge state fraction
$I(q)$	Ionization potential of an ion of charge q
$I^*(q)$	Excitation of an ion of charge q
$k_n{}^c$, $k_n{}^l$	Ratio between cross sections for multiple- and single-electron capture or loss, Eq. (2.14)

[12] Ryding *et al.* (1971a) present a graph with equilibrium fractions of 12-MeV iodine ions in fluorocarbon vapors and in conventional gases and foils; however, except for the fluorocarbon stripper, the distributions refer to 10 MeV and not to 12 MeV. Thus, in reality, the effect of the fluorocarbon is less pronounced than one would assume from their graph.

$\bar{k}$	Broadening factor of the width of charge state distributions due to multiple-electron capture and loss, d/d_0, Eq. (2.16)
κ	$2\pi b/\lambda$
λ	de Broglie wave length
m, M	Projectile mass
m_e	Electron mass
n	Number of electrons captured or lost by an ion in a single charge-changing collision
ν, ν^*	Quantum numbers
P	Target gas pressure
q	Charge of an ion
q_T	Effective charge of a target atom during an encounter
$\bar{q}$	Average charge of ions in a beam, Eq. (2.6)
$\bar{q}_{\text{eff}}$	Effective charge of ions deduced from energy loss measurements, Eq. (5.12)
r_0	Impact parameter
ρ	Target gas density in molecules/cm^3
s	Skewness of equilibrium charge state distributions, Eq. (2.9)
$\sigma(q, q')$	Cross section for a charge-changing process $q \rightarrow q'$ of an ion in a single encounter, in cm^2/molecule
σ_c, σ_l	Charge-changing cross section for electron capture or loss in cm^2/molecule
σ_t	Total charge-changing cross section, Eq. (2.2a)
σ^*	Charge-changing cross section of an excited ion
σ'	Cross section for a collision between two particles with relative velocity v, accompanied by an energy transfer of $\sim m_e v^2/2$
t	Time
τ	Lifetime of excited states of ions
u	Orbital velocity of an electron
v	Projectile velocity
v_0	Bohr velocity $[e^2/\hbar = c/127 = 2.188 \times 10^8$ cm/sec)
x	Target thickness in cm^2/molecule
x_∞	Equilibrium target thickness
$Y(q)$	Normalized nonequilibrium charge state fractions
Z	Atomic number of projectile ions
Z_T	Atomic number of target atoms

ACKNOWLEDGMENTS

I wish to express my thanks to Professor Arthur K. Kerman for his inspiration in the writing of this article. In addition I am grateful to Professor Lee Grodzins for his continued support and his most valuable comments and criticism. I am also indebted to Dr. Peter H. Rose and Dr. Andrew Wittkower for many helpful discussions and for communication of experimental results. Thanks are also extended to the many authors who made their data available to me prior to publication.

REFERENCES

Allison, S. K., 1958, Rev. Mod. Phys. **30,** 1137.
——, and M. Garcia-Munoz, 1962, in *Atomic and Molecular Processes*, edited by D. R. Bates (Academic, New York).
Almqvist, E., C. Broude, M. A. Clark, J. A. Kuehner, and A. E. Litherland, 1962, Can. J. Phys. **40,** 954.
Angert, N., B. Franzke, A. Möller, and Ch. Schmelzer, 1968, Phys. Letters **27A,** 28; see also N. Angert, 1968, Unilac Report 5-68, Universität Heidelberg (unpublished); N. Angert (private communication).
Barkas, W. H., 1963, in *Nuclear Research Emulsions* (Academic, New York), Vol. I, p. 371.
Baron, E., 1972, IEEE Transactions on Nuclear Science NS-**19,** No. 2, 256.
Bates, D. R., 1962, in *Atomic and Molecular Processes*, edited by D. R. Bates (Academic, New York), p. 549.
——, and A. Dalgarno, 1953, Proc. Phys. Soc. (London) **A66,** 972.
——, and R. McCarrol, 1962, Adv. in Phys. **11,** 39.
——, and R. A. Mapleton, 1967, Proc. Phys. Soc. **90,** 909.
Bell, G. I., 1953, Phys. Rev. **90,** 548.
Bethe, H., and J. Ashkin, 1953, in *Experimental Nuclear Physics*, edited by E. Segré (Wiley, New York), Vol. I, p. 282.
——, and E. E. Salpeter, 1957, in *Quantum Mechanics of One- and Two-Electron Atoms* (Springer Verlag, Berlin), pp. 320–322.
Bethge, K., P. Sandner, and H. Schmidt, 1966, Z. Naturforsch. **21a,** 1052.
——, and G. Günther, 1964, Z. Angew. Phys. **17,** 548.
Beringer, R., and W. Roll, 1957, Rev. Sci. Instr. **28,** 77.
Betz, H. D., G. Hortig, E. Leischner, Ch. Schmelzer, B. Stadler, and J. Weihrauch, 1966, Phys. Letters **22,** 643. See also H. D. Betz, 1965, Unilac report 5-65, Universität Heidelberg (unpublished), and E. Leischner, 1966, Unilac Report 1-66, Universität Heidelberg (unpublished).
——, and Ch. Schmelzer, 1967, Unilac Report 1–67, Universität Heidelberg (unpublished).
——, and L. Grodzins, 1970, Phys. Rev. Letters **25,** 211.
——, 1970, Phys. Rev. Letters **25,** 903.
——, G. Ryding, and A. B. Wittkower, 1971a, Phys. Rev. **A3,** 197.
——, L. Grodzins, A. B. Wittkower, and G. Ryding, 1971, 1971b, Phys. Rev. Letters **26,** 871.
——, and H. W. Schnopper, 1972, European Conference on Nuclear Physics, Aix-en-Provence, June 26–July 1.
——, J. P. Delvaille, K. Kalata, H. W. Schnopper, A. R. Sohval, K. W. Jones, and H. E. Wegner, 1972, Proc. of the International Conference on Inter Shell Ionization Phenomena, Atlanta, April 17–21 (North-Holland Publ. Co., to be published).
——, and A. B. Wittkower, 1972a, Phys. Rev. (unpublished).
——, and A. B. Wittkower, 1972b, Phys. Rev. (unpublished).
Bloom, S. D., and G. D. Sauter 1971, Phys. Rev. Letters **26,** 607.
Bohr, N., 1940, Phys. Rev. **58,** 654.,
——, 1941, Phys. Rev. **59,** 270.
——, 1948, Kgl. Danske Videnskab. Selskab, Mat.-Fys. Medd. **18,** No. 8.
——, and J. Lindhard, 1954, Kgl. Danske Videnskab. Selskab, Mat.-Fys. Medd. **28,** No. 7.
Booth, W., and I. S. Grant, 1965, Nucl. Phys. **63,** 481.
Borovik, E. S., F. I. Busol, V. B. Yuferov, and E. I. Sibenko, 1963, Zh. Tekh. Fiz. **33,** 973 [Sov. Phys.-Tech. Phys. **8,** 724 (1964)].
Brandt, W., and R. Laubert, 1970, Phys. Rev. Letters **24,** 1037.
Bridwell, L. B., L. C. Northcliffe, S. Datz, C. D. Moak, and H. O. Lutz, 1967, Phys. Rev. **149,** 276.
Brinkmann, H. C., and H. A. Kramers, 1930, Proc. Acad. Sci. Amsterdam **33,** 973.
Brown, M., 1972, Phys. Rev. A **6,** 229.
——, and C. D. Moak, 1972, Phys. Rev. **B6,** No. 1 (in press).
Brunings, J. H., and J. K. Knipp, 1941, Phys. Rev. **59,** 919.
——, J. K. Knipp, and E. Teller, 1941, Phys. Rev. **60,** 657.
Busol, F. I., V. B. Yuferov, and E. I. Sibenko, 1964, Zh. Tekh. Fiz. **34,** 2156 [Sov. Phys.-Techn. Phys. **9,** 1661 (1965)].
Carlson, T. A., C. W. Nestor, N. Wasserman, and J. D. McDowell, 1970, Atomic Data **2,** 63.
——, C. W. Nestor, and J. D. McDowell, 1971, Oak Ridge National Laboratory Report ORNL-4721.

Cline, C. K., T. E. Pierce, K. H. Purser, and M. Blann, 1969, Phys. Rev. **180,** 450.
Cumming, J. B., and V. P. Crespo, 1967, Phys. Rev. **161,** 287.
Dagnac, R., D. Blanc, and D. Molina, 1970, J. Phys. B **3,** 1239.
Dalgarno, A., 1964, in *Atomic and Molecular Processes,* edited by M. R. McDowell (North-Holland Publ. Co., Amsterdam), p. 609.
Datz, S., H. O. Lutz, L. B. Bridwell, C. D. Moak, H. D. Betz, and L. D. Ellsworth, 1970, Phys. Rev. A **2,** 430.
——, C. D. Moak, H. O. Lutz, L. C. Northcliffe, and L. B. Bridwell, 1971, Atomic Data **2,** 273.
Dawton, R. H., 1961, Nucl. Instr. Methods **11,** 326.
Desclaux, J. P., 1972, Computer Phys. Commun. (to be published).
Dmitriev, I. S., 1957, Zh. Eksperim. i. Teor. Fiz. **32,** 570 [Sov. Phys. JETP **5,** 473 (1957)].
——, V. S. Nikolaev, L. N. Fateeva, and Ya. A. Teplova, 1962a, Zh. Eksperim. i Teor. Fiz. **42,** 16 [Sov. Phys. JETP **15,** 11 (1962)].
——, V. S. Nikolaev, L. N. Fateeva, and Ya. A. Teplova, 1962b, Zh. Eksperim. i Teor. Fiz. **43,** 361 [Sov. Phys. JETP **16,** 259 (1963)].
——, and V. S. Nikolaev, 1963, Zh. Eksperim. i. Teor. Fiz. **44,** 660 [Sov. Phys. JETP **17,** 447 (1963)].
——, and V. S. Nikolaev, 1964, Zh. Eksperim. i Teor. Fiz. **47,** 615 [Sov. Phys. JETP **20,** 409 (1965)].
——, Ya. M. Zhileikin, and V. S. Nikolaev, 1965, Zh. Eksperim. i Teor. Fiz. **49,** 500 [Sov. Phys. JETP **22,** 352 (1966)].
Drukarev, G. F., 1959, Zh. Eksperim. i Teor. Fiz. **37,** 847 [Sov. Phys. JETP **37,** 603 (1960)].
——, 1967, Zh. Eksperim. i Teor. Fiz. **52,** 498 [Sov. Phys. JETP **25,** 326 (1967)].
Fano, U., and W. Lichten, 1965, Phys. Rev. Letters **14,** 627.
Fogel, I. M., L. I. Krupnik, and V. A. Ankudinov, 1956, Zh. Tekh. Fiz. **26,** 1208 [Sov. Phys.-Tech. Phys. **1,** 1181 (1956)].
Franzke, B., N. Angert, A. Möller, and Ch. Schmelzer, 1967, Phys. Letters **25A,** 769; and B. Franzke, 1967 (private communication).
——, N. Angert, and Ch. Schmelzer, 1971, Abs. International Conference on Physics of Electronic and Atomic Collisions, Amsterdam, edited by L. M. Branscomb *et al.* (North-Holland Publ. Co., Amsterdam), p. 542.
——, N. Angert, and Ch. Schmelzer, 1972, IEEE NS-**19,** No. 2, 266; B. Franzke (private communication).
Fulmer, C. B., and B. L. Cohen, 1958, Phys. Rev. **109,** 94.
Gerasimenko, V. K., and L. N. Rozentsveig, 1956, Zh. Eksperim. i Teor. Fiz. **31,** 684 [Sov. Phys. JETP **4,** 509 (1957)].
Gilbody, H. B., R. Browning, and G. Levy, 1968, J. Phys. B **1,** 863.
——, K. F. Dunn, R. Browning, and C. J. Latimer, 1970, J. Phys. B **3,** 1105.
——, 1971 (private communication).
Gluckstern, R. L., 1955, Phys. Rev. **98,** 1817.
Grodzins, L., R. Kalish, D. Murnick, R. J. Van de Graaf, F. Chmara, and P. H. Rose, 1967, Phys. Letters **24B,** 282. See also F. M. Flasar, Mass. Inst. of Technology, 1967 (unpublished); L. Grodzins (private communication).
Hall, T., 1950, Phys. Rev. **79,** 504.
Harrison, K. G., and M. W. Lucas, 1971, Phys. Letters **35A,** 402.
Heckmann, H. H., B. L. Perkins, W. G. Simon, F. M. Smith, and W. H. Barkas, 1960, Phys. Rev. **117,** 544.
——, E. L. Hubbard, and W. G. Simon, 1963, Phys. Rev. **129,** 1240.
Hubbard, E. L., and E. J. Lauer, 1955, Phys. Rev. **98,** 1814.
Hvelplund, P., E. Laegsgard, J. Olsen, and E. H. Pedersen, 1970, Nucl. Instr. Meth. **90,** 315.
——, E. Laegsgaard, and E. H. Pedersen, 1972, Nucl. Inst. Meth. **101,** 497; and P. Hvelplund, private communication.
Jackson, J. D., and H. Schiff, 1953, Phys. Rev. **89,** 359.
Kalish, R., L. Grodzins, F. Chmara, and P. H. Rose, 1969, Phys. Rev. **183,** 431.
Kessel, Q. C., 1970, Phys. Rev. **A2,** 1881.
Knipp, J. K. and E. Teller, 1941, Phys. Rev. **59,** 659.
Kulcinsky, G. L., A. B. Wittkower, and G. Ryding, 1971, Nucl. Instr. Meth. **94,** 365.
Lamb, W. E., 1940, Phys. Rev. **58,** 696.
Lasssen, N. O., 1951a, Kgl. Danske Videnskab. Selskab, Mat.-Fys. Medd. **26,** No. 5.
——, 1951b, Kgl. Danske Videnskab. Selskab, Mat.-Fys. Medd. **26,** No. 12.
Layton, J. K., R. F. Stebbings, R. T. Brackmann, W. L. Fite, W. R. Ott, C. E. Carlston, A. R. Comeaux, G. D. Magnuson, and P. Mahadevan, 1967, Phys. Rev. **161,** 73.
Lichten, W., 1967, Phys. Rev. **164,** 131.
Lindhard, J., M. Scharff, and H. E. Schiøtt, 1963, Kgl. Danske-Videnskab. Selskab, Mat.-Fys. Medd. **33,** No. 14.
Litherland, A. E., E. Almqvist, B. H. Andrews, C. Broude, and J. A. Kuehner, 1963, Bull. Am. Phys. Soc. **8,** 75. See also H. R. Andrews, E. Almqvist, C. Broude, M. A. Eswaran, J. A. Kuehner, and A. E. Litherland, 1963, The Tandem Quarterly, **1,** (High Voltage Engineering, Burlington, Mass., 1963), Vol. 1, p. 1.
Lo, H. H., and W. L. Fite, 1970, Atomic Data **1,** 305.
Löwdin, P. O., 1959, J. Molec. Spectry. **3,** 46.
Lucas M. W., and K. G. Harrison, 1972, J. Phys. B. **5,** L20.
Lutz, H. O., J. Stein, S. Datz, and C. D. Moak, 1972, Phys. Rev. Letters **28,** 8.
Macdonald, J. R., and F. W. Martin, 1971, Phys. Rev. **A4,** 1965.
——, S. M. Ferguson, T. Chiao, L. D. Ellsworth, and S. A. Savoy, 1972, Phys. Rev. A **5,** 1188.
Main, B., 1967 (private communication).
Martin, F. W. and L. C. Northcliffe, 1962, Phys. Rev. **128,** 1166.
——, 1965, Phys. Rev. **140,** A75.
Meyer, L., 1971, Phys. Status Solidi **44,** 253.
Moak, C. D. and M. D. Brown, 1966, Phys. Rev. **149,** 244.
——, H. W. Schmitt, F. J. Walter, and G. F. Wells, 1963, Rev. Sci. Instr. **34,** 853.
——, 1967 (private communication).
——, H. O. Lutz, L. B. Bridwell, L. C. Northcliffe, and S. Datz, 1967, Phys. Rev. Letters **18,** 41.
——, H. O. Lutz, L. B. Bridwell, L. C. Northcliffe, and S. Datz, 1968, Phys. Rev. **176,** 427.
Möller, A., N. Angert, B. Franzke, and Ch. Schmelzer, 1968, Phys. Letters **27A,** 621; See also A. Möller, 1968, Unilac Report 6-68, Universität Heidelberg (unpublished); A. Möller (private communication).
Nikolaev, V. S., 1957, Zh. Eksperim. i Teor. Fiz. **33,** 534 [Sov. Phys. JETP **6,** 417 (1957)].
——, L. N. Fateeva, I. S. Dmitriev, and Ya. A. Teplova, 1957, Zh. Eksperim. i Teor. Fiz. **33,** 306 [Sov. Phys. JETP **6,** 239 (1957)].
——, I. S. Dmitriev, L. N. Fateeva, and Ya. A. Teplova, 1960, Zh. Eksperim. i Teor. Fiz. **39,** 905 [Sov. Phys. JETP **12,** 627 (1961)].
——, I. S. Dmitriev, L. N. Fateeva, and Ya. A. Teplova, 1961a, Zh. Eksperim. i. Teor. Fiz. **40,** 989 [Sov. Phys. JETP **13,** 695 (1961)].
——, L. N. Fateeva, I. S. Dmitriev, and Ya. A. Teplova, 1961b, Zh. Eksperim. i Teor. Fiz. **41,** 89 [Sov. Phys. JETP **14,** 67 (1962)].
——, I. S. Dmitriev, Ya. A. Teplova, and L. N. Fateeva, 1963, Izv. Acad. Nauk SSSR, Ser. Fiz. **27,** 1078 [Bull. Acad. Sci. USSR, Phys. Ser. **27,** 1049 (1963)]; see also V. S. Nikolaev, I. S. Dmitriev, L. N. Fateeva, and Ya. A. Teplova, 1962, Izv. Acad. Nauk SSSR, Ser. Fiz. **26,** 1430 [Bull. Acad. Sci. USSR Phys. Ser. **26,** 1455 (1962)].
——, 1965, Usp. Fiz. Nauk **85,** 679 [Sov. Phys. Usp. **8,** 269 (1965)].
——, 1966, Zh. Eksperim. i Teor. Fiz. **51,** 1263 [Sov. Phys. JETP **24,** 847 (1967)].
——, and I. S. Dmitriev, 1968, Phys. Letters **28A,** 277.
Northcliffe, L. C., 1960, Phys. Rev. **120,** 1744.
——, 1963, Ann. Rev. Sci. **13,** 67.
——, and R. F. Schilling, 1970, Nucl. Data, Sect. **A7,** 233.
Oppenheimer, J. R., 1928, Phys. Rev. **31,** 349.
Papineau, A., 1956, Compt. Rend. **242,** 2933.
Petrov, L. A., V. A. Karnaukhov, and D. D. Bogdanov, 1970, Zh. Eksperim. i Teor. Fiz. **59,** 1926 [Sov. Phys. JETP **32,** 1042 (1971)].
Pierce, T. E., and M. Blann, 1968, Phys. Rev. **173,** 390; note that the exponent 2.5 in Eq. (6) should read 5.0.
Pivovar, L. I., M. T. Novikov, and V. M. Tubaev, 1963, Zh. Eksperim. i Teor. Fiz. **46,** 471 [Sov. Phys. JETP **19,** 318 (1964)].
——, V. M. Tubaev, and M. T. Novikov, 1965a, Zh. Eksp. Teor. Fiz. **48,** 1022 [Sov. Phys. JETP **21,** 681 (1965)].

——, M. T. Novikov, and A. S. Dolgov, 1965b, Zh. Eksp. Teor. Fiz. **49,** 734 [Sov. Phys. JETP **22,** 508 (1966)].
——, M. T. Novikov, and A. S. Dolgov, 1966, Zh. Eksp. Teor. Fiz. **50,** 537 [Sov. Phys. JETP **23,** 357 (1966)].
——, L. I. Nikolaichuk, and F. M. Trubchaninov, 1967b, Zh. Eksp. Teor. Fiz. **52,** 1160 [Sov. Phys. JETP **25,** 770 (1967)].
——, G. A. Krivonosov, and V. M. Tubaev, 1967b, Zh. Eksp. Teor. Fiz. **53,** 1872 [Sov. Phys. JETP **26,** 1066 (1968)].
——, L. I. Nikolaichuk, and A. N. Grigor'ev, 1969, Zh. Eksperim. i Teor. Fiz. **57,** 432 [Sov. Phys. JETP **30,** 236 (1970)].
——, and L. I. Nikolaichuk, 1970, Zh. Eksperim. i Teor. Fiz. **58,** 97 [Sov. Phys. JETP **31,** 55 (1970)].
Reynolds, H. L., D. W. Scott, and A. Zucker, 1954, Phys. Rev. **95,** 671.
Roll, P. G. and F. E. Steigert, 1960a, Nucl. Phys. **17,** 54.
——, and F. E. Steigert, 1960b, Phys. Rev. **120,** 470.
Roos, M., P. H. Rose, A. B. Wittkower, N. B. Brooks, and R. R. Bastide, 1965, Rev. Sci. Instr. **36,** 544.
Rose, P. H., K. H. Purser, and A. B. Wittkower, 1965, IEEE Transactions on Nuclear Science, NS-**12,** No. 3, 251.
Russek, A., 1963, Phys. Rev. **132,** 246.
Ryding, G., A. B. Wittkower, and P. H. Rose, 1969a, Phys. Rev. **184,** 93.
——, A. B. Wittkower, and P. H. Rose, 1969b, Phys. Rev. **185,** 129.
——, A. B. Wittkower, G. H. Nussbaum, A. C. Saxmann, R. Bastide, Q. Kessel, and P. H. Rose, 1970a, Phys. Rev. **A1,** 1081.
——, A. B. Wittkower, G. H. Nussbaum, A. C. Saxmann, and P. H. Rose, 1970b, Phys. Rev. **A2,** 1382.
——, H. D. Betz, and A. B. Wittkower, 1970c, Phys. Rev. Letters **24,** 123.
——, A. B. Wittkower, and P. H. Rose, 1971a, Particle Accelerators **2,** 13.
——, A. B. Wittkower, and P. H. Rose, 1971b, Phys. Rev. **A3,** 1658.
Schiff, H., 1954, Can. J. Phys. **32,** 393.
Schlachter, A. S., D. H. Loyd, P. J. Bjorkholm, L. W. Anderson, and W. Haeberli, 1968, Phys. Rev. **174,** 201.
Schmitt, H. W., and F. Pleasonton, 1966, Nucl. Instr. Meth. **40,** 204.
Schnopper, H. W., H. D. Betz, J. P. Delvaille, K. Kalata, A. R. Sohval, K. W. Jones, and H. E. Wegner, 1972, Proc. of the International Conference on Inner Shell Ionization Phenomena, Atlanta, April 17–21, (North-Holland Publ. Co., to be published).
Sellin, I. A., D. J. Pegg, P. M. Griffin, and W. W. Smith, 1972, Phys. Rev. Letters **28,** 1229.
Senashenko, V. S., V. S. Nikolaev, and I. S. Dmitriev, 1968, Zh. Eksp. Teor. Fiz. **54,** 1203 [Sov. Phys. JETP **27,** 643 (1968)].
Smith, P. L., and W. Whaling, 1969, Phys. Rev. **188,** 36.
Stephens, K. G., and D. Walker, 1954, Phil. Mag. **45,** 543.
Stier, P. M., C. F. Barnett, and G. E. Evans, 1954, Phys. Rev. **96,** 973.
Strauss, M. G., and R. Brenner, 1965, Rev. Sci. Instr. **36,** 1857.
Teplova, Ya. A., V. S. Nikolaev, I. S. Dmitriev, and L. N. Fateeva, 1962, Zh. Eksp. Teor. Fiz. **42,** 44 [Sov. Phys. JETP **15,** 31 (1962)].
Thomas, E. W., and G. D. Bent, 1967, Phys. Rev. **164,** 143.
——, 1967, Phys. Rev. **164,** 151.
Toburen, L. H., M. Y. Nakai, and R. A. Langley, 1968, Phys. Rev. **171,** 114.
Utterback, N. G., and T. Griffith, 1966, Rev. Sci. Instr. **37,** 866.
Vinogradov, A. V., and V. P. Shevel'ko, 1970, Zh. Eksp. Teor. Fiz. **59,** 593 [Sov. Phys. JETP **32,** 323 (1971)].
Welsh, L. M., K. H. Berkner, S. N. Kaplan, and R. V. Pyle, 1967, Phys. Rev. **158,** 85.
Williams, E. J., 1939, Proc. Roy. Soc. (London) **169,** 531.
——, 1940, Phys. Rev. **58,** 292.
Wittkower, A. B. and H. B. Gilbody, 1967, Proc. Phys. Soc. **90,** 353.
——, and G. Ryding, 1971, Phys. Rev. A, **4,** 226.
——, and H. D. Betz, 1971a, VII International Conference on Physics of Electronic and Atomic Collisions, Amsterdam, edited by L. M. Branscomb *et al.* (North-Holland Publ. Co. Amsterdam), p. 498.
——, and H. D. Betz, 1971b, J. Phys. B **4,** 1173.
——, and H. D. Betz, 1972a, U.S. Atomic Energy Commission, Division of Technical Information, AEC Critical Review Series (to be published).
——, and H. D. Betz, 1972b, Phys. Rev. A (unpublished).
Wolke, R. L., 1968, Phys. Rev. **171,** 301.